Universitat Internacional de Catalunya
Departament de Ciències Bàsiques

Tesis doctoral

Iron Regulatory Protein/Iron Responsive Element (IRP/IRE) system: associated diseases and new target mRNAs (PPP1R1B)

Ferran Celma Nos

Iron Regulatory Protein/Iron Responsive Element (IRP/IRE) system: associated diseases and new target mRNAs (PPP1R1B)

FERRAN CELMA NOS

TESIS DOCTORAL

UNIVERSITAT INTERNACIONAL DE CATALUNYA, 2022

DIRECTORES:

Dr. MAYKA SÁNCHEZ FERNÁNDEZ

Dr. GONZALO HERNÁNDEZ VIEDMA

PROGRAMA DE DOCTORADO EN CIENCIAS DE LA SALUT

DEPARTAMENTO DE CIENCIAS BÁSICAS

IRON METABOLISM: REGULATION AND DISEASES GROUP

A mi mateix…

SUMMARY

Iron is a biometal involved in many physiological processes essential for life. Regulation of both systemic and cellular iron homeostasis is crucial for health. The IRP/IRE post-transcriptional regulatory system is in charge to control iron uptake, utilization, storage and export at cellular level. There are two iron regulatory proteins (IRP1 and IRP2) which recognize and bind conserved mRNA motifs named iron responsive elements (IREs). These IREs are located in the mRNA untranslated regions (UTR) of genes involved in iron metabolism. IRP/IRE binding is produced under cellular iron depletion conditions, modifying the expression of several proteins related with cellular iron acquisition, mobilization and storage. Depending on the location of the IREs in the target mRNA, the binding of the IRPs regulates differentially its expression. When IREs are present in the 3' UTR their binding to the IRPs stabilize the mRNA, protecting it from degradation and increasing its translation. On the other hand, translation is inhibited when IRPs bind IREs located in the 5' UTR. IRP/IRE system missregulation leads to human diseases denoting the importance of this post-transcriptional gene regulation. As part of my thesis (objective 1) we describe new cases of patients with Hereditary Hyperferritinemia Cataract Syndrome (HHCS) with mutations in the *FTL* IRE (Paris1 c.-160A>G and Madrid/Philadelphia c.-167G>T mutations) and we did an exhaustive revision of all literature reported cases. In my thesis objective 2, we also contributed to the characterization of a *Slc11a2* IRE knock-in mouse model to dissect the Dmt1 3' IRE function in iron homeostasis. A genome-wide study made by our group, in order to characterize all the mRNAs that interact with the IRPs, identified 263 mRNAs that are potential IRP-target genes (44 mRNAs bind both IRPs, 102 bind specifically IRP1 and 117 bind specifically IRP2). The objective 3 of my thesis is focused on the characterization of one of these novel IRP-target mRNAs: *PPP1R1B* (DARPP-32 protein). DARPP-32 is a dopaminergic neurotransmission integrator which its main function is to inhibit protein phosphatase 1 (PP1). We identified a functional 5'IRE in mouse Ppp1r1b mRNA that binds *in vitro* to IRP1. Further, DARPP-32 protein expression is downregulated in two human cell lines under iron deprivation by an iron chelator and upregulated with an iron source, in agreement with an IRP/IRE regulation by a 5'IRE.

RESUMEN

El ferro és un biometall implicat en molts processos fisiològics essencials per a la vida. La regulació de l'homeòstasi del ferro tant sistèmica com cel·lular és crucial per a la salut. El sistema de regulació post-transcripcional IRP/IRE s'encarrega de controlar l'absorció, utilització, emmagatzematge i exportació de ferro a nivell cel·lular. Hi ha dues proteïnes reguladores del ferro (IRP1 i IRP2) que reconeixen i s'uneixen a motius d'ARNm conservats anomenats elements sensibles al ferro (IREs). Aquests IREs es troben a les regions no traduïdes de l'ARNm (UTR) dels gens implicats en el metabolisme del ferro. La unió IRP/IRE es produeix en condicions d'esgotament del ferro cel·lular, modificant l'expressió de diverses proteïnes relacionades amb l'adquisició, la mobilització i l'emmagatzematge de ferro cel·lular. Depenent de la ubicació dels IREs a l'ARNm diana, la unió dels IRP en regula de manera diferent la seva expressió. Quan els IREs estan presents al 3'UTR, la seva unió a les IRPs estabilitzen l'ARNm, protegint-lo davant la degradació i augmentant la seva traducció. D'altra banda, la traducció s'inhibeix quan les IRPs s'uneixen a IREs situats al 5'UTR. La mala regulació del sistema IRP/IRE condueix a malalties humanes que denoten la importància d'aquesta regulació gènica post-transcripcional. Com a part de la meva tesi (objectiu 1) descrivim nous casos de pacients amb Síndrome d'Hiperferritinèmia Hereditària amb Cataractes (HHCS) amb mutacions a l'IRE del gen *FTL* (mutacions Paris1 c.-160A>G i Madrid/Philadelphia c.-167G>T) i vam fer una revisió exhaustiva de tots els casos reportats en la literatura. En el meu objectiu 2 de tesi, també hem contribuït a la caracterització d'un model *knock-in* de ratolí per al IRE de *Slc11a2* per estudiar la funció del 3' IRE de Dmt1 en l'homeòstasi del ferro. Un estudi de tot el genoma realitzat pel nostre grup, per tal de caracteritzar tots els ARNm que interaccionen amb els IRP, va identificar 263 ARNm que són gens potencials objectiu IRP (44 ARNm s'uneixen a tots dos IRP, 102 s'uneixen específicament a IRP1 i 117 s'uneixen específicament a IRP2). L'objectiu 3 de la meva tesi es centra en la caracterització d'un d'aquests nous ARNm objectiu IRP: *PPP1R1B* (proteïna DARPP-32). DARPP-32 és un integrador de neurotransmissió dopaminèrgica que la seva funció principal és inhibir la proteïna fosfatasa 1 (PP1). Hem identificat un 5'IRE funcional a l'ARNm de *Ppp1r1b* del ratolí que s'uneix in vitro a IRP1. A més, l'expressió de la proteïna DARPP-32 es regula a la baixa en dues línies cel·lulars humanes sota privació de ferro per un quelant de ferro i es regula amb una font de ferro, d'acord amb una regulació IRP/IRE per un 5'IRE.

Table of contents

I. LIST OF FIGURES

II. LIST OF TABLES

III. LIST OF ABBREVIATIONS

A - Adenosine

ABCB7 - ATP-binding cassette subfamily B member 7

ACO1 / IRP1 - aconitase 1, soluble

ACO2 - aconitase 2, mitochondrial

ADP adenosine diphosphate

AHMIO1 Anemia, hypochromic microcytic, with iron overload 1

AKT serine/threonine kinase

ALAS delta aminolevulinate synthase

ALAD aminolevulinic acid dehydratase

ASAT Sideroblastic Anemia with Spinocerebellar Ataxia

ATP adenosine triphosphate

BMP bone morphogenetic protein

C cytosine

CDC14A cell division cycle 14A

CDK1 Cyclin-Dependent Kinase 1

cDNA Complementary deoxyribonucleic acid

CDS Coding DNA sequence

CIA Cytosolic Assembly Machinery

CK Casein Kinase

CLPX Caseinolytic Mitochondrial Matrix Peptidase Chaperone subunit X

CP Ceruloplasmin

CPO Coproporphyrinogen Oxidase

DARPP-32 Dopamine and cAMP regulated Phosphoprotein of 32-kDa

DCYTB Cytochrome B Reductase 1

DFO Deferoxamine

DMT1 / SLC11A2 Divalent Metal Transporter 1 / solute carrier family 11 (proton-coupled divalent metal ion transporter), member 2

EMSA Electrophoretic Mobility Shift Assay

EPO Erythropoietin

EPP Erythropoietic Protoporphyria

ETC Electron Transport Chain

FAC Ferric Ammonium Citrate

FBXL5 F-box and leucine-rich repeat protein 5

Fe Iron

Fe^{+2} ferrous iron ion

Fe^{+3} ferric iron ion

FECH ferrochelatase

Fe/S iron-sulfur

FLVCR1 Feline leukemia virus subgroup receptor 1

FPN1 / SLC40A1 ferroportin-1 / solute carrier family 40 (iron-regulated transporter),

member 1

FRDA Friedreich's ataxia

FTH1 ferritin heavy chain

FTL ferritin light chain

FTMT ferritin mitochondrial

FXN frataxin

G guanosine

GAPDH Glyceraldehyde-3-phosphate Dehydrogenase

GLRX5 glutaredoxin 5

Gox / Hao1 glycolate oxidase / liver hydroxyacid oxidase 1

GTP guanosine triphosphate

H+ proton

H_2O_2 hydrogen peroxide HAMP hepcidin antimicrobial peptide

HAMP Hepcidin Antimicrobial Peptide

Hb Hemoglobin

HFE hemochromatosis

HFE2 / HJV hemochromatosis type 2 (juvenile) / hemojuvelin

HH Hereditary Hemochromatosis

HHCS Hereditary Hyperferritinemia – Cataract Syndrome

HIF1β hypoxia inducible factor-1 beta

HIF2α / EPAS1 hypoxia inducible factor-2 alpha / endothelial PAS domain protein 1

HML hereditary myopathy with lactic acidosis

HMOX1 heme oxygenase (decycling) 1

HSC20 Heat Shock Protein Cognate 20

HSPA9 Heat Shock Protein family A (Hsp70) member 9

IRE Iron Regulatory Element

IREB2 / IRP2 Iron-Responsive Element Binding Protein 2

IRP Iron Regulatory Protein

ISCU Iron-Sulfur Cluster assembly enzyme

ISD11 Iron-Sulfur protein biogenesis, desulfurase-interacting protein 11

JAC1 / HSCB HscB mitochondrial iron-sulfur cluster co-chaperone

KI Knock out

KO Knock in

LIP Labile Iron Pool

MCV Mean Corpuscular Value

mRNA messenger Ribonucleic Acid

NCOA4 Nuclear Receptor Coactivator 4

NEF Nucleotide Exchange Factor

NFS1 cysteine desulfurase

NGS Next Generation Sequencing

NMDAR N-methyl-D-aspartate Receptor

NTBI Non Transferrin Bound Iron

O_2 Oxygen

OH- Hydroxide ion

●OH Hydroxyl radical

OMIM Online Mendelian Inheritance in Man database

PBGD porphobilinogen deaminase

PCBP1 poly-r(C)-Binding Protein-1

PCR polymerase chain reaction

PFN2 profilin 2

PHDs Prolyl Hydroxylase

PKA Protein Kinase A

PKG Protein Kinase G

PP1 Protein Phosphatase 1

PP2A Protein Phosphatase 2A

PP2B Protein Phosphatase 2B

PP2C Protein Phosphatase 2C

PPIX protoporphyrin IX

PPO protoporphyrinogen oxidase

PPP1R1B Protein Phosphatase 1 Regulatory subunit 1B

pVHL von Hippel-Lindau E3 ubiquitin ligase

qPCR quantitative polymerase chain reaction

RNS Reactive Nitrogen Specie

ROS Reactive Oxygen Specie

S sulfur

SD standard deviation

Sdh succinate dehydrogenase

SDS-PAGE Sodium Dodecyl Sulphate - PolyAcrylamide Gel Electrophoresis

SLC11A2 (see DMT1)

SLC22A17 solute carrier family 22, member 17

SLC40A1 (see FPN1)

SLC48A1/HRG1 solute carrier family 48 (heme transporter), member 1 / heme responsive gene 1

STEAP3 STEAP family member 3, metalloreductase

TCA tricarboxylic acid cycle

TF transferrin

TFR1 transferrin receptor 1

TFR2 transferrin receptor 2

TMPRSS6 transmembrane protease serine 6

U uracil

UROD uroporphyrinogen decarboxylase

UROS uroporphyrinogen III synthase

UTR untranslated region

XLEPP X-linked Erythropoietic Protoporphyria

XLSA X-linked sideroblastic anemia

ZIP14 / SLC39A14 Zrt-, Irt-like protein 14 / solute carrier family 39 (zinc transporter), member 14

ZIP8 / SLC39A8 Zrt-, Irt-like protein 8 / solute carrier family 39 (zinc transporter), member 8

1. Introduction:

Iron (Fe) is the most common metal element on Earth. It is a biometal involved in many physiological processes essential for life, such as oxygen transport, cellular respiration and many metabolic reactions. For this reason, it is considered as an essential micronutrient.

Inorganic iron has a wide range of oxidation states (from -2 to +6) but its reduced form (ferrous iron, Fe^{2+}) and oxidized form (ferric iron, Fe^{3+}) have the most biological importance. The ability of iron to change its oxidative state is the reason why iron is used by living organisms. However, this reactive capacity can be toxic in some conditions where iron is in excess, because through the Fenton's reaction, free ferrous ion could react with hydrogen peroxide (H_2O_2) and produce highly reactive hydroxyl radicals:

$$Fe^{2+} + H_2O_2 \rightarrow Fe^{3+} + OH^- + \cdot OH$$

These free radicals, also called Reactive Oxygen Species (ROS), interact with cellular structures and cause protein oxidation, lipid peroxidation and DNA damage. This molecular damage leads to cell death and, consequently, organ dysfunction.

Iron deficiency leads to anemia, a major world-wide public health problem, while iron overload is toxic and increases the oxidative stress of body tissues leading to inflammation, cell death, systemic organ dysfunction and cancer (Dev & Babitt, 2017; Hentze, Muckenthaler, Galy, & Camaschella, 2010). Due to these effects and the impact that iron has on health when it is out of balance, living organisms need a tight regulation of iron concentration both at systemic and cellular levels.

1.1.Iron in our body

Healthy human adults have about 3-5 g of iron in their bodies. A large amount of this element is in the form of hemoglobin inside the red blood cells (Gkouvatsos, Papanikolaou, & Pantopoulos, 2012). The liver and the spleen act as iron reservoir organs, storing iron into the liver hepatocytes and in specialized macrophages located in both organs. In addition, skeletal muscles contain iron associated to myoglobin, which functions as an oxygen storage under hypoxic conditions (Souza, Brunetto, & Nunes, 2016).

Iron is acquired from our diet through the enterocytes in the duodenum. Once absorbed, it is released into the plasma through the membrane transporter ferroportin (FPN). Ferric iron is insoluble and to solve this problem it is bound to a glycoprotein called transferrin (TF) that acts as an iron transporter in the blood. This way of transporting iron also avoids the ROS production of free excessive iron. The Fe^{+3}-TF complex is then internalized by cells through transferrin receptor 1 (TFR1) endocytosis (Thorstensen & Romslo, 1990). Iron will be stored mainly in the liver (also in the spleen) and directed to the bone marrow where it will be used to support erythropoiesis. Iron contained in senescent red blood cells will be recycled by splenic macrophages that will phagocyte old erythrocytes (Figure 1.1). It is important to remark

that there are no active mechanisms for iron excretion and iron loss are the consequence of bleeding or desquamation of epithelial surfaces (Green et al., 1968).

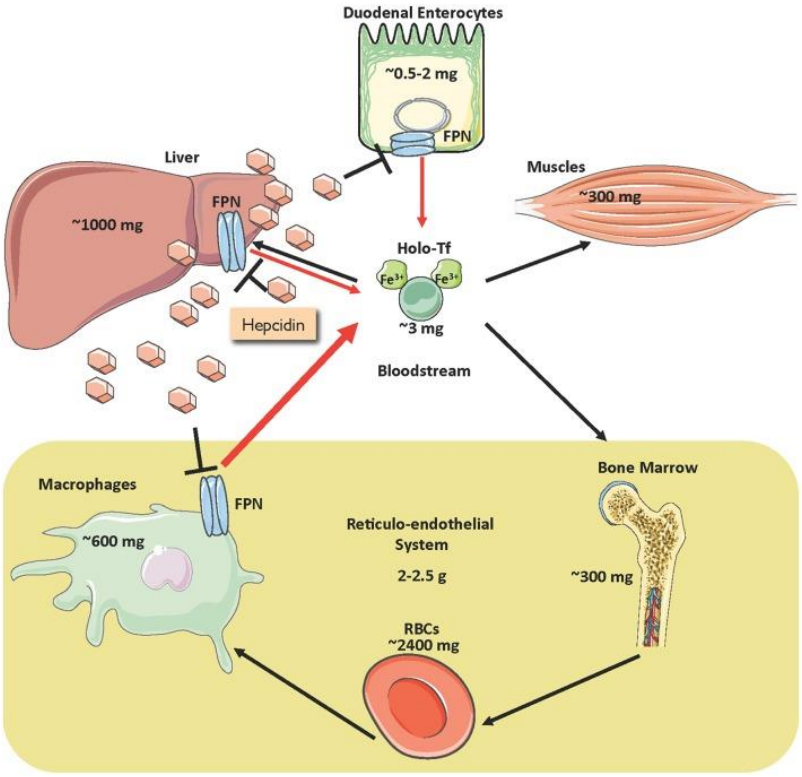

Figure 1.1: Systemic iron regulation. Dietary iron proceeding from our diet is absorbed by enterocytes and released at bloodstream where binds with TF. Iron is stored mainly in the liver, but it could be stored in other tissues such skeletal muscle. Bone marrow uses iron to produce red blood cells (RBC) which, in turn, will be recycled by macrophages that release this iron into the bloodstream again. (Sebastiani, Wilkinson, & Pantopoulos, 2016). Picture used with permission from Sebastiani *et al.* 2016.

1.2.Systemic iron regulation

The consequences of imbalance body iron levels can be fatal for the organism, hence a complex mechanism evolved to control iron absorption, storage and mobilization. The main systemic iron regulator is a small peptide hormone called hepcidin, which is coded by the *HAMP* gene and its role is to maintain systemic iron homeostasis. Hepcidin was firstly identified as an antimicrobial peptide (Krause et al., 2000) and afterwards it was discovered to be upregulated in the liver of iron overloaded mice (Pigeon et al., 2001). The *HAMP* gene knockout mice present an iron overload phenotype (Nicolas et al., 2001) confirming the role of hepcidin in iron regulation.

Hepcidin is synthesized in the liver by hepatocytes and secreted into the bloodstream (where it can be found free or bounded to plasma proteins). Other organs can also express lower levels of hepcidin such as heart, kidney, pancreas or hematopoietic cells (Kulaksiz, H. et al., 2005; Kulaksiz, Hasan et al., 2008; Merle, Fein, Gehrke, Stremmel,

& Kulaksiz, 2007; Peyssonnaux et al., 2006). Hepcidin binds to ferroportin (FPN), the membrane cellular iron export protein, causing its internalization and degradation leading to a reduction in the release of iron into the circulation from macrophages and the reduction of iron absorption in the duodenum (Qiao et al., 2012).

When the body is iron overloaded, hepcidin secretion increases, resulting in a reduction in the iron plasma concentration. Hepcidin is also upregulated during infections to reduce iron availability to halt the growth of pathogens (Armitage et al., 2011).

On the contrary, when iron levels are low, hepcidin production is repressed allowing iron duodenal absorption and release from macrophages (Anderson, G. J. & Frazer, 2017). If the rate of erythropoiesis needs to be increased due to hypoxia conditions or after bleeding, hepcidin is also repressed to allow the mobilization of iron from storage tissues to the bone marrow (Pak, Lopez, Gabayan, Ganz, & Rivera, 2006; Peyssonnaux et al., 2007).

1.3.Cellular iron regulation

Apart from the maintenance of systemic iron regulation, iron control is also needed at the cellular level. To avoid cellular iron toxicity, cells need to coordinate cellular iron uptake, storage and excretion.

1.3.1. Cellular iron uptake:

Cellular iron uptake is mainly mediated by the endocytosis of transferrin by its receptor transferrin receptor 1 (TFR1). Transferrin can bind up to two iron atoms (Tf-2Fe^{+3}), but in physiological conditions TF is not fully saturated. Transferrin circulates in plasma and the complex (2Fe^{+3}-TF/TFR1) is internalized by clathrin dependent endocytosis into endosomes. The endosome membrane contains a proton pump which decreases internal pH. Acidic conditions induce iron release from transferrin (Dautry-Varsat, Ciechanover, & Lodish, 1983). Free iron (Fe^{3+}) is then reduced to Fe^{2+} by the metalloreductase Six-Transmembrane Epithelial Antigen of Prostate 3 (STEAP3) (Ohgami et al., 2005; Ohgami, Campagna, McDonald, & Fleming, 2006). Finally, ferrous iron is transported to the cytoplasm by the divalent metal transporter 1 (DMT1) and the vesicle will be recycled to the plasma membrane, transferrin with no iron bound (apo-TF) is released to the plasma and TFR1 is ready to re-start another endocytic cycle. Figure 1.2 summarizes the TF/TFR1 endocytic pathway.

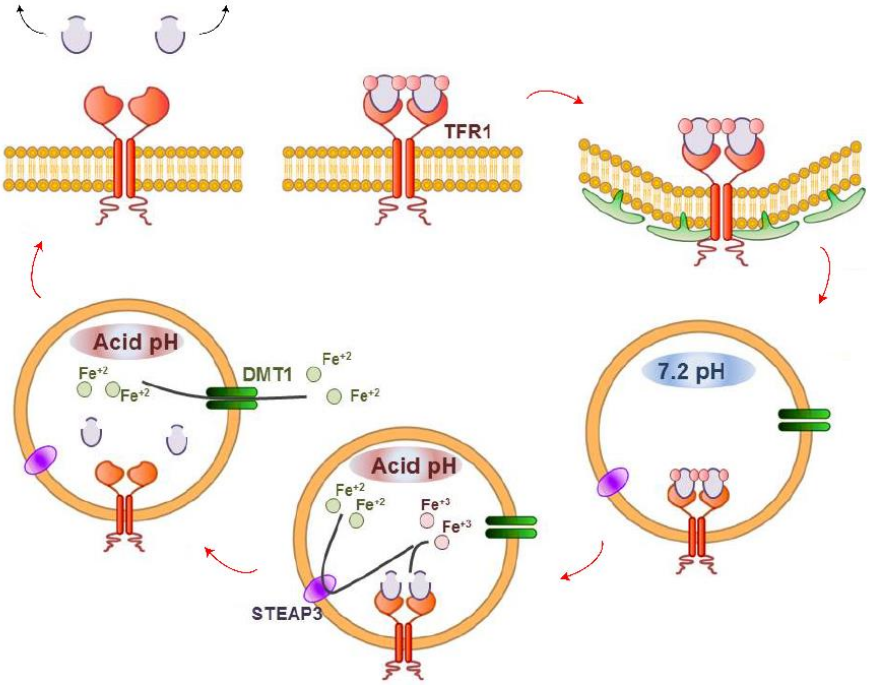

Figure 1.2: Transferrin - Transferrin receptor 1 (TFR1) endocytosis pathway. Schematic cycle of iron uptake by receptor-mediated endocytosis of iron loaded transferrin through transferrin receptor 1. Picture from Dr. Sanchez lab, courtesy of Dr. Marc Vila.

Interestingly, hypotransferrinemic (hpx/hpx) mice (Trenor, Campagna, Sellers, Andrews, & Fleming, 2000), have a mutation in the transferrin gene leading to a very low concentration of transferrin in plasma, similarly to what happens in human cases of congenital atransferrinemia (OMIM #209300) (Goldwurm et al., 2000). The clinical characteristic of congenital atransferrinemia is anemia with hepatic iron overload. Development of iron overload in non-hematopoietic tissues indicates that there are other mechanisms to introduce iron into the cells independent of the TF-TFR1 endocytic pathway. The fraction of iron that circulates in plasma not bound to any protein is called non-transferrin bound iron (NTBI). In atransferrinemia, iron in plasma and NTBI are high and this iron excess is rapidly taken up by hepatocytes (Zimelman, Zimmerman, McLean, & Weintraub, 1977) and T lymphocytes probably to eliminate potential iron toxicity (Arezes et al., 2013). Many transporters and channels have been speculated and involved in NTBI uptake from the plasma to the hepatocytes, being DMT1 an important player (Shindo et al., 2006). In addition, metalloproteins like ZIP14 and ZIP8 participate in NTBI uptake (Pinilla-Tenas et al., 2011; Wang, C. et al., 2012). Finally, in cardiomyocytes, calcium channels provide another pathway for iron entry (Oudit et al., 2003).

1.3.2. Cellular iron utilization:

A small fraction of uptaken iron becomes part of the cellular labile iron pool (cLIP) which is the fraction of the cellular iron that is in the cytoplasm. This iron is bound to low molecular weight chelators as citrates, sugar, ascorbate, ADP, ATP or other nucleotides (Petrat et al., 2003). Therefore, it will be metabolized quickly in the cell. A

bigger amount of uptaken iron is distributed to the mitochondria, where it is used to synthesize Fe/S clusters or heme. The mechanism for iron transport into the mitochondria is not fully understood, but it is postulated that porins may allow the passage of iron across the outer mitochondrial membrane (Lane et al., 2015; Paul, Manz, Torti, & Torti, 2017). Another hypothesis for iron transport into the mitochondria involves an isoform of DMT1 found in the outer mitochondrial membrane of HEK293 cells, which is the responsible of import ferrous iron into the intermembrane space (Wolff, Garrick, Zhao, Garrick, & Thévenod, 2014; Wolff et al., 2014). In the inner mitochondrial membrane there are two principal iron importers: mitoferrin and mitoferrin2 (Paradkar, Zumbrennen, Paw, Ward, & Kaplan, 2009; Shaw et al., 2006). In erythroblast cells, which need the greater amount of iron, this is imported into the mitochondria directly from the TRF1 endosomal vesicles, where DMT1 pumps iron directly into the mitochondria through an unknown channel, in a process known as the "kiss and run" mechanism (Hamdi et al., 2016).

Iron in the mitochondria is used for prosthetic groups biosynthesis such heme and Fe/S clusters. Heme is an essential iron-containing group present in several heme proteins including the oxygen transport hemoglobin protein. The biogenesis of heme requires 8 steps that take place in both the mitochondria and the cytoplasm. The first and rate limiting step is catalyzed by the mitochondrial matrix enzyme 5- aminolevulinic acid synthase (ALAS). This enzyme catalyzes the condensation of glycine and succinyl-CoA to form 5- aminolevulinic acid (ALA). Two isoforms of ALAS exist; ALAS1, expressed ubiquitously, and the erythroid-specific isoform known by ALAS2. In humans, loss of function mutations in the *ALAS2* gene leads to the genetic disease X-linked sideroblastic anemia (XLSA, OMIM #300751), which is characterized by ineffective erythropoiesis and mitochondrial iron deposition in maturing erythroblasts (Cotter, Baumann, & Bishop, 1992). In addition, gain-of-function mutations of *ALAS2* gene are responsible for X-linked Erythropoietic Protoporphyria (XLEPP, OMIM #300752). The enzymatic product ALA is modified in the cytoplasm by aminolevulinic acid dehydratase (ALAD) which condensate two molecules of ALA to form the monopyrrole porphobilinogen (PBG). Four molecules of PBG are deamined and condensed by porphobilinogen deaminase (PBGD) to conform the linear tetrapyrrole hydroxymethylbilane (HMB). HMB is the substrate of Uroporphyrinogen III synthase (UROS) producing uroporphyrinogen III. The last cytoplasmic step is the decarboxylation of uroporphyrinogen III by uroporphyrinogen decarboxylase (UROD) to form coproporphyrinogen. This intermediate comes back to the mitochondria and is oxidated by the coproporphyrinogen oxidase (CPO) forming protoporphyrinogen IX. Protoporphyrinogen oxidase (PPO) oxidates the protoporphyrinogen IX to form protoporphyrin IX (PPIX). Finally, the mitochondrial enzyme ferrochelatase (FECH) inserts the ferrous iron ion into the PPIX ring (Figure 1.3). The loss of activity of ferrochelatase causes Erythropoietic Protoporphyria (OMIM #177000) a disease that results in toxic accumulation of protoporphyrin IX (Lamoril et al., 1991).

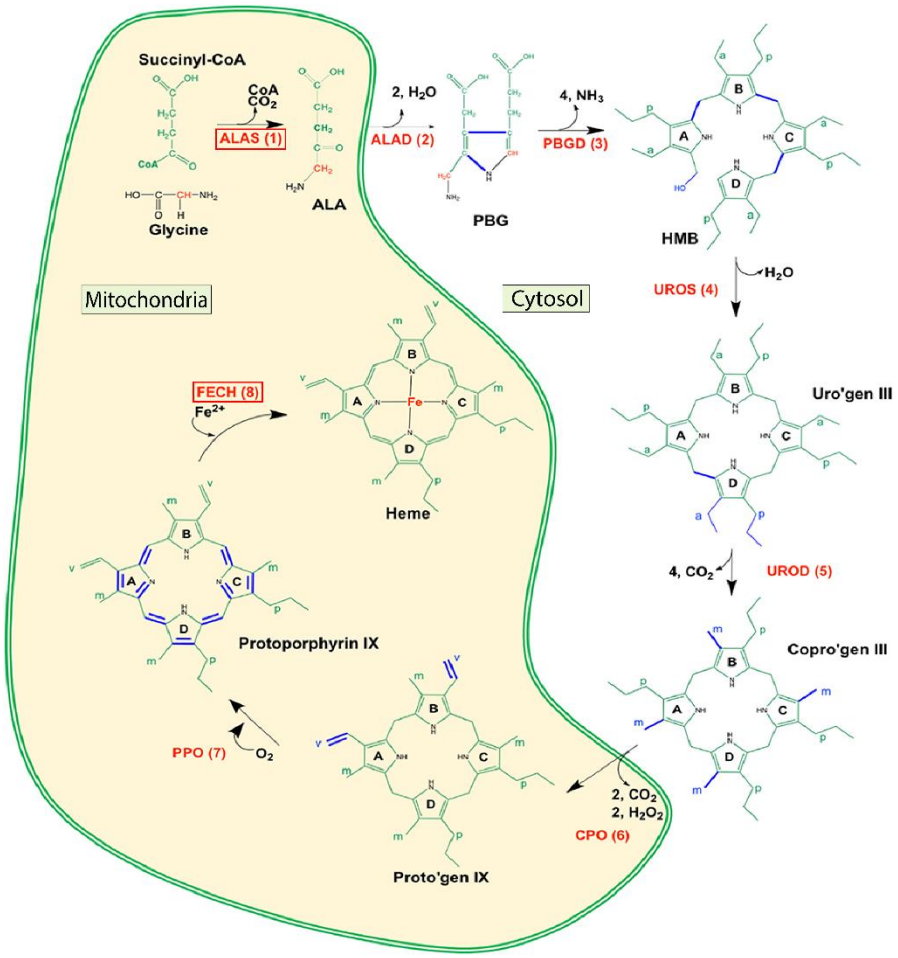

Figure 1.3: Heme biosynthesis. The eight steps in heme biosynthesis are labeled in red; ALAS, d-aminolevulinic acid synthase; ALAD, aminolevulinic acid dehydratase; PBGD, porphobilinogen deaminase; UROS, uroporphyrinogen III synthase; UROD, uroporphyrinogen decarboxylase; CPO, coproporphyrinogen oxidase; PPO, protoporphyrinogen oxidase; FECH, ferrochelatase. The bonds that change between substrates are colored blue. The number after the enzyme name indicates the enzymatic step. Substrates and enzymes within the yellow shading with double green line are located within the mitochondria. Enzymes which mutations produce human diseases are marked with a red box. Picture modified from (Phillips, 2019).

Iron-sulfur clusters are prosthetic groups with diverse and important functions involved in redox reactions. The synthesis pathway for Fe/S clusters is well known in prokaryotic and in yeasts leading to the description of more than 20 essential molecules that later were identified and studied in eukaryotes (Lill & Mühlenhoff, 2008). The process can be divided in two phases: the transiently assemble of Fe/S cluster on a proteic scaffold called ISCU (Agar et al., 2000). During this phase, the sulfur comes from the L-cysteine amino acid when it is desulfurated by the cysteine desulfurase complex NFS1-ISD11 (Gerber, Mühlenhoff, & Lill, 2003) and frataxin (FXN) is proposed as an iron-donor (Bulteau et al., 2004). The second phase consists in the transfer of the Fe/S cluster to

the acceptor apoproteins. The exact mechanism of Fe/S assembly is not yet fully understood, but the process is facilitated by “chaperone” molecules as HSPA9 and HSC20 (Maio & Rouault, 2015). Figure 1.4 summarizes Fe/S synthetic pathway. A cytoplasmic iron–sulfur protein assembly machinery (CIA) also exists (Balk, Pierik, Netz, Mühlenhoff, & Lill, 2004), but CIA requires an intermediate to assemble the Fe/S structure that is produced by the mitochondrial machinery (Pandey, Pain, Dancis, & Pain, 2019). It has been hypothesized that the mitochondrion provides via the ABC transporter ABCB7 cytosol a "X" substance essential for Fe/S cluster protein maturation (Kispal, Csere, Guiard, & Lill, 1997). Mutations in Fe/S biogenesis genes lead to impairment of Fe/S containing proteins and also to a cellular iron homeostasis deregulation (Richardson et al., 2010). Importantly, iron regulatory protein 1 (IRP1) is an Fe/S containing protein (see section 1.4). Therefore, mutations in the Fe/S machinery proteins are associated with hematological and neurodegenerative human diseases for example Friedreich Ataxia, a disease caused by mutations in the *FXN* gene.

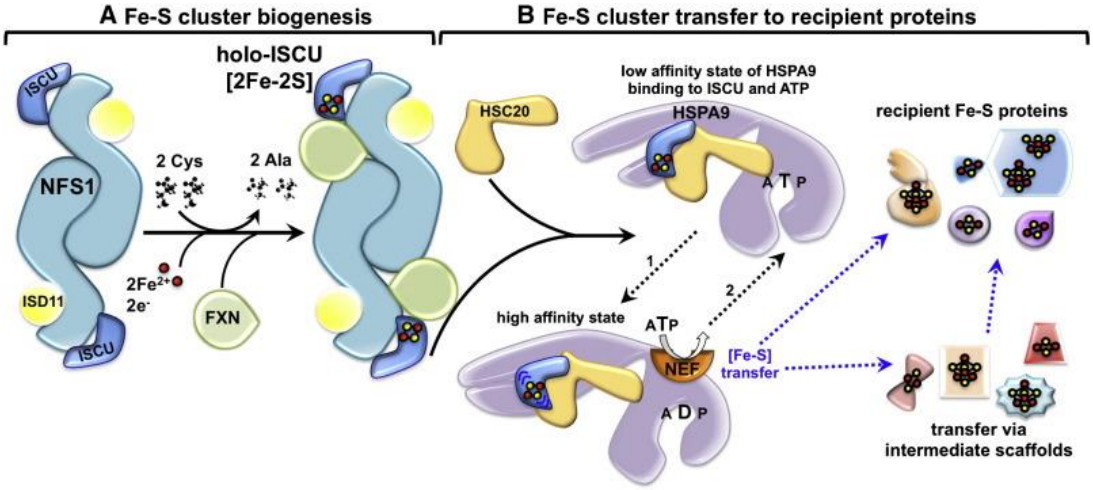

Figure 1.4: Fe/S cluster biogenesis in mammalian cells. (A) Assembly of a nascent Fe–S cluster upon the scaffold protein ISCU. A cysteine desulfurase complex NFS1-ISD11 forms a dimer to which monomers of the primary scaffold ISCU bind at either end. ISD11 is a structural component of the core complex in eukaryotes, required for the activity of NFS1. Frataxin (FXN) is part of the core complex, potentially binding in a pocket-like region between NFS1 and ISCU. The cluster assembles upon ISCU when iron is provided together with the reducing equivalents that allow achievement of the final electronic configuration of the cluster. **(B)** Cluster transfer to recipient apoproteins. A dedicated chaperone/cochaperone (HSPA9/HSC20) system facilitates cluster transfer from the primary scaffold ISCU to recipient apoproteins or to intermediate carriers. A nucleotide exchange factor (NEF) exchanges ADP with ATP and completes the ATPase cycle of the chaperone. Picture from Maio & Rouault, 2015.

1.3.3. Cellular iron storage:

The iron not used for heme or Fe/S cluster synthesis must be exported, using FPN, or stored in a redox-inactive form inside cells (i.e. inside the ferritins) to avoid the ROS production associated with free iron. Ferritins are heteropolymers made of 24 subunits of heavy (FTH) and light (FTL) chains forming a spherical shell surrounding a cavity capable of accommodating up to 4500 atoms of iron as ferric oxohydroxide (Wang, W., Knovich, Coffman, Torti, & Torti, 2010). Ferritins L and H have a conserved 3D structure and are ubiquitously expressed, but their ratio is tissue specific. For instance, H-ferritin is predominant in heart and brain, while L-ferritin is predominant in liver and spleen. Ferritins H and L have different functions; FTH carries on the ferroxidase activity, converting ferrous iron in ferric iron, while FTL provides a nucleation center to iron deposition. It has been proposed that PCBP1 [poly-r(C)-binding protein-1] is the molecule which chaperones iron to FTH for being oxidized (Leidgens et al., 2013). If cells require iron, it can be released from ferritin. Although the exact release mechanism is not clear yet, it involves the lysosomal pathway (Bradley, Le Brun, & Moore, 2016; Kidane, Sauble, & Linder, 2006). A mitochondrial ferritin isoform (FTMT) also exists, that produces homopolymers similar to ferritin heavy chain (Arosio, P. & Levi, 2010). However, this isoform have a tissue restricted expression in testis and the erythroid progenitors of patients with sideroblastic anemia (Santambrogio et al., 2007).

A glycosilated form of FTL is secreted into the body fluids: serum, cerebrospinal and synovial fluids. Serum ferritin provides clinical information about the total amount of iron stored in the body and it is used to diagnose iron-related diseases (Arosio, P., Ingrassia, & Cavadini, 2009). Low levels of serum ferritin indicate iron deficiency (Lopez, Cacoub, Macdougall, & Peyrin-Biroulet, 2016). However, high levels of serum ferritin may indicate an inflammatory condition as ferritin is an acute phase protein (Gulhar, Ashraf, & Jialal, 2021; Kernan & Carcillo, 2017) or an iron overload condition (Cullis, Fitzsimons, Griffiths, Tsochatzis, & Thomas, 2018).

Mutations in ferritin genes produce different diseases depending on its location. Mutations on *FTL* gene can produce: hereditary hyperferritinemia with cataract syndrome (HHCS) (OMIM#600886) produced by mutations in the 5' IRE region (see section 1.6.2.1), neuroferritinopathy (OMIM#606159) mostly produced by mutations in the C-terminal gene region, benign hyperferritinemia (or hyperferritinemia without iron overload) (OMIM#600886) due to mutations in the N-terminal gene region, autosomal dominant L-ferritin deficiency and autosomal recessive L-ferritin deficiency (OMIM#615604) produced by mutations in the coding region of *FTL* gene (Cadenas et al., 2019). On the other hand, a mutation in the 5' UTR (untranslated region) of *FTH1* mRNA causes an iron overload syndrome (OMIM #615517). Moreover, *FTH* gene is essential for life as the knockdown of *Fth* gene in mice is embryonic lethal (Ferreira et al., 2000).

1.3.4. Cellular iron export:

Iron export is a way to eliminate the excess of cellular iron that is not needed in the cell. This function is important in different cells as enterocytes or macrophages to maintain a non-toxic level of iron and to supply for iron to cells that have an increased need of it. Ferroportin (FPN) is the only known iron export transporter in vertebrates. The

disruption of the ferroportin gene (*Slc40a1*) in mice is embryonic lethal because of an impaired transfer of maternal iron to the embryos through the extraembryonic visceral endoderm (Donovan et al., 2005). Selective ferroportin inactivation in mouse embryos, in sites different from extraembryonic visceral endoderm and placenta, results in viable pups presenting with severe anemia and iron accumulation in enterocytes, macrophages, and hepatocytes; this fact remarks the important role of ferroportin in those cell types (Donovan et al., 2005). FPN exports ferrous iron (Fe^{2+}), so it acts coordinated with a cooper-dependent ferroxidase (that converts ferrous iron (Fe^{2+}) into ferric iron (Fe^{3+})) that can be ceruloplasmin (CP), expressed in all cell types, or hephaestin that it is specifically expressed in enterocytes (De Domenico et al., 2007). Besides elemental iron, cells may also export iron bound to ferritin, through a not yet fully known mechanism (Leimberg, Prus, Konijn, & Fibach, 2008) as well as heme. Feline leukemia virus subgroup receptor 1 (FLVCR1) facilitates heme export in differentiating erythroblasts, macrophages and liver hepatocytes (Keel et al., 2008); by this way, erythropoietic cells maintain a correct cellular heme levels, as excess of heme is toxic. Constitutive and total *Flvcr1* knockout mice are embryonic lethal, while the deletion of *Flvcr1* gene at birth in mice causes a severe macrocytic anemia associated with an early erythropoietic blockage (Keel et al., 2008).

1.4.Regulation of iron homeostasis: IRP/IRE network

As we described above, several mechanisms to control cellular iron uptake, storage, utilization and export exist. This regulation is coordinated by iron-sensitive post transcriptional regulatory machinery composed by the iron regulatory proteins (IRPs) and the iron responsive elements (IREs). IREs are *cis*-regulatory motifs located in the 5' and 3' untranslated regions (UTRs) of target mRNAs involved in iron homeostasis (Anderson, C. P., Shen, Eisenstein, & Leibold, 2012).

1.4.1. Iron Regulatory Proteins (IRPs):

Two iron regulatory proteins exist in mammals: IRP1, encoded by *ACO1* gene, and IRP2, encoded by *IREB2* gene. They are homologous genes that belong to the aconitases family which participates in the tricarboxylic acid (TCA) cycle. It also exists a mitochondrial aconitase enzyme gene (*ACO2*) which could be the origin of IRP1 through genetic divergence, followed by a duplication that produced the *IREB2* gene. Aconitases are enzymes that have a 4Fe-4S cluster in their catalytic site and isomerise citrate to isocitrate. Both, IRP1 and IRP2 are expressed ubiquitously, but IRP1 is more abundant in kidney, brown fat and liver than IRP2 which is more abundant than IRP1 in brain, intestine, and spleen (Meyron-Holtz et al., 2004). IRP1 is a cytosolic aconitase with 30% amino acid sequence identity (100% in the catalytic core) to mitochondrial aconitase (ACO2), however, the Fe/S cluster of IRP1 is easily lost upon iron depletion (Rouault et al., 1992). Crystal structure of IRP1 shows that it is very similar to the one of ACO2 structure. IRP1 have four globular domains with a catalytic site at the interface between domains 1-3 and 4 where the 4Fe-4S cluster is accommodated coordinated by cysteine residues (Dupuy et al., 2006). Disassembly of the Fe/S cluster upon iron depletion induces a switch to an open conformation that allows interaction with the IRE (Walden et al., 2006). In IRP1 both aconitase and RNA binding activity are mutually

exclusive and the switch between IRP1 catalytic center conformations is reversible, so IRP1 is a bifunctional protein (Rouault et al., 1992).

On the other hand, IRP2 contains an additional 73 amino acids at the N-terminus compared to IRP1; the role of this domain is unknown, although it was initially thought to be involved in iron-dependent degradation of IRP2 when the cell is iron replete (Iwai, Klausner, & Rouault, 1995; Kühn, 2015). Contrary to IRP1, IRP2 does not have aconitase activity and it does not assemble an Fe/S cluster (Guo, Yu, & Leibold, 1994). Unlike IRP1, IRP2 structure has not yet been crystallographically resolved but has been predicted upon IRP1 structure (Zumbrennen, Wallander, Romney, & Leibold, 2009).

1.4.2. Iron Responsive Elements (IREs):

IRE is a conserved RNA element of 25-30 nucleotides that conforms a hairpin structure. These RNA motifs are evolutionarily conserved and they can be located in the 3' or 5' UTRs of mRNAs. A canonical IRE structure is composed of a 6-nucleotide apical loop 5'-CAGYGX-3', where Y denotes C or U and X denotes A, C or U, on a stem of five paired nucleotides, a small asymmetrical bulge with an unpaired cytosine on the 5' strand of the stem, and an additional lower stem of variable length (Wilkinson & Pantopoulos, 2014) as described in the Figure 1.5. The apical loop sequence "AGY" forms a pseudo-triloop through the first C and fifth G union which stabilizes the IRE structure. This pseudo-triloop and the C bulge are very important for the interaction with the IRPs (Addess, Basilion, Klausner, Rouault, & Pardi, 1997; Walden et al., 2006). IREs are present in the mRNAs of genes that encode proteins involved in iron metabolism: iron uptake (TFR1, DMT1), iron storage (FTH, FTL), heme synthesis (ALAS2), energy metabolism (ACO2, *Drosophila* succinate dehydrogenase, Sdh), oxygen sensing (hypoxia inducible factor-2 alpha (HIF2α), gene EPAS1), and iron export (FPN) (Muckenthaler, Galy, & Hentze, 2008; Sanchez, Galy, Muckenthaler, & Hentze, 2007) (Figure 1.6).

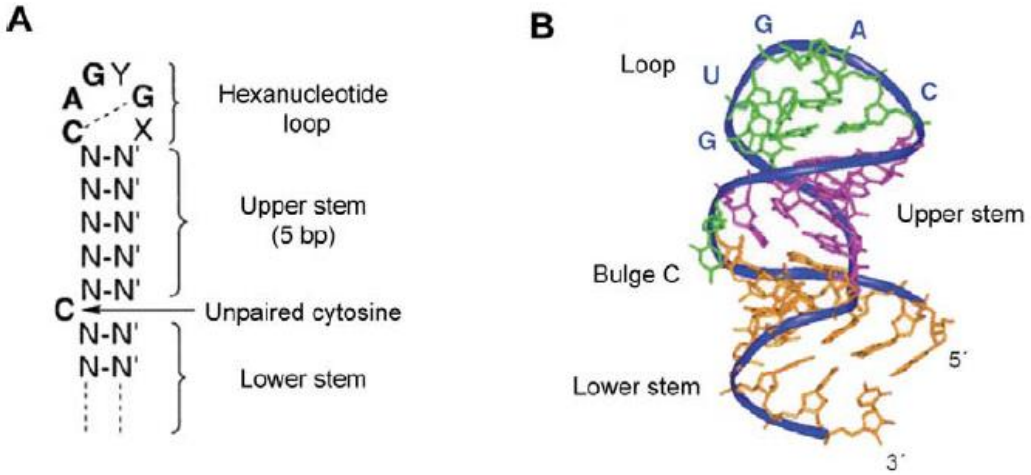

Figure 1.5: IRE conformation. (A) The schematic IRE construction. 6 hexanucleotide loop contain conserved CAGYGX sequence (Y means C or U and X means C, A or U). The upper stem seems to work as a molecular ruler to orient the C bulge and the loop for optimal interaction with the IRPs. **(B)** The nuclear magnetic resonance structure of the consensus IRE is depicted (Addess et al., 1997). Picture from (Zhang, Deliang, Meyron-Holtz, & Rouault, 2007).

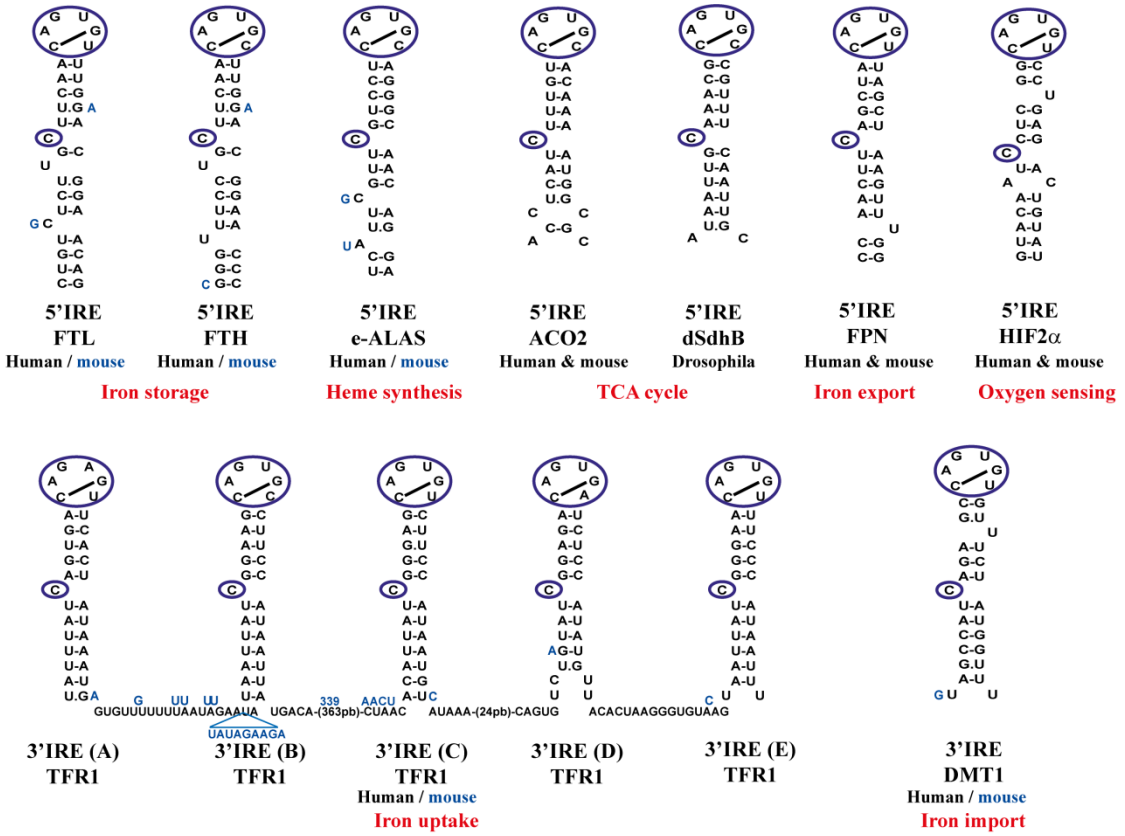

Figure 1.6: Functional IREs. Classical and well-recognized IREs are represented in the picture. All motifs present a C-bulge on the 5' strand of the stem and an apical loop composed by six nucleotides (5'-CAGYGX-3') (blue circles). In the top part of the picture there are the mRNAs carrying IREs in the 5' UTR and the 3' UTR IREs are in the bottom part. TFR1 have 5 IREs named from A to E. Nucleotides in blue indicate sequence differences among human and mouse IREs. The function of the encoded protein is in red. FTL: L-ferritin; FTH: H-ferritin; ALAS2: erythroid-specific delta aminolevulinate synthase; dSdhB: Drosophila succinate dehydrogenase B; FPN: ferroportin; HIF2α: hypoxia inducible factor-2 alpha; TFR1: transferrin receptor 1; DMT1: divalent metal ion transporter 1. Picture from Joshi et al. 2012.

1.4.3. Post-transcriptional regulation of IRP-target mRNAs:

IRPs and IREs work together to regulate the expression of iron metabolism genes. Their interaction is promoted by iron deficiency conditions and abolished in iron-replete cells by different mechanisms (explained in 1.4.4. section). As we see above, IREs can be located in the 3' or 5' UTRs. Depending on the location of the IREs in the target mRNA, the binding of the IRPs differentially regulates its expression. When cellular iron is low, the IRE present in the 3' UTR binds to the IRP, stabilizing the mRNA, and this interaction protects it front endonuclease degradation increasing its translation, this is the case of transferrin receptor 1 (*TFRC*) mRNA (Casey, Koeller, Ramin, Klausner, & Harford, 1989). In contrast, in mRNAs with a 5' UTR IRE, the IRP binding represses mRNA translation avoiding the association of the small ribosomal subunit to the mRNA, as in the case of ferroportin or ferritins mRNAs (Muckenthaler, M., Gray, & Hentze, 1998). Figure 1.7 summarizes this regulation.

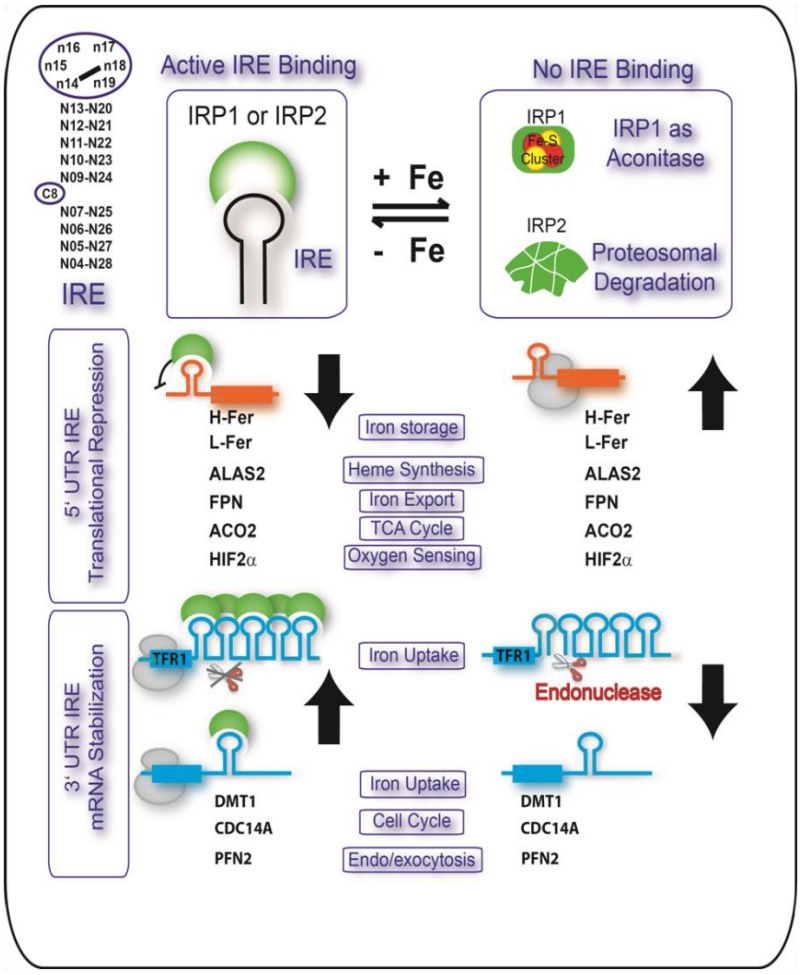

Figure 1.7: A summary of the IRP - IRE interaction. On top, from left to right, we could see an IRE structure and the interaction between IRPs and IREs, which is modulated by cellular iron concentration. On the bottom, we see first IREs located in the 5' UTR. When IRP binds to IRE, the mRNA translation is repressed. Several genes are showed. Below, we see IREs located in the 3' UTR. In this case, the interaction with the IRP stabilized the mRNAs and promotes its translation. The list of genes is showed. Figure courtesy of Dr. Mayka Sanchez.

1.4.4. Regulation of IRPs:

To maintain correct iron levels, IRP activity must be coordinated with cellular iron levels. As mentioned above, IRP1 has two mutually exclusive functions: cytosolic aconitase or as RNA binding protein that regulates the expression of proteins involved in iron metabolism. This is possible due to its reversible Fe/S cluster switch, which at the same time correlates with cellular iron status and Fe/S biogenesis. Nevertheless, the exact mechanism by which iron deficiency triggers the loss of the cluster is not fully understood. *In vitro* studies revealed that aconitase activity is disrupted when IRP1 loses the forth labile iron of the cluster (4Fe/4S → 3Fe/4S), but this is insufficient to acquire RNA binding activity; showing that it is necessary an additional alteration in the protein complex (Haile et al., 1992). Low cellular iron is the signal through which

cytosolic aconitase becomes an iron regulatory protein, although reactive oxygen species (ROS) and reactive nitrogen species (RNS) also promote the loss of the fourth iron of the cluster and activate IRP1 activity (Castro, Tórtora, Mansilla, & Radi, 2019). Contradictorily, other studies claim that IRP1 binding activation is not a direct oxidative effect on IRP1; rather, its activation may involve other signaling pathways related with calcium signaling, mitogen-activated protein kinase cascades, tyrosine phosphorylation, regulation of phosphatases and phospholipases, or activation of transcription factors (Caltagirone, Weiss, & Pantopoulos, 2001; Torres & Forman, 2000).

Despite the contradictions in the literature, the “Fe/S switch” is widely accepted as the mechanism controlling IRP1 activity, supported by the observation that the total levels of c-aconitase/IRP1 protein do not vary in response to iron changes (Haile et al., 1992). Under physiological conditions, IRP1 exists predominantly in the cytosolic aconitase form (Meyron-Holtz et al., 2004). Besides, the c-aconitase pool can be up to 100-fold more abundant than the IRE-binding form of IRP1 and even severe iron deficiency increases IRE-binding IRP1 pool no more than 4-folds, showing that a small fraction of cytosolic aconitase is recruited for acting as RNA binding protein (Chen, Schalinske, & Eisenstein, 1997). Moreover, different *in vitro* and *in vivo* studies, using an IRP1 that has not the capability to assemble Fe/S cluster, showed an iron-mediated IRP1 degradation (Clarke et al., 2006; Sheftel, Stehling, & Lill, 2010). This could suggest that IRP1 degradation may be a mechanism to prevent excessive RNA binding activity when the “Fe/S switch” is not effective.

By contrast, IRP2 is regulated and degraded by F-box and leucine-rich repeat protein 5 (FBXL5), a part of the E3 ubiquitin-ligase complex, which contains an iron-sensitive hemerythrin like domain. Hence, in iron or oxygen deficiency, the centre of the hemerythrin domain is destabilized, leading to FBXL5 degradation and subsequently IRP2 stabilization. On the other hand, when iron or oxygen are in excess, the hemerythrin domain is stable and FBXL5 is allowed to interact with IRP2 and target it for proteasomal degradation (Moroishi, Nishiyama, Takeda, Iwai, & Nakayama, 2011; Salahudeen et al., 2009; Vashisht et al., 2009). In addition, FBXL5 interacts with the IRE-binding state of IRP1 and also targets it to proteasomal degradation. This mechanism may be a way to insurance to avoid excessive activation of IRP1-IRE binding in conditions when the Fe/S cluster biogenesis is impaired (Johnson, Deck, Nizzi, & Eisenstein, 2017).

1.5.The IRP/IRE regulatory system in physiology

The IRP/IRE regulatory system has been extensively studied. The generation and characterization of mouse models with constitutive and tissue-specific *Irp1* and *Irp2* gene ablation (Table 1.1) has provided a substantial amount of information about the implication of the IRP/IRE system in physiological processes. The most important physiological events where IRPs are involved are duodenal iron absorption, erythropoiesis and liver iron storage.

Table 1.1: Phenotypic features of mouse models with global or tissue-specific *Irp1* and/or *Irp2* genetic ablation/activation. Modified from Wilkinson et. al. 2014.

Mouse model	Site of modification	Reference	Phenotype	Phenotype references
Irp1 -/-	Global	(Meyron-Holtz *et al.* 2004, Galy *et al.* 2005)	Polycythemia, stress erythropoiesis, splenomegaly and increased expression of erythropoietin	(Anderson *et al.* 2013, Ghosh *et al.* 2013, Wilkinson and Pantopoulos 2013)
			Pulmonary hypertension, cardiac hypertrophy and fibrosis. Mice succumb to hemorrhages when fed with iron-deficient diet	(Ghosh *et al.* 2013, Wilkinson and Pantopoulos 2013)
			Increased expression of Dmt1, Fpn1 and DcytB mRNAs in the duodenum	(Anderson *et al.* 2013)
			Misregulation of ferritin and Tfr1 expression in the kidney and brown fat	(Meyron-Holtz *et al.* 2004)
			Efficient inflammatory signaling response to tupertine	(Viatte *et al.* 2009)
			Increased ferroportin expression in splenic macrophages and decreased hepcidin mRNA levels in the liver	(Wilkinson and Pantopoulos 2013)
Irp2-/-	Global	(LaVaute *et al.* 2001, Galy *et al.* 2005, Zumbrennen-Bullough *et al.* 2014)	Microcytic hypochromic anemia with mild duodenal and hepatic iron overload and splenic iron deficiency	(Cooperman *et al.* 2005, Galy *et al.* 2005)
			Reduced Tfr1 expression in erythroid precursors	(Cooperman *et al.* 2005, Galy *et al.* 2005)
			High levels of protoporphyrin IX in erythroid precursors	(Cooperman *et al.* 2005)
			Increased ferritin levels in all tissue	(Cooperman *et al.* 2005)
			Iron overload in neurons and progressive neurodegeneration	(LaVaute *et al.* 2001)
			Efficient inflammatory signaling response to tupertine	(Viatte *et al.* 2009)
			Lower motor neuronal degeneration with spinal cord axonopathy	(Jeong *et al.* 2011)
			Mild neurological and behavioral defects, as well as nociception	(Zumbrennen-Bullough *et al.* 2014)
			Minor performance deficits in specific neurologic tests (coordination, balance)	(Galy *et al.* 2006)
Irp2-/-	Liver-specific	(Ferring-Appel *et al.* 2009)	Mild hepatic iron overload	(Ferring-Appel *et al.* 2009)
Irp2-/-	Intestinal-specific	(Ferring-Appel *et al.* 2009)	Mild duodenal iron overload	(Ferring-Appel *et al.* 2009)
Irp2-/-	Macrophage-specific	(Ferring-Appel *et al.* 2009)	No pathology	(Ferring-Appel *et al.* 2009)
Irp1-/- Irp2-/-	Global	(Smith *et al.* 2006)	Embryonic lethality at the blastocyst stage	(Smith *et al.* 2006)
Irp1+/- Irp2-/-	Global	(Smith *et al.* 2004)	More severe presentation of neuronal pathology than the *Irp2-/-* mice	(Smith *et al.* 2004)
			Neuronal pathology partially rescued by the pharmacological activation of Irp1	(Ghosh *et al.* 2008)
Irp1-/- Irp2-/-	Liver-specific	(Galy *et al.* 2010)	Lethality within 1-2 weeks after birth due to liver failure. Mitochondrial dysfunction	(Galy *et al.* 2010)
Irp1-/- Irp2-/-	Intestinal-specific	(Galy *et al.* 2008)	Growth retardation, early death (within 30 days) due to dehydration. Increased expression of ferritin and ferroportin and decreased expression of Tfr1 and Dmt1	(Galy *et al.* 2008)
Irp1-/- Irp2-/-	Adult ligand-induced intestinal specific	(Galy *et al.* 2013)	Increased expression of ferritin leading to "mucosal block", in spite of increased expression of ferroportin and Dmt1	(Galy *et al.* 2013)
Irp1 gain-of-function due to expression of a constitutive active Irp1 transgene	Global	(Casarrubea *et al.* 2013)	Macrocytic erythropenia due to impaired erythroid differentiation	(Casarrubea *et al.* 2013)
Irp2 gain-of-function due to disruption of *Fbxl5*	Global	(Moroishi *et al.* 2011, Ruiz *et al.* 2013)	Embryonic lethality. Lethality was prevented by simultaneous ablation of *Irp2*	(Moroishi *et al.* 2011, Ruiz *et al.* 2013)
Irp2 gain-of-function due to disruption of *Fbxl5*	Liver-specific	(Moroishi *et al.* 2011)	Hepatic iron overload, steatohepatitis and low hepcidin mRNA levels. Mice succumb to liver failure when fed with high-iron diet	(Moroishi *et al.* 2011)

1.5.1. Mouse models with IRP1 and/or IRP2 deficiency:

Irp1 and *Irp2* gene inactivation (double knockout) in mice leads to embryonic lethality at the blastocyst stage, suggesting that the IRP/IRE system plays an important role in early stages of development (Smith, Ghosh, Ollivierre-Wilson, Hang Tong, & Rouault, 2006). On the contrary, mice that have a single deletion of *Aco1* or *Ireb2* genes are viable. This remarks the functional redundancy of the two IRPs (Galy, Ferring, & Hentze, 2005a; LaVaute et al., 2001; Meyron-Holtz et al., 2004; Zumbrennen-Bullough et al., 2014). However, single *Irp1*-/- or *Irp2*-/- mice display different phenotypes likely due to different subsets of target genes or tissue-specific roles. Initially, *Irp1*-/- mice were described to lack any overt phenotype under standard laboratory conditions apart from mild ferritin and Tfr1 dysregulation in kidneys and brown fat, where *Irp1* expression is higher (Galy et al., 2005a; Meyron-Holtz et al., 2004). Nowadays, different groups have reported that *Irp1*-/- mice develop polycythemia, alterations of iron metabolism together with pulmonary hypertension and cardiac hypertrophy (Anderson, S. A., Nizzi, Chang, Deck, Schmidt, Galy, Damnernsawad, Broman, Kendziorski, Hentze, Fleming, Zhang, & Eisenstein, 2013a; Ghosh et al., 2013; Wilkinson & Pantopoulos, 2013). The polycythemic phenotype is related to the inability of *Irp1* to bind and regulate Hif2α mRNA IRE and to inhibit its translation, causing a translational de-repression of this protein which leads to increased erythropoietin (EPO) expression causing reticulocytosis, polycythemia, and suppression of hepatic hepcidin mRNA (Ghosh et al., 2013; Zimmer et al., 2008). In addition, if *Irp1*-/- knockout mice are treated with an iron-deficient diet, they die due to hemorrhages (Ghosh et al., 2013). But, if mice have a normal diet, polycythemia is corrected after the 10^{th} week of age explaining why *Irp1*-/- polycythemic phenotype was not recognized in the past (Wilkinson & Pantopoulos, 2013).

Three independent groups have generated different mice *Irp2*-/- strains: (Galy et al., 2005a; LaVaute et al., 2001; Zumbrennen-Bullough et al., 2014). All *Irp2*-/- knockout mouse strains present elevated iron levels in the duodenum and liver together with increased ferritin and decreased Tfr1 expression, but the iron content is reduced in the spleen with reduced ferritin expression. These physiological conditions cause the mice to develop microcytic hypochromic anemia and erythropoietic protoporphyria associated with altered body iron distribution (Cooperman et al., 2005; Galy et al., 2005b). In addition, it has been reported that an *Irp2*-/- mouse strain generated by LaVaute *et. al.* displays a lower motor neuronal degeneration and spinal cord axonopathy; the outcome of this phenotype is worse and more severe in *Irp1*+/- *Irp2*-/- mice (Jeong et al., 2011; Smith et al., 2004). Moreover, *Irp2*-/- mouse strains generated by LaVaute *et al.* develop late-onset neurodegeneration and iron overload in the white matter areas of the brain (LaVaute et al., 2001). Interestingly, a drug that converts c-aconitase to Irp1 RNA-binding form, called Tempol, restore iron homeostasis by stabilizing Tfr1 mRNA and repressing ferritin synthesis. Hence, this drug is able to mitigate the neuronal defects of both *Irp2*-/- and *Irp1*+/- *Irp2*-/- mice (Ghosh et al., 2008). Controversially, the *Irp2*-/- mouse strain generated by Galy *et. al.* who used a different knockout strategy, does not display signs of neurodegeneration, brain iron deposits or mitochondriopathy, and only presents minor motor coordination and balance defects. Zumbrennen-Bullough *et al.* have generated the third *Irp2*-/- mouse

strain that confirms the erythropoietic abnormalities (Zumbrennen-Bullough et al., 2014). Despite of the iron deposition in brain white matter and in oligodendrocytes, this mouse strain does not develop signs of neurodegeneration and just presents a mild impairment in locomotion, exploration, motor coordination/balance and nociception. The different phenotype showed by the three *Irp2*-/- mouse strains could be due to environmental issues, genetic background, the different gene ablation strategies or a combination of them.

Mouse strains with tissue-specific *Irp1* and *Irp2* deletion has been generated to overcome the embryonic lethality of double IRPs deficiency *in vivo* and to study its effects in adult mice. The different mouse models described so far with global or tissue-specific *Irp1* and/or *Irp2* genetic ablation or activation are detailed in Table 1.1 (adapted from Wilkinson *et al.* 2014). These *in vivo* models (explained in the next sections) have increased our understanding of the role of the IRP/IRE system in key tissues involved in systemic iron metabolism.

1.5.2. The IRP/IRE regulatory system in dietary iron absorption:

Our organism lacks any active mechanism to excrete iron, and iron losses are due to bleeding or desquamation of epithelial surfaces (Green et al., 1968). Hence, to regulate total iron content in our body duodenal iron absorption is subject to exhaustive control through transcriptional, post-transcriptional and post-translational mechanisms. Several key molecules in dietary iron absorption are post-transcriptionally controlled by IRP/IRE regulatory system, as seeing in Figure 1.8.

Two main forms of iron are taken up by duodenal enterocytes: heme and inorganic iron. Nowadays, inorganic iron absorption is better understood than heme duodenal absorption as it is yet not clear what protein acts as the main duodenal heme transporter. High iron concentration, either serum or hepatic, induces hepcidin secretion. Hepcidin binds to FPN inducing its internalization and subsequent proteasomal degradation (Nemeth et al., 2004; Vogt et al., 2021). In addition, hepcidin induces intestinal ubiquitin-dependent proteasome degradation of DMT1, avoiding systemic inorganic iron absorption (Brasse–Lagnel et al., 2011). In iron deficient enterocytes, HIF2α activates the transcription of DMT1 and FPN to provide iron to the plasma (Mastrogiannaki et al., 2009; Shah, Matsubara, Ito, Yim, & Gonzalez, 2009; Taylor et al., 2011). HIF2α and FPN present IREs in their 5' UTR while DMT1 presents an IRE in its 3' UTR. Thus, they are direct targets of the IRP/IRE regulatory system (see section 1.4.2.). Interestingly, both DMT1 (Hubert & Hentze, 2002) and FPN (Zhang, De-Liang, Hughes, Ollivierre-Wilson, Ghosh, & Rouault, 2009) include mRNA isoforms lacking the IRE sequence, that instead can therefore escape IRP regulation. There is evidence that in duodenum, Dmt1 IRE-containing isoforms are the predominant compared to the non-IRE isoforms perhaps to ensure a minimum iron absorption (Galy et al., 2013). Overall, the duodenal iron absorption is doubly regulated by the IRP/IRE system, directly by IRE-binding and indirectly through modification of HIF2α expression.

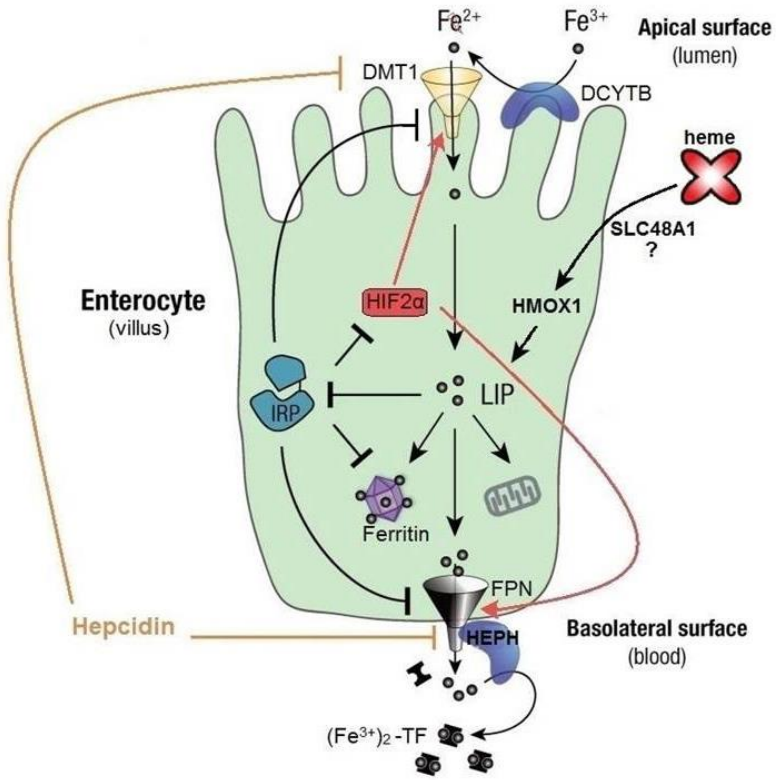

Figure 1.8: The IRP/IRE regulatory system in dietary iron absorption. In a diet rich in meat, heme accounts for two-thirds of dietary iron supply; heme is transported by the putative heme-carrier SLC48A1 and then degraded by the action of heme oxygenase to release iron. Transport of inorganic iron requires iron to be converted to its reduced form (Fe^{2+}) either by a reducing agent in the lumen of the gut or by the reductase DCYTB. Iron is then transported across the membrane by the DMT1 transporter. Cytoplasmic iron is therefore exported into the bloodstream via the basolateral transporter ferroportin in conjunction with the ferroxidase hephaestin and loaded onto apo-transferrin. Duodenal enterocytes also express ferritin, which limits excessive iron transfer to the circulation (Vanoaica et al. 2010) while TFR1 expression is limited to the precursor cells in the crypts that cannot uptake dietary iron (Waheed et al., 1999). DMT1: divalent metal ion transporter; DCYTB: duodenal cytochrome B; SLC48A1: solute carrier family 48, member 1; HMOX1: heme oxygenase 1; HIF2α: hypoxia inducible factor-2 alpha; IRP: iron regulatory protein; LIP: labile iron pool; FPN: ferroportin; HEPH: hephaestin. Picture modified from Muckenthaler et al. 2008.

Total or tissue-specific deletion of *Irp1* and/or *Irp2* affects the normal duodenal iron absorption. The different phenotypic characterization of Irps mouse models are described in Table 1.1. *Irp1*-/- mice have high level of duodenal Dmt1 and ferroportin, probably due to the derepression of Hif2α by the lack of Irp1 and the subsequent transcriptional activation of Fpn and Dmt1 by Hif2α (Anderson, S. A. et al., 2013a). *Irp2*-/- and intestinal-specific *Irp2*-/- mice present mild duodenal iron overload, with increased ferritin levels but no altered ferroportin or Dmt1 expression (Ferring-Appel, Hentze, & Galy, 2009; Galy et al., 2005b). These data suggest that Irp1 is the main regulator of Dmt1 and ferroportin in the duodenum.

Mice with intestinal-specific inactivation of both Irp1 and Irp2 die shortly after birth due to malabsorption and dehydration. These mice also presented mitochondriopathy and alterations in intestinal structure, showing the importance of the IRPs for intestine function and survival (Galy, Ferring-Appel, Kaden, Gröne, & Hentze, 2008). Moreover, mice display reduced Dmt1 and Tfr1 expression and increased ferritin and ferroportin levels, in agreement with IRP absence. Interestingly, blood parameters revealed no signs of systemic iron deficiency; this could be explained due to a compensation caused by the high expression levels of ferroportin that pumps iron to plasma. At the same time, enterocytes limit Tfr1 expression to avoid iron uptake from the bloodstream (Waheed et al., 1999).

Galy *et. al.* also generated a mouse strain with duodenal-specific tamoxifen-inducible Irp1 and Irp2 ablation conducted at adult age (Galy et al., 2013). These mice have normal intestine structure, but present reduced Tfr1 expression, overexpression of ferritins and Fpn and an unexpected upregulation of Dmt1. This observation differs from what was observed in pups with constitutive intestinal-specific Irp1 and Irp2 ablation (Galy et al., 2008), suggesting that the IRP system might regulate Dmt1 expression in young mice but not in adult life. Despite of Dmt1 upregulation, duodenal-specific tamoxifen-inducible Irp1 and Irp2 KO mice showed iron absorption impairment. This phenotype is known as “mucosal block” and it is due to the effect of ferritin upregulation, which chelates iron and impedes the delivery to the bloodstream as pointed by other independent studies that show ferritin importance in iron absorption (Ferreira et al., 2000; Vanoaica, Darshan, Richman, Schümann, & Kühn, 2010). Nevertheless, mice clinical chemistry parameters remain within the nonpathological range, with only a slight decrease of plasma iron concentration (Galy et al., 2013).

1.5.3. The IRP/IRE regulatory system in hepatic function:

The liver has a key role in iron metabolism, as it is the main organ implicated in iron storage and mobilization. It also produces several molecules which have critical roles on the regulation of the systemic iron homeostasis. Liver produces relevant proteins in iron homeostasis including: transferrin, a serum iron transporter; ceruloplasmin, a ferroxidase; and hepcidin, the hormone responsible of the systemic regulation of iron (Graham, Chua, Herbison, Olynyk, & Trinder, 2007; Muckenthaler et al., 2008). Moreover, the liver expressed molecules HFE, HJV and TFR2 detect changes in body iron and adjust them by modifying hepcidin expression (D’Alessio, Hentze, & Muckenthaler, 2012).

Hepatocytes are in charge of intracellular iron storage via the ferritins. Sequestered iron can be mobilized by ferritin degradation via NCOA4 (Nuclear Receptor Coactivator 4). In iron-deficient cells, NCOA4 interacts with FTH and targets the ferritin complex for degradation in autolysosomes, a process called “ferritinophagy”. This process is conversely suppressed in iron-loaded cells due to increased NCOA4 turnover (Muckenthaler, Rivella, Hentze, & Galy, 2017). The impairment of iron storage or mobilization pathways leads to miss-regulation of iron homeostasis and, consequently, metabolic diseases. Iron overload is the main phenotype in disorders where there is a dysfunction of liver iron-related proteins.

Mutations affecting the IRP/IRE system in hepatocytes cause systemic iron disorders. Irp1 and Irp2 liver-specific knock out mice die 1 or 2 weeks after birth due to liver failure and mitochondrial dysfunction (Galy et al., 2010). These pups have reduced level of hepatic hepcidin and internal bleeding in the brain and intestines, profound liver damage and hepatic steatosis (abnormal lipid accumulation) and hepatocytes apoptosis. The hepatocytes of these mice show high expression of ferritin and ferroportin and diminished expression of transferrin receptor 1 and Dmt1, in agreement with a mechanism of IRP/IRE regulation. Consequently, hepatocytes show upregulation of iron storage and export whereas iron uptake is reduced producing iron deficiency in hepatic cells. Iron deficient hepatocytes present mitochondriopathy (swollen mitochondria with abnormal cristae structures). Mitochondria require high amounts of iron for synthesis of heme and Fe/S clusters, essential cofactors for the electron transport chain (ETC) and the TCA cycle. Hepatic failure in liver-specific Irp1 and Irp2 knockout mice is probably due to the defect of mitochondrial energy metabolism (Galy et al., 2010).

On the other hand, mice with global or liver specific single Irp2 ablation manifest hepatic iron overload and increased ferritin expression (Ferring-Appel et al., 2009; Galy et al., 2005).

Mouse model with liver-specific *Fbxl5* gene ablation highlights the importance of IRP/IRE system in the liver (Moroishi et al., 2011; Ruiz, Walker, Anderson, Eisenstein, & Bruick, 2013). Fbxl5 promotes Irp2 degradation, thus Fblx5 inactivation leads to an increase in Irp2 expression. *Fbxl5* liver-specific knockout mice are viable but their hepatocytes present mitochondriopathy, oxidative stress and steatosis. These mice also present high IRP activity and, consequently an increased iron uptake that produce hepatic iron overload. *Fbxl5* liver-specific knockout mice subjected to high iron diet develop acute liver failure and die within two weeks (Moroishi et al., 2011).

Global *Fbxl5* knockout mice are embryonic lethal as a consequence of iron overload and oxidative stress in embryos. Simultaneous depletion of both Fbxl5 and Irp2 restores mouse viability, but not with Irp1 (Moroishi et al., 2011).

All of these mouse models highlight the importance of the IRP/IRE regulatory system in maintaining a correct iron homeostasis both at the systemic and hepatic level.

1.5.4. The IRP/IRE regulatory system in erythropoiesis:

Erythropoiesis is the process by which red blood cells (RBCs) are produced. It occurs mainly in the bone marrow in adult humans and in the spleen in mice. It has been estimated that adult humans produce more than 2.5 $x10^6$ erythrocytes per second, whereas adult mice make approximately 7000 erythrocytes per second (Paulson, Ruan, Hao, & Chen, 2020). About 200 billion of RBCs are produced everyday requiring more than $2x10^{15}$ iron atoms (Li, Q. & Kang, 2017). Hence, most iron in body is used in erythropoiesis (Wilkinson & Pantopoulos, 2014). The IRP/IRE regulatory system plays an important role in several points of this process.

In iron deficiency conditions, erythroid precursor cells will have priority for iron utilization over cells in other tissues, for the proper and sufficient production of RBCs

(Finch, 1994). An increment of erythropoiesis leads to stimulation for increasing iron absorption by duodenal enterocytes and increase of iron egression by macrophages (Wilkinson & Pantopoulos, 2014). Erythropoietin (EPO), a hormone secreted by the kidney and, to a lesser extent by the liver, is secreted following erythropoiesis stimulation during hypoxia and controls erythroid cell maturation (Franke, Gassmann, & Wielockx, 2013). The hypoxia inducible factor-2 alpha (HIF2α) activates EPO transcription. In normoxia and in the presence of Fe^{2+} and 2-oxoglutarate, HIF-1α and HIF-2α are hydroxylated by prolyl hydroxylases (PHDs) and degraded by the proteasome (Muckenthaler et al., 2017). On the contrary, in hypoxia or iron deficiency conditions, PHDs lack the essential O_2 or Fe^{2+} and HIF-2α is stabilized and accumulates in the nucleus recruiting HIF-1β, which is constitutively stable and expressed, and all together activate EPO transcription (Muckenthaler et al., 2017). Consequently, a low oxygen concentration produces an increment of EPO production which leads to proliferation and maturation of erythroid cells increasing blood oxygen binding capacity. In addition, iron deficiency also inhibits the PDH proteins in cultured cells and in humans explaining how iron chelators promote EPO expression (Muckenthaler, M., Rivella, Hentze, & Galy, 2017). Furthermore, HIF2α have a 5'UTR IRE that controls its expression by the IRPs (Sanchez et al., 2007). In iron deficiency conditions, IRPs bind to HIF2α 5'UTR IRE and reduce its expression; therefore reducing EPO levels and limiting the generation of hypochromic and microcytic erythrocytes (Figure 1.9). Actually, Irp1 knockout mice shows signs of Hif2α activation and elevated EPO which leads to polycythemia and splenomegaly due to extramedullary erythropoiesis (Anderson, S. A., Nizzi, Chang, Deck, Schmidt, Galy, Damnernsawad, Broman, Kendziorski, Hentze, Fleming, Zhang, & Eisenstein, 2013b; Ghosh et al., 2013; Wilkinson & Pantopoulos, 2013). However, Irp2 knockout mice present hypochromic microcytic anemia (Cooperman et al., 2005; Galy et al., 2005) whereas tissue-specific Irp2 knockout in hepatocytes, macrophages or enterocytes mice do not develop hematological defects (Ferring-Appel et al., 2009) demonstrating that microcytic anemia is a local defect in RBC precursors of Irp2 knockout mice.

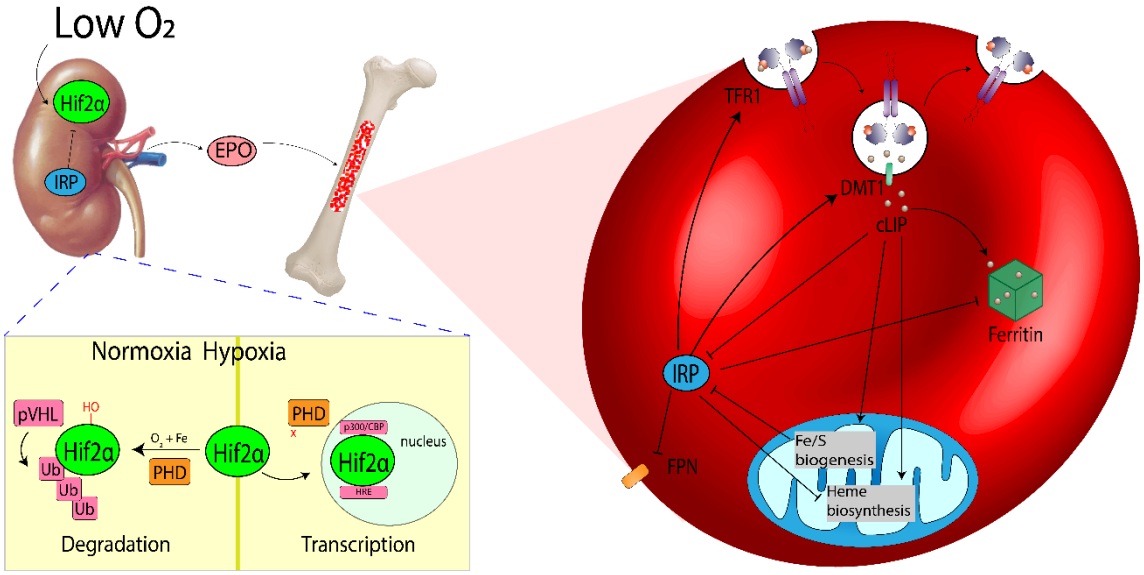

Figure 1.9: The IRP/IRE regulatory system in erythropoiesis. The IRP/IRE system controls the production of the erythropoietin hormone in the kidney through HIF2α expression and subsequently affecting bone marrow erythropoiesis. To guarantee the adequate iron supply for hemoglobin production, the IRP/IRE system coordinates the expression of TFR1, DMT1, ferritin and FPN in developing enterocytes. HIF2α: hypoxia inducible factor-2 alpha; EPO: erythropoietin; PHD: prolyl-hydroxilases; pVHL: von Hippel-Lindau E3 ubiquitin ligase; HRE: hypoxia responsive element; IRP: iron regulatory protein; cLIP: cellular labile iron pool; DMT1: divalent metal ion transporter; TFR1: transferrin receptor 1; FPN: ferroportin.

RBCs iron acquisition strongly depends on the transferrin – transferrin receptor 1 axis. Transgenic mice with Tf (Trenor et al., 2000) and Tfr1 (Levy, Jin, Fujiwara, Kuo, & Andrews, 1999) deficiency presents severe hypochromic microcytic anemia and parenchymal iron overload highlighting the capacity of other tissues to obtain iron by alternative pathways but not in the erythroid precursors. Actually, Dmt1 is also involved in iron uptake via Tfr1 and Dmt1 knockout mice present impaired iron acquisition in RBC precursors (Fleming, M. D. et al., 1998). Both TFR1 and DMT1 have 3'UTR IREs, consistent with their role in incrementing iron uptake in low iron conditions. Irp2 knockout mice have high ferritin expression coupled with low Tfr1 expression in bone marrow erythrocytes, suggesting insufficient iron uptake (Cooperman et al., 2005; Galy et al., 2005). In addition, in Irp2 knockout mice, Alas2 is not repressed and, consequently, mice present erythropoietic protoporphyria due to heme synthesis acceleration in its first limiting enzymatic step resulting in the accumulation of protoporphyrin IX, which is toxic and it cannot be converted to heme by ferrochelatase due to iron absence (Cooperman et al., 2005). Moreover, the inactivation of one allele of Irp1 aggravates the anemia of Irp2-/- mice (Smith et al., 2004).

Several Fe/S biogenesis defects, which lead to secondary IRP1 activation, produce ALAS2 repression and anemia both in human and zebrafish model (Camaschella et al., 2007; Wingert et al., 2005; Ye et al., 2010). All these data together show that IRP1 participates in the control of ALAS2 and TFR1 in erythroid, but IRP2 is their main regulator.

Erythroid cells also express ferroportin (FPN) (Zhang, De-Liang et al., 2009). Besides hepcidin regulation (mentioned in section 1.2) FPN also has an IRE in its 5'UTR mRNA and it is regulated by IRPs (Abboud & Haile, 2000). This gene has two mRNA isoforms, the canonical, FPN1A, which has the IRE, and FPN1B, that undergoes an alternative splicing that results in a non-IRE isoform. The FPN1B is expressed in enterocytes and in early stages of erythroid differentiation as possible mechanism to avoid toxic iron accumulation if iron uptake exceeds mitochondrial iron utilization (Zhang, De-Liang et al., 2009). In terminal stages of erythroid differentiation, when cells need important amounts of iron for heme synthesis, FPN1A becomes the predominant isoform to allow IRPs to repress FPN expression, limiting iron export (Zhang, De-Liang et al., 2009).

To sum up, the IRP/IRE system coordinates different processes to guarantee production of hemoglobin in maturing erythroblasts. The main genes in this process are ferritins (FTL and FTH), TFR1, DMT1, ALAS2 and FPN. Schranzhofer and collaborators showed that IRE-containing mRNAs avoid IRP regulation during terminal differentiation in murine erythroid progenitors, where the expression of Alas2 and ferritin are uncoordinated and Tfr1 mRNA levels are elevated even in iron overload conditions (Schranzhofer et al., 2006). To explain this unexpected finding, the authors proposed that in mature erythroblasts substantial mRNA transcription may lead to an excess of IRE containing mRNAs over available IRP molecules (Schranzhofer et al., 2006).

1.6.The IRP/IRE in human diseases

Mutations in the IRP/IRE regulatory system can lead to several human diseases. These mutations can be in the IRPs or in the IREs. Recently, it was described the first mutation that affects directly one IRP: bi-allelic mutations of *IREB2* gene were reported in 2 patients affected by neurodegeneration and microcytic hypochromic anemia refractory to iron supplementation (Cooper, Stark, Lunke, Zhao, & Amor, 2019; Costain et al., 2019). In addition, there are several described mutations affecting the iron responsive elements disturbing its binding with the IRPs that also cause IRP/IRE-related human diseases.

1.6.1. Human diseases due to mutations in the IRPs

Recently, the first two cases of mutations in the *IREB2* gene were described. Both patients are compound heterozygotes. Table 1.2. summarizes this disease.

1.6.1.1. IRP2 mutations

The proband of the first case is a 16-years old male with profound early developmental delays. At nine years old he developed generalized tonic-clonic seizures needing antiepileptic drugs. Basically, he is dependent for all aspects of self-care. Brain magnetic resonance imaging (MRI) showed the loss of cerebral volume at 18 month of age, moderate loss of white matter accentuated in the brain frontal regions. Moreover, patient presents retinal dysfunction and microcytic hypochromic anemia refractory to iron supplementation (Costain et al., 2019). A genetic test reveal that the proband is a compound heterozygous (NM_004136.2; c.[1069G>T, p.G357X];[1255C>T, p.R419X]) with two nonsense mutations (Costain et al., 2019)

The second proband is a 10-year old male with similar clinical features. Since birth the patient present early and profound developmental delays, and episodes of neutropenia. At 4 years the proband needed a nasogastric tube for feeding. Gastric troubles went worse and finally feeds cannot be introduced and the proband died from fungal sepsis and malnutrition. The genetic test reveal that he is a compound heterozygous NM_004136.4; c.[2353G>A, p.(G785R)];[1329_1331del, p.(S444del)] with a missense mutation and 3 bp in frame deletion (Cooper et al., 2019).

Human clinical features were consistent with *Ireb2* knockout mice which present progressive neurodegeneration with neuronal loss and iron accumulation in axons and oligodendrocytes, mild anemia and erythropoietic protoporphyria (Cooperman et al., 2005; LaVaute et al., 2001). Hematological parameters in the first described patient show mild elevated serum ferritin, elevated zinc protoporphyrin, but normal serum transferrin and iron levels (Costain et al., 2019). Molecular studies with patient's lymphoblast extracts reveal upregulated FTH, downregulated TFR1 and increased IRP1 binding activity consistent with IRP2 loss. Importantly, all abnormalities present in patient's lymphoblast were reversed with lentiviral restoration of IRP2 expression (Costain et al., 2019). In the second described patient full blood count was normal, but ocasionally he had mild microcytic anaemia. This proband, as the previous one, also present elevated serum ferritin levels and normal serum transferrin and iron levels (Cooper et al., 2019). Molecular studies were not possible due to the death of the patient.

Table 1.2: Human disorders due to mutations in the IRPs.

Human disease	Gene	Phenotype	Inheritance	OMIM	Reference
Neurodegeneration with choreoathetosis and microcytic anemia	*IREB2*: bi-allelic loss of function	Neurodegenerative early onset with choreoathetoid movement disorder and microcytic anemia	AR	#618451	(Cooper et al., 2019; Costain et al., 2019)

1.6.2. Human diseases due to mutations in the IREs of IRE-containing mRNAs.

Missregulation in the expression of genes involved in iron metabolism causes several disorders summarized in Table 1.3.

Table 1.3: Human disorders due to mutations in IREs

Human disease	Gene	Phenotype	Inheritance	OMIM	Reference
Hereditary Hyperferritinemia-Cataract Syndrome (HHCS)	*FTL*: point mutations and deletions in the IRE that impair IRPs' binding	Elevated serum ferritin in the absence of iron overload or inflammation. Tendency to the development of bilateral cataract in early age	AD	#600886	(Beaumont, C. et al., 1995; Bonneau et al., 1995; Girelli et al., 1995); other papers report many other mutations
Autosomal dominant iron overload syndrome	*FTH1*: point mutation in the IRE that increases IRPs' binding	Reduction of FTH1 expression leading to an iron overload syndrome similar to Hereditary Hemochromatosis	AD	#615517	(Kato et al., 2001)
Clinical severity modifier in EPP	*ALAS2*: heterozygous point mutation and CPLX heterozygous mutation	Clinical severity modifier in EPP	Digenism (CPLX + ALAS2)	-	(Ducamp et al., 2021)
Hemochromatosis with mutation of ferroportin gene	*FPN*: point mutation located 7 nucleotides downstream the IRE, not demonstrated effect on IRP binding	Phenotype similar to Hereditary Hemochromatosis	AD?	-	(Liu, W. et al., 2005)

1.6.2.1. Hereditary Hyperferritinemia – Cataract Syndrome (HHCS):

Hereditary hyperferritinemia-cataract syndrome (HHCS) (OMIM #600886) is a rare disease characterized by high serum ferritin levels, congenital bilateral cataracts and the absence of tissue iron overload (Table 1.2). It was first independently described in 1995 by two research teams in France and Italy (Beaumont, C. et al., 1995; Bonneau et al., 1995; Girelli et al., 1995). The geographical distribution of HHCS patients is worldwide. Even so, its global prevalence is not defined, but in Australian population was estimated to be 1 in 200.000 (Craig et al., 2003). HHCS is due to mutations in the iron responsive element (IRE) located in the 5'UTR of the Ferritin L mRNA (*FTL*). Mutations in the 5'UTR IRE of the *FTL* mRNA lead to the loss of the interaction between IRPs and the *FTL* IRE, losing the IRP-induced translation repression. As a consequence, an excessive level of ferritin is produced, accumulating in the serum and finally depositing in the lens causing bilateral congenital cataracts. HHCS is an autosomal dominant inherited disease and mutations are in heterozygous state in almost all reported families. However, there are few cases with *de novo* mutations (Arosio, C. et al., 1999; Cao, McMahon, Wang, O'Connor, & Clarkson, 2010; Craig et al., 2003; Hernández Martín, Cervera Bravo, & Balas Pérez, 2008; Hetet, Devaux, Soufir, Grandchamp, & Beaumont, 2003; McLeod, Craig, Gumley, Roberts, & Kirkland, 2002; Muñoz-Muñoz et al., 2013) and only three cases with homozygous mutations (Álvarez-Coca-González et al., 2010; Giansily-Blaizot, Cunat, Moulis, Schved, & Aguilar-Martinez, 2013; Luscieti et al., 2013). At least 47 mutations have been described in *FTL* IRE as causative of HHCS, including 36 single mutations, 9 deletions and 2 insertion-deletions (Figure 1.10). Due to the phenotypical variability regarding serum ferritin levels, ocular involvement and the age of onset of the cataracts, some authors attempted to find out a relationship between the disease severity and the

position of the mutation in the IRE structure. Thus, mutations that affect the most important IRE structure, as the hexanucleotide loop or the C-bulge nucleotide, lead to more elevated ferritin levels and probably early onset cataracts than mutations that affect other IRE regions as the upper or lower stems (Allerson, Cazzola, & Rouault, 1999; Luscieti et al., 2013). However, relatives who share same mutations present phenotypic variability. This suggests that other environmental or genetic factors could contribute in the development of clinical symptoms (Girelli et al., 2001). The HHCS patients do not have any other clinical symptoms rather than early appearance of bilateral cataracts. Patients diagnosed with HHCS are treated by undergoing surgical intervention when they suffer visual impairment, usually in adult stage. A differential diagnosis is crucial because HHCS is usually misdiagnosed as hereditary hemochromatosis (HH) due to the detection of hyperferritinemia that is a common biochemical sign present in both diseases. As a consequence of HHCS misdiagnosis with HH, some HHCS patients were treated with periodic phlebotomies that are the adequate treatment for HH. However, phlebotomies are contraindicated in HHCS as they lead to anemia in HHCS patients. For an extensive literature revision of FTL 5' IRE mutations see Annex I and Annex I.I (section 8.1.4.) and the supplementary data of my paper Ferran Celma Nos *et al. (*2021) *"Hereditary Hyperferritinemia Cataract Syndrome: Ferritin L Gene and Physiopathology behind the Disease-Report of New Cases"* IJMS.

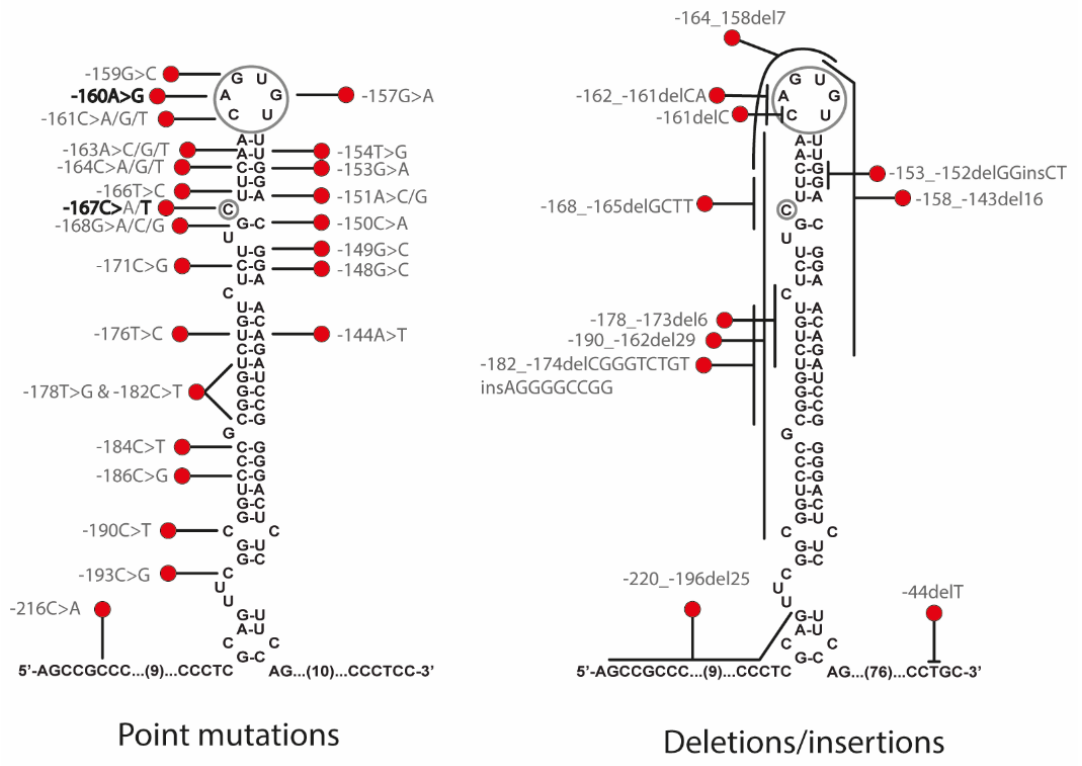

Figure 1.10: Summary of all reported mutations that cause HHCS. Point mutations are on the left and deletions/insertions are depicted on the right. A grey circle marks the C-bulge and the hexanucleotide loop. Picture from Celma Nos *et al.* 2021. See Annex I, page 99.

1.6.2.2. Autosomal dominant iron overload syndrome

An autosomal dominant iron overload syndrome (OMIM #615517) was described just in a single Japanese patient (Kato et al., 2001) (Table 1.2). The proband had a heterozygous point mutation in the IRE of H-ferritin mRNA (NM_002032.2; c.[-164A>T];[=]) (Figure 1.11). This mutation leads to high serum ferritin levels, elevated transferrin saturation and iron deposits in the liver and bone marrow. Mutated *FTH1* IRE presents a higher IRP affinity, more than wildtype, demonstrated by electrophoretic mobility shift assay (EMSA) analysis. Consistently, the liver of the proband showed a diminished expression of H-ferritin and increased levels of L-ferritin. Studies in COS-1 cells, carrying the *FTH1* mutation, reveal low iron incorporation within ferritin despite an increased cellular iron uptake. The *Fth1* KO mouse is embryonic lethal due to massive iron deposits in agreement with the iron overload present in this patient (Ferreira et al., 2000). In the patient the decrease of FTH will produce cytosolic iron accumulation, possibly due to the decrease of ferroxidase activity, as a consequence of impaired iron incorporation into the ferritin cage.

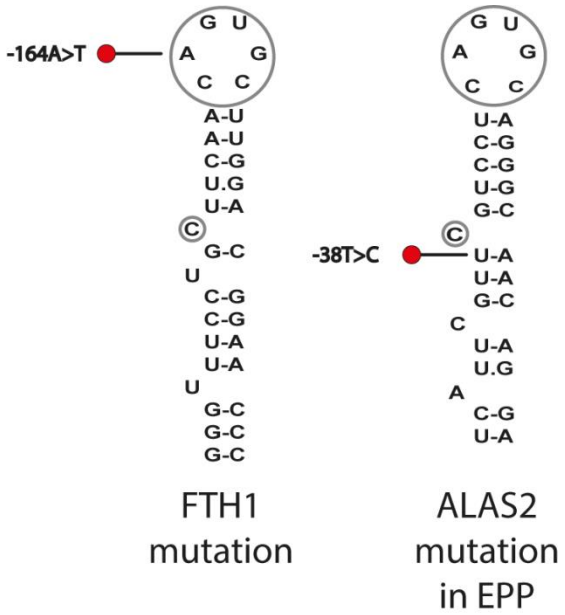

Figure 1.11: Mutations in FTH1 and ALAS2 IREs. (Left) mutation in human *FTH* IRE causative for AD iron overload syndrome. (Right) mutation in human *ALAS2* IRE as a clinical modifier of EPP. A grey circle marks the C-bulge and the hexanucleotide loop.

1.6.2.3. A mutation in *ALAS2* IRE as a clinical severity modifier in EPP

Erythropoietic Protoporphyria (EPP2) (OMIM #618015) is a disease caused by mutations in the coding region of *FECH*, *ALAS2* and *CLPX* genes. Recently, it was described the first EPP case caused by a digenism. The proband presents a mutation in the *CLPX* gene and another mutation in the IRE of *ALAS2* mRNA (Figure 1.11). The ALAS2 IRE mutation abrogates IRP binding and contributes to a greater accumulation of porphyrin in erythrocytes leading to severe EPP (Ducamp et al., 2021). EPP symptoms in the patient were photosensitivity, accumulation of zinc-chelated erythroid PPIX and microcytic iron deficiency anemia.

1.6.3. Human diseases due to mutations in genes that contain an IRE

Several human diseases are caused by mutations in genes that contain an IRE, but mutations are located outside the IRE region. This situation produces a misregulation that affects the IRP/IRE posttranscriptional regulatory system. Table 1.4. contains a summary of these disorders.

Table 1.4: Human disorders due to mutations in genes that contains an IRE.

Human disease	Gene	Phenotype	Inheritance	OMIM	Reference
Anemia, hypochromic microcytic, with iron overload 1 (AHMIO1)	SLC11A2: compound heterozygous or homozygous mutations.	Severe hypochromic microcytic anemia and hepatic iron overload	AR	#600523	(Bardou-Jacquet et al., 2011; Barrios et al., 2012; Beaumont, Carole et al., 2006; Blanco, Kannengiesser, Grandchamp, Tasso, & Beaumont, 2009; Casale et al., 2018; De Falco et al., 2012; Iolascon et al., 2006; Priwitzerova et al., 2004)
X-linked Sideroblastic Anemia (XLSA)	ALAS2: mutations in the coding or promoter region that produce reduced enzyme activity	Moderate to severe sideroblastic anemia and iron accumulation secondary to the ineffective erythropoiesis	X-linked	#300751	(Peto, Pippard, & Weatherall, 1983)
X-linked Erythropoietic Protoporphyria (XLEPP)	ALAS2: gain of function mutations located in the C-terminal region of the protein	Severe photosensitivity associated to decreased iron stores	X-linked dominant	#300752	(Whatley et al., 2008)
Ferroportin disease (previously known as Hereditary hemochromatosis type 4A	*SLC40A1:* mutations that lead to loss of function of the gene	Generally asymptomatic with no tissue damage and further complications. With age, tissue damage in the liver can occur which in some cases can lead to fibrosis	AD	#606069	(Pietrangelo et al., 1999)
Non-HFE hemochromatosis (previously known as hemochromatosis type 4B)	*SLC40A1:* mutations that lead to loss of Hepcidin binding region and subsequently the FPN dysregulation.	Characterized by liver iron overload	AD	#606069	(Njajou et al., 2001)
Familiar erythrocytosis	*EPAS1*: gain-of-function mutations resulting in constitutive activation of EPO signaling	Increased levels of serum hemoglobin, hematocrit and erythrocyte mass, associated with elevated or inappropriately normal erythropoietin serum levels	AD	#611783	(Percy et al., 2008)
Immunodeficiency 46 (IMD46)	*TFRC*: amino acid substitution producing TfR1 disruption	Primary immunodeficiency resulting in severe childhood infections. Decreased numbers of memory B cells. Non hematologic disorders.	AR	#616740	(Jabara et al., 2015)

1.6.3.1. Mutations in *SCL11A2* gene (DMT1 protein):

DMT1 (encoded by the *SLC11A2* gene) is essential for iron uptake, both at the systemic level in the duodenal non-heme iron absorption and at the cellular level in the transferrin endocytosis cycle (Gunshin et al., 1997). Mutations in *SLC11A2* gene cause hypochromic microcytic anemia and iron overload (OMIM #206100) (Iolascon, De Falco, & Beaumont, 2009) due to deficient duodenal iron absorption and erythroid iron utilization. So far, 8 patients have been reported worldwide with bi-allelic mutations in the *SLC11A2* gene since the first case described in 2005 (Mims et al., 2005). Although patient present hepatic iron overload, *Slc11a2* KO mutant mice do not. Authors attributed this observation to the fact that humans present higher heme iron absorption than mice and can compensate the DMT1 intestinal impairment. Interestingly, two out of the eight reported cases did not present the hepatic iron overload phenotype (Blanco et al., 2009; Casale et al., 2018).

I have contributed to the characterization of a new mouse model (knock-in mouse) which lacks part of the *Dmt1* IRE (see Results and Discussion and the paper Tybl et al 2020 in Annex II).

1.6.3.2. Mutations in *ALAS2* gene (in the coding region)

ALAS2 gene encodes the first enzyme of heme biosynthesis (see section 1.3.2). It is located on the X-chromosome. Mutations in this gene cause 2 different diseases: X-linked Sideroblastic Anemia (XLSA) and X-linked Erythropoietic Protoporphyria (XLEPP) (Table 1.3). XLSA (OMIM #300751) is characterized by loss of function mutations in the *ALAS2* gene leading to ineffective erythropoiesis. The main clinical symptoms are hypochromic microcytic anemia, bone marrow ringed sideroblasts and a systemic iron overload secondary to chronic ineffective erythropoiesis (Fleming, Mark D., 2002). On the other hand, XLEPP (OMIM #300752) is produced by gain-of-function mutations in *ALAS2* gene. This disorder produces accumulation of protoporphyrin IX (PPIX). Patients show photosensitivity associated with decreased iron stores and zinc-chelated erythroid PPIX (Ducamp et al., 2013).

1.6.3.3. Mutations in *SLC40A1* gene (FPN protein)

Mutations in *SLC40A1* gene, encoding ferroportin, cause 2 different diseases: Ferroportin disease and non-HFE Hereditary Hemochromatosis.

Ferroportin disease (OMIM #606069), previously known as Hereditary hemochromatosis type 4A, is an autosomal dominant disorder caused by loss of function mutations in the *SLC40A1* gene. Mutations affect the localization of FPN to the cell membrane and/or iron export function (Détivaud et al., 2013; Schimanski et al., 2005); consequently, iron remains sequestrated into the cells. Patients present normal or low transferrin saturation, hyperferritinemia and systemic iron accumulation, mainly in macrophages (Montosi et al., 2001).

On the other hand, non-HFE Hereditary Hemochromatosis, previously known as hereditary hemochromatosis type 4B, is produced by gain of function mutations in the *SLC40A1* gene. These mutations affect the interaction between FPN and hepcidin impairing the binding, interaction or the internalization of FPN. Consequently, there is

an increased expression of FPN in the cell membrane leading a constitutive iron export from the cells. Patients with these mutations present a phenotype similar to hereditary hemochromatosis, including high serum ferritin, high transferrin saturation and iron overload, mostly affecting hepatocytes (Détivaud et al., 2013; Drakesmith et al., 2005; Njajou et al., 2001).

In addition, Liu and collaborators reported a mutation close to the 5' IRE of ferroportin gene in a Japanese patient (Table 1.3). The proband presents the non-HFE hereditary hemochromatosis (HH) typical phenotype: iron overload in liver and spleen, chronic hepatitis, impaired glucose tolerance, skin pigmentation and high serum iron levels, serum ferritin and transferrin saturation (Liu, W. et al., 2005). The patient carry a heterozygous mutation (NM_014585.5; c.[-188A>G];[=]) that has not passed to her children, suggesting an autosomal inheritance compatible with non-HFE HH. Interestingly, a new gen (*BMP6*) has been identified as a cause of dominant HH (Daher et al., 2016), but it was not studied in that family. Unfortunately, there are no studies with the mutation described in the FPN 5'UTR to test whether it affects the IRP/IRE binding.

An irradiation-induced mouse model with a heterozygous microdeletion in the promoter region of FPN leading to the lack of the IRE, presents elevated levels of FPN which lead to increased iron uptake and reticuloendothelial iron overload. Moreover, mice with heterozygous IRE lack present erythropoietin-dependent polycythemia while mice with homozygous mutation present hypochromic microcytic anemia (Mok et al., 2004).

1.6.3.4. Mutations in *EPAS1* gene (HIF2α protein)

Familiar erythrocytosis type 4 (ECYT4) (OMIM #611783) is an autosomal dominant disease produced by gain-of-function mutations in the *EPAS1* gene encoding HIF2 α protein. It is characterized by increased serum red blood cell mass and hemoglobin concentration as well as elevated serum erythropoietin (EPO) (Percy et al., 2008).

1.6.3.5. Mutations in *TFRC* gene (TFR1 protein)

Immunodeficiency 46 (OMIM #616740) is an autosomal recessive disorder produced by mutations in the *TFRC* gene. It was described in a single consanguineous family producing primary immunodeficiency which results in severe childhood infections (Jabara et al., 2015). In addition, these family members had decreased numbers of memory B cells, impaired immunoglobulin class-switching, and decreased proliferative responses of T cells (Jabara et al., 2015).

1.6.4. Human diseases due to mutations in genes involved in Fe/S cluster biosynthesis and therefore affecting the IRP1 activity

Another group of diseases related with the IRP/IRE system are those that affect the Fe/S cluster formation altering the IRP1 functionality (Table 1.5). In this group of diseases, mutations impair the synthesis of Fe/S cluster (process done in the mitochondria) resulting in a diminished number and activity of Fe/S proteins and, consequently, mitochondrial iron accumulation (Sheftel et al., 2010). With less Fe/S cluster production, IRP1 is constitutively active and its binding to IREs lead to

pathogenic deregulation of iron homeostasis. Examples of such diseases are reported in Table 1.5.

Table 1.5: Human diseases due to mutations affecting IRP1 activity. This table is not an exhaustive revision table for mutations in genes affecting Fe/S cluster formation, rather a table to illustrate diseases in which the impairment of the Fe/S cluster synthesis has been linked with IRP1 activation.

Human disease	Gene	Phenotype	Inheritance	OMIM	Reference
Friedreich's ataxia (FRDA)	*FXN*: GAA triplet expansion (in 97% of the cases) or point mutations leading to FXN deficiency	Spinocerebellar ataxia with cardiomyopathy	AR	#229300	(Campuzano et al., 1996; Delatycki et al., 1999)
Sideroblastic anemia and spinocerebellar ataxia (ASAT)	*ABCB7*: missense mutations	Spinocerebellar ataxia and mild sideroblastic anemia	XR	#301310	(Allikmets et al., 1999)
Autosomal recessive pyridoxine-refractory sideroblastic anemia	*GLRX5*: point mutation affecting splicing and leading to GLRX5 deficiency and Fe/S cluster biogenesis defect	Sideroblastic anemia with hepatosplenomegaly and iron overload	AR	#205950	(Camaschella et al., 2007; Liu, G. et al., 2014)
Sideroblastic anemia 4 (SIDBA4)	*HSPA9:* heterozygous mutation	Sideroblastic anemia	AR	#182170	(Schmitz-Abe et al., 2015)
Sideroblastic anemia 5 (SIDBA5)	*HSCB:* loss of function mutations	Sideroblastic anemia. Patients may also develop thrombocytopenia or pancytopenia	AR	#619523	(Crispin et al., 2020)
Hereditary myopathy with lactic acidosis (HML)	*ISCU*: missense mutation altering mRNA splicing resulting in reduced levels of ISCU protein and Fe/S cluster biogenesis defect	Myopathy with lactic acidosis characterized by childhood onset of exercise intolerance with muscle tenderness, cramping, dyspnea, and palpitations	AR	#255125	(Mochel et al., 2008)

1.6.4.1. Friedreich's Ataxia

Friedreich's Ataxia (FRDA) (OMIM #229300) is an autosomal recessive inheritance disease (prevalence 1 in 50000) with onset in preadolescent age. In 95-98% of the cases it is caused by reduction in frataxin (FXN) protein levels in the mitochondria due to a homozygous GAA triplet expansion in the first intron of the frataxin gene (*FXN*). Healthy people have about 35 repetitions, but patients could have GAA repetitions ranging from 100 to 1000. The number of repetitions correlates with disease severity and onset age (Patel & Isaya, 2001). FRDA is characterized by spinocerebellar ataxia, hypertrophic cardiomyopathy and increased risk of diabetes (Parkinson, Boesch, Nachbauer, Mariotti, & Giunti, 2013). The pathology evolves in a time-lapse of 10-15 years with progressive loss of movement coordination. Thus, patients require wheelchair and assistance in daily activities and they also lose communicative skills, but do not present cognitive impairment. The exact function of FXN is not known, but several studies confirmed that it is involved in Fe/S biogenesis (Cavadini, O'Neill, Benada, & Isaya, 2002). Hence, reduced availability of Fe/S cluster promotes IRP1 binding to IREs constitutively. In addition, IRP2 activity is promoted by cytosolic iron depletion (Li, K., Besse, Ha, Kovtunovych, & Rouault, 2008).

Despite FRDA patients present a dysregulation in iron metabolism; they do not present hematologic problems derivate to the mutation. Some clinical trials use iron chelators to

diminish oxidative stress and iron accumulation with inconsistent yield (Pandolfo et al., 2014).

1.6.4.2. Sideroblastic anemias

Sideroblastic anemias (SAs) are a group of inherited and acquired bone marrow disorders defined by pathological iron accumulation in the mitochondria of erythroid precursors (Cartwright & Deiss, 1975; Ducamp & Fleming, 2019). Its name comes from a characteristic morphological feature: the presence of ringed sideroblasts, produced by iron-laden mitochondria encircling erythroblast nuclei. Most frequent SA is due to mutations in *ALAS2* gene that affect heme synthesis (see section 1.6.3.2.). Other SA are due to mutations in genes involved in Fe/S cluster (see below).

1.6.4.2.1. Sideroblastic anemia and spinocerebellar ataxia

Sideroblastic Anemia with Spinocerebellar Ataxia (ASAT) (OMIM #301310) (Table 1.5) is an ultra-rare disease that affects few families in the world with recessive X-linked inheritance. ASAT is caused by missense mutations in the *ABCB7* gene, which encodes an ATP-binding cassette (ABC) transporter involved in Fe/S clusters export from mitochondria to cytosol, located in the inner mitochondrial membrane. Alterations in *ABCB7* gene provokes an alteration in iron homeostasis similar to FXN deficiency. This gene is significantly expressed in bone marrow and cerebellum. Hemizygous patients with ASAT present since early infancy non-progressive or slow-progressive spinocerebellar ataxia and cerebellar hypoplasia. Moreover, patients develop mild hypochromic microcytic anemia with high levels of free protoporphyrin IX and a characteristic iron accumulation in bone marrow erythroblasts (ringed sideroblasts). Heterozygous females only present hematological signs. In this scenario, mitochondrial enzymes with Fe/S clusters are not altered, but the cytosolic Fe/S proteins are reduced. This reduction in cytosolic Fe/S clusters impairs aconitase activity promoting IRP1-mRNA binding activity.

Together with *ABCB7*, other mutations in genes implicated in biogenesis of Fe/S clusters produce sideroblastic anemia, such glutaredoxin 5 (*GLRX5*), heat shock protein family A member 9 (*HSPA9*) or heat shock cognate B (*HSCB*) (Crispin et al., 2020).

1.6.4.2.2. Autosomal recessive sideroblastic anemia due to GLRX5 mutations

Two patients have been reported with Sideroblastic anemia and mutation in glutarredoxin 5 gene (Camaschella et al., 2007; Liu, G. et al., 2014) (Table 1.4). Camaschella and collaborators reported a patient with a homozygous mutation in *GLRX5* gene (NM_016417.2; c.[294A>G];[294A>G]. Interestingly, this substitution does not change the amino acid sequence, but alter the splicing of the mRNA. The patient present hypochromic microcytic anemia, hepatosplenomegaly, iron overload and low number of ringed sideroblasts. Liu and collaborators described a patient with two heterozygous missense mutations on the coding region, K101Q and L148S. Patient presents severe anemia, hepatosplenomegaly, anisocytosis, mild erythroid hyperplasia and low number of ringed sideroblast.

1.6.4.2.3. Sideroblastic anemia 4

Sideroblastic anemia 4 (SIDBA4) (OMIM #182170) is caused by mutations in *HSPA9* gene which encodes a mitochondrial chaperone from the HSP70 family of heat shock proteins. It is also involved in export of Fe/S clusters from mitochondria to the cytosol (Schmitz-Abe et al., 2015). Patients present ringed sideroblasts and some cases mild anemia.

1.6.4.2.4. Sideroblastic anemia 5

Sideroblastic anemia-5 (SIDBA5) (OMIM #619523) is an autosomal recessive hematologic disorder. Recently, Crispin and collaborators reported the first patient who has mutated the *HSCB* gene, a partner of *HSPA9*, with a frameshift mutation (Crispin et al., 2020). The patient reported by Crispin and collaborators present hypochromic microcytic anemia with ringed sideroblasts that evolve in pancytopenia, mild neutropenia and moderate thrombocytopenia.

1.6.4.3. Hereditary myopathy with lactic acidosis (HML)

Finally, intronic mutations in *ISCU* gene lead to hereditary myopathy with lactic acidosis (HML) (OMIM #255125) (Table 4). The disease is caused by incorrect mRNA splicing promoting decreased levels of the ISCU protein (Mochel et al., 2008; Olsson, Lind, Thornell, & Holmberg, 2008). It is a rare disease found in northern Swedish descendent families with an autosomal recessive inheritance. HML affects overall skeletal muscle and is characterized by exercise intolerance, muscle tenderness, cramping, dyspnea and palpitations. ISCU protein assists in the Fe/S formation in mitochondria; a deficiency of ISCU decreases the synthesis of Fe/S and mitochondrial activity. As a result, cytosolic levels of Fe/S are low increasing IRP1 binding with IREs.

1.7.Novel IRPs target mRNAs

Several studies from our and other groups have reported additional IREs or IRE-like structures, apart from canonical ones, in mRNAs of genes that *a priori* were not related with iron metabolism (Luscieti et al., 2017; Sanchez et al., 2006; Yanatori, Richardson, Dhekne, Toyokuni, & Kishi, 2021). Therefore, the IRP/IRE regulatory system can be wider than initially thought. My supervisor, Dr. Mayka Sanchez tried to define the limits of the IRP/IRE regulatory network using a high throughput genome-wide approach by specifically immunoprecipitating IRP-mRNA complexes and then analyzing the obtained mRNAs (Sanchez et al., 2011).

In detail, Sanchez and collaborators extracted RNA from mouse duodenum, liver, brain, spleen and bone marrow and incubated these mRNAs with recombinant IRP1 or IRP2. Finally, RNA-protein complexes were immunoprecipitated with specific antibodies and mRNAs were identified with Affymetrix microarrays. With this approach, we have identified 263 mRNAs that can interact with IRPs (44 mRNAs bind both IRPs, 102 bind specifically IRP1 and 117 bind specifically IRP2), including all 9 known murine IRP-binding mRNAs (*Ftl1*, *Ftl2*, *Fth1*, *Slc40a1*, *Alas2*, *Aco2*, *Epas1*, *Slc11a2* and *Tfrc*) used as positive controls (Figure 1.12).

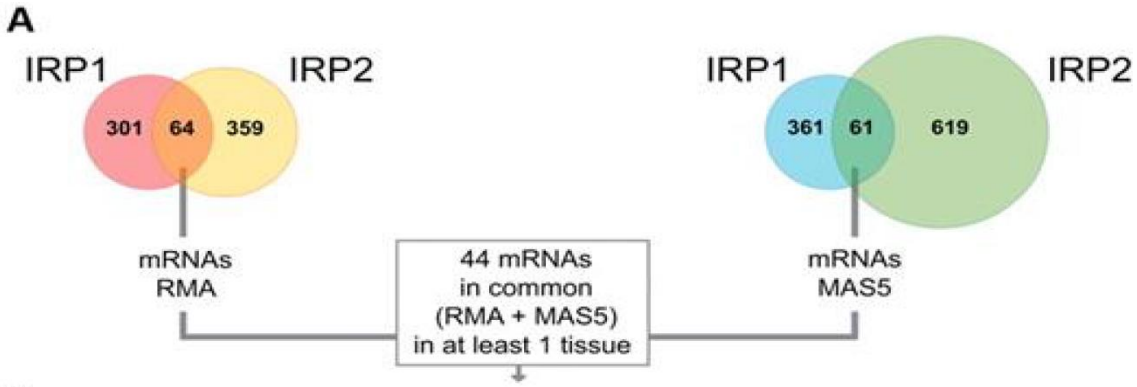

B

Gene Symbol	IRP1 Duodenum	IRP1 Liver	IRP1 Bone Marrow	IRP1 Spleen	IRP1 Brain	IRP2 Duodenum	IRP2 Liver	IRP2 Bone Marrow	IRP2 Spleen	IRP2 Brain	IRE motif Position	IRE motif Species
Ftl1	■	■	■	■	■	■	■	■	■	■	5′	*Mm/Hs*
Tfrc	■	■	■	■	■	■	■	■	■	■	3′	*Mm/Hs*
Lrpap1	■	■	■	■	■	■	■	■	■	■	3′	*Mm*
Slc40a1	■	■	■	■	■	■	■	□	■	■	5′	*Mm/Hs*
Aco2	■	■	■	■	■	■	■	□	■	■	5′	*Mm/Hs*
Ftl2	■	■	■	■	■	□	■	■	■	□	5′	*Mm/Hs*
Slc11a2	■	■	■	■	■	■	■	□	■	□	3′	*Mm/Hs*
0610007L01Rik	■	■	■	■	■	■	■	□	■	□	n.d.	
Ccdc45	■	■	■	■	■	■	■	□	■	□	n.d.	
Epas1	■	■	■	■	■	■	■	□	■	□	5′	*Mm/Hs*
Cxcl16	■	■	■	■	■	■	■	□	■	□	3′	*Mm*
Fxyd5	■	■	■	■	■	■	□	□	■	□	5′	*Hs*
Ormdl1	■	■	■	■	■	■	■	□	□	□	3′	*Hs*
Gyg	■	■	■	■	■	□	□	□	■	□	CDS	*Mm/Hs*
Garnl1	■	□	■	■	■	■	■	■	■	■	5′-CDS	*Mm*
Egr2	■	□	■	■	■	■	■	■	■	■	CDS	*Mm*
A430093A21Rik	□	■	■	■	■	■	■	□	■	■	CDS	*Mm*
Alas2	□	■	■	■	■	□	■	□	■	■	5′	*Mm/Hs*
Fth1	□	■	■	■	■	□	□	■	■	■	5′	*Mm/Hs*
Pfn2	■	■	■	■	□	■	■	□	■	□	n.d.	
8430410A17Rik	■	□	■	■	■	□	□	□	■	■	CDS	*Mm*
Trp53inp2	■	■	■	□	■	■	■	□	□	□	3′	*Hs*
Kcnf1	■	□	■	□	■	■	□	■	■	■	3′	*Mm*
Hao1	□	■	■	□	■	□	■	□	□	■	3′	*Mm*
Mkrn1	■	■	□	□	■	■	■	□	□	□	n.d.	
Gstm6	■	■	□	□	■	■	■	□	□	□	3′	*Mm*
Pdcl3	□	□	■	■	□	■	■	□	■	■	n.d.	
AI45035/Pex12	■	□	□	□	■	■	□	□	■	■	n.a.	*Mm*
Arflp2	■	□	□	□	■	■	□	□	■	■	n.d.	
BC051227	□	□	□	■	■	■	□	□	■	□	CDS	*Mm*
Ppp1r1b	■	□	□	□	■	■	□	□	□	■	5′	*Mm*
Gstt3	■	■	□	□	□	■	■	□	□	□	CDS	*Mm*
D5Ertd255e	□	□	■	■	□	□	□	■	■	□	n.d.	
Dlg2	□	□	■	□	■	□	□	□	■	■	CDS/3′	*Mm/Hs*
Lnx1	■	□	□	□	■	■	□	□	□	□	n.d.	
Lsm12	□	■	□	■	□	□	□	□	■	□	n.d.	
Pabpc4l	□	■	□	■	□	□	□	□	■	□	CDS	*Mm*
4930579E17Rik	□	■	□	□	■	□	□	□	□	■	3′	*Mm*
Dhx32	■	□	□	■	□	■	□	□	□	□	n.d.	
Ankrd29	□	□	□	■	□	■	□	□	■	■	3′	*Hs*
Dirc2	□	□	□	□	■	■	■	□	□	■	n.d.	
Nr4a3	□	□	□	■	□	□	□	□	■	■	5′	*Hs*
2010107G12Rik	■	□	□	□	□	■	□	□	□	□	CDS	*Mm*
Pyroxd1	■	□	□	□	□	■	□	□	□	□	CDS	*Hs*

Figure 1.12: Novel mRNA targets for IRP1 and IRP2. (A) Number of mRNAs detected as enriched in IRP1, IRP2, or both IRPs by microarrays with MAS5, RMA, or a combined (MAS5 + RMA) mathematical data analysis. **(B)** Virtual heatmap representing the 44 identified mRNAs that are bound by both IRPs in at least one of the 5 studied tissues. Affymetrix-positive probes were grouped by gene and reported in each of the rows. Known IRE-containing mRNAs are shown in green. Red and black squares indicate positive or lacking IP enrichment, respectively, relative to mock IPs in 2 independent biologic replicas. Predicted IREs by SIREs program in mouse (*Mus musculus*, *Mm*.) or human (*Homo sapiens*, *Hs*.) databases and their positions also are indicated. N.d. denotes that an IRE motif was not detected using the SIREs bioinformatic program; n.a. denotes no-available information; and 3′ or 5′ denotes the 3′ or 5′IRE. The mouse Ppp1r1b gene is highlighted in blue. Picture modified from Sanchez et al 2011.

In addition, these IRP immunoprecipitated mRNAs were tested with the bioinformatics web tool SIREs (Searching for IREs) (Campillos, Cases, Hentze, & Sanchez, 2010) to predict the existence of putative IRE motifs in their sequence. Among the IRP immunoprecipitated mRNA by both IRP1 and IRP2 there was the *Ppp1r1b* gene (Figure 1.12, marked in blue).

1.7.1. PPP1R1B: a novel IRP-target mRNA candidate

Therefore, my thesis is focused in the characterization of this novel IRP-target mRNA: Protein Phosphatase 1 Regulatory inhibitor subunit 1B (*PPP1R1B*). In the next section I will describe what is known so far about the structure and function of *PPP1R1B*.

PPP1R1B human gene is located on the 17q12 chromosome and encodes an enzyme called DARPP-32 (Dopamine and cAMP regulated Phosphoprotein of 32-kDa). Darpp-32 was firstly characterized as an inhibitor of protein phosphatase 1 (PP1) by the Nobel Prize Paul Greengard and collaborators in 1980s (Walaas, S. I., Aswad, & Greengard, 1983).

1.7.2. PPP1R1B transcripts and proteins

Human *PPP1R1B* gene has eight exons and its translation results in three different transcript variants produced by alternative promoter usage and alternative splicing at the first exon generating two protein isoforms: DARPP-32 or t-DARPP-32 (truncated) (Avanes, Lenz, & Momand, 2019). Figure 1.13 summarizes human *PPP1R1B* transcript variants and protein isoforms.

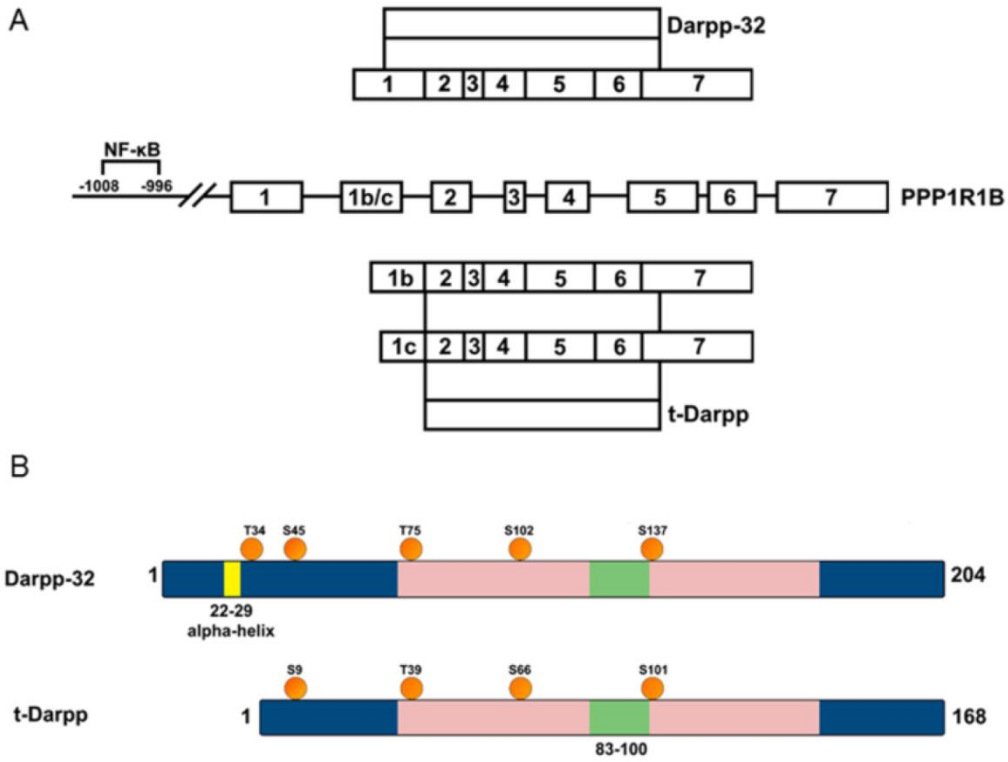

Figure 1.13: Gene structure, transcripts and proteins products of human *PPP1R1B* gene. (A) Canonical transcripts and the two documented protein products. Inclusion of exon 1 creates a transcript that produces DARPP-32. Inclusion of exon 1b or exon 1c creates a transcript that produces t-DARPP-32. NF-kB transcription factor binding sites were described in the promoter of the gene. **(B)** Schematic diagram showing motifs and phosphorylation sites on DARPP-32 and t-DARPP-32. Picture modified from Avanes et al 2019.

DARPP-32 is a neurotransmission integrator. The activation of the dopamine receptor 1 promotes the generation of cAMP, leading to PKA-mediated phosphorylation of DARPP-32 on its Threonine 34, resulting in PP1 inhibition. On the other hand, the activation of dopamine receptor 2 or N-methyl-D-aspartate receptor (NMDAR), an ionotropic glutamate receptor, leads to dephosphorylation of pThr34-DARPP-32 via calcineurin impeding the PP1 inhibition (RW.ERROR - Unable to find reference:doc:618ba4e58f0831dacc25667a; Halpain, Girault, & Greengard, 1990; Svenningsson et al., 2004). The truncated isoform of DARPP-32 lacks the firsts 36 N-terminal amino acids. Therefore, PKA cannot phosphorylate the Thr34, so t-DARPP-32 loses its ability to inhibit PP1. This truncated isoform is associated with tumorigenesis, inducing cell proliferation and resistance to apoptosis both *in vitro* and *in vivo* (Christenson & Kane, 2014; Denny & Kane, 2015; El-Rifai et al., 2002; Vangamudi et al., 2010). In addition, the expression of t-DARPP-32 in the central nervous system has been implicated in the pathogenesis of schizophrenia and cognitive disorders (Kunii et al., 2011; Svenningsson et al., 2004).

1.7.3. DARPP-32 and t-DARPP-32: tissue expression

In adults, human *PPP1R1B* is expressed in brain regions responsive to dopamine signaling including the caudate, putamen, nucleus accumbens, cerebral and cerebellar cortex (Berger, Febvret, Greengard, & Goldman-Rakic, 1990; Brené et al., 1994; Brené et al., 1995; Ouimet, Miller, Hemmings, Walaas, & Greengard, 1984). *PPP1R1B* is also expressed in the duodenum, colon, fat and some glandular tissues such as salivary gland or testis (Fagerberg et al., 2014) (Figure 1.14). Additionally, both DARPP-32 and t-DARPP-32 has been shown to be overexpressed in cancerogenous tissues from breast, colon, esophageal, gastric, lung and prostate (Alam et al., 2018; Belkhiri, Zhu, & El-Rifai, 2016; Ebihara et al., 2004).

The mouse Darpp-32 tissue expression is quite different to human. Mice presents restricted expression pattern, where Darpp-32 is mainly expressed in basal ganglia, specifically in nucleus accumbens. It is also expressed in salivary gland and small intestine according to BioGPS (Figure 1.14). It contrasts to human DARPP-32 expression that is more extended in brain. The tissue expression pattern of mouse *Ppp1r1b* is in agreement with its immunoprecipitation by IRPs only in duodenum and brain from the 5 tested tissues (Figure 1.12).

Figure 1.14: Human PPP1R1B tissue gene expression. (A) The PPP1R1B gene expression in different tissues. **(B)** PPP1R1B isoform differential expression in the same tissues. A putative IRE-like hairpin is represented in the isoform 1. Images are modified from GTEx (Genotype-Tissue Expression).

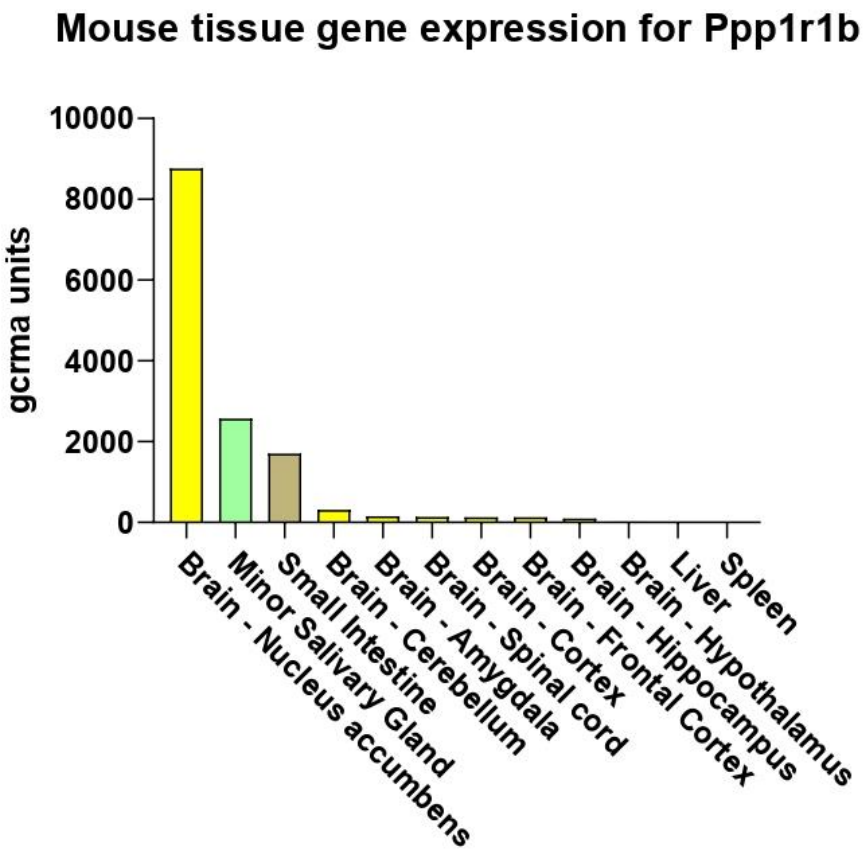

Figure 1.15: Mouse *Ppp1r1b* tissue expression. Graphic representation of mouse *Ppp1r1b* tissue expression in gcrma units. Data from BioGPS.

1.7.4. Role of DARPP-32 and t-DARPP-32

The activity of DARPP-32 depends on its phosphorylation status at multiple regulatory sites, including in its aminoacidic residues Thr34, Thr75, Ser102 (analogue of mouse Ser97), and Ser137 (analogue of mouse Ser130). The phosphorylation pattern is dependent on the dynamic balance between activation of protein kinases and phosphatases (Scheggi, De Montis, & Gambarana, 2018). When DARPP-32 is phosphorylated at Thr34 by protein kinase A (PKA) it binds and inhibits PP1 (Hemmings, Williams, Konigsberg, & Greengard, 1984). On the contrary, when it is phosphorylated by cyclin-dependent kinase 5 (CdK5) at Thr75, DARPP-32 becomes a PKA inhibitor, resulting in PP1 activation (Bibb et al., 1999). Casein kinase 1 and 2 (CK1 and CK2) also phosphorylate DARPP-32 on Ser137 and Ser102 respectively (Walaas, Sven Ivar, Hemmings, Greengard, & Nairn, 2011). Phosphorylation of Ser137 increases phosphorylation of Thr34 through inhibition of PP2B promoting dopaminergic signaling via the cAMP/PKA/DARPP-32/PP-1 pathway. Finally, the phosphorylation of Ser102 residue enhances the interaction between DARPP-32 and adducins. DARPP-32 phosphorylation-target residues are summarized in Figure 1.16.

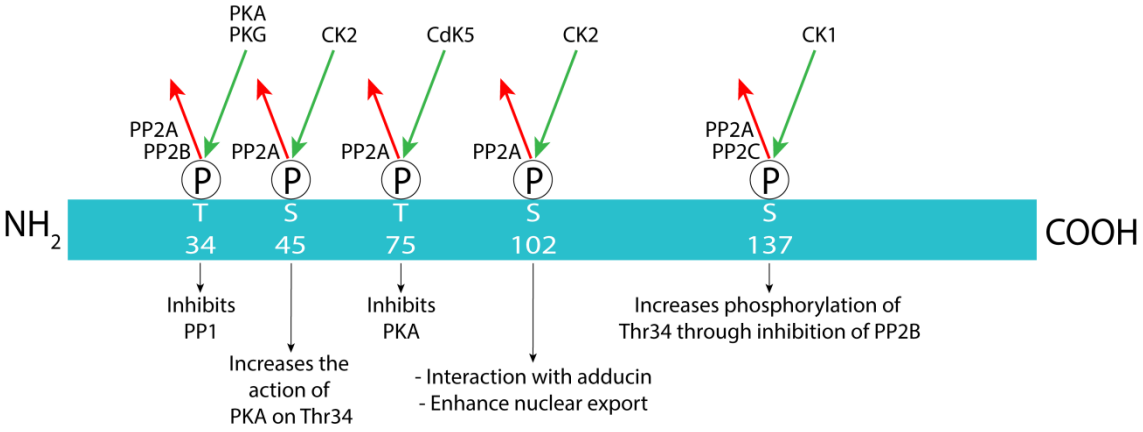

Figure 1.16: Phosphorylation-target residues of DARPP-32. Schematic representation of human DARPP-32 and its *in vivo* phosphorylation residues (Thr-34, Ser-45, Thr-75, Ser-102 and Ser-137). Kinases are indicated above by green arrows (phosphorylation) and protein phosphatases beside by red arrows (dephosphorylation). The role of the phosphorylation is described below each residue. P, phosphate; T, Threonine; S, Serine; PKA, Protein kinase A; PKG, Protein kinase G; PP2A, Protein phosphatase 2A; PP2B, Protein phosphatase 2B; PP2C, Protein phosphatase 2C; CK1, casein kinase 1; CK2, Casein kinase 2; CdK5, Cyclin-dependent kinase 5 Picture modified from Yger *et. al.*

Adducins are a family of proteins that regulate the assembly of the spectrin-actin network providing physical support to the plasma membrane. Adducins also participates in several molecular pathways as substrate for protein kinase A and C (PKA, PKC) and tyrosine kinase phosphorylation (Kiang & Leung, 2018). Moreover, adducin also participates in the endocytosis pathway by modulating actin cytoskeleton (Torielli et al., 2008). DARPP-32 modifies the cytoskeleton via adducins by two different ways. On one hand, by directly interacting with adducin, impairing the stabilization of the actin cytoskeleton. As shown in the figure 1.16, the phosphorylation of Ser102 (Ser 97 in mouse) increase the interaction between adducines and DARPP-32 (Engmann et al., 2015). On the other hand, DARPP-32 also indirectly modifies the state of phosphorylation of adducins via inhibition of PKA. pThr75-DARPP-32 inhibits PKA, which in turn inhibits PP2A leading to an excess of pSer713-adducin. The phosphorylation of this residue impedes the assembly of the spectrin-actin network (Engmann et al., 2015). PKC can phosphorylate adducin on its Ser713 and PP2A dephosphorylates this same adducin residue. Moreover, pThr75-DARPP-32 inhibits pSer713-adducin dephosphorylation through inhibition of PKA, preventing interaction with spectrin-actin network (Engmann et al., 2015). Figure 1.17 summarizes the interaction between adducin and DARPP-32 proteins.

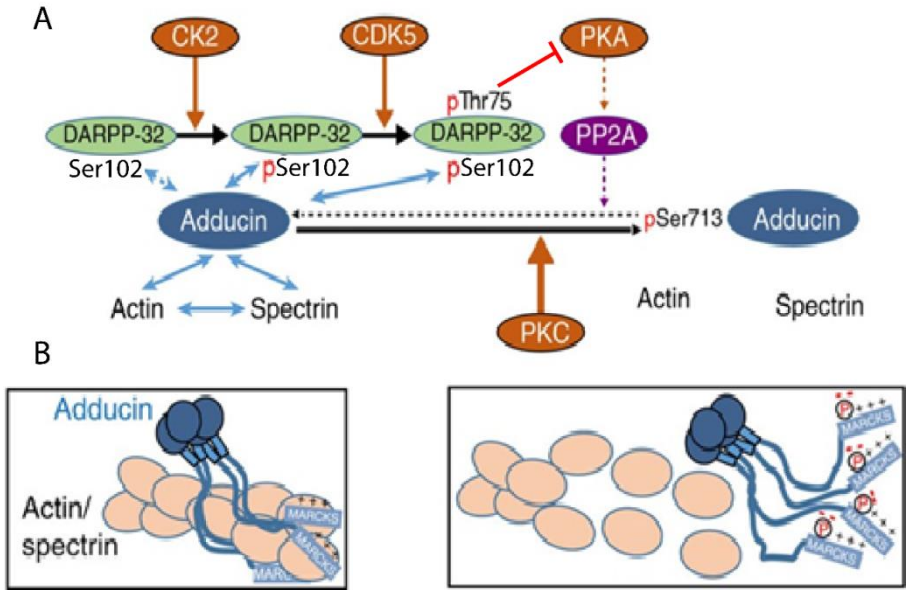

Figure 1.17: Model of human DARPP-32 and β-adducin interactions. (A) DARPP-32 can interact with β-adducin and this interaction is increased by phosphorylation of DARPP-32 on Ser102 by casein kinase II (CK2). When DARPP-32 is phosphorylated by cyclin-dependent kinase 5 (CdK5) on its Thr75 it inhibits PKA. Since PKA activates protein phosphatase 2A (PP2A), which dephosphorylates β-adducin Ser713, pThr75-DARPP-32 increases β-adducin phosphorylation level (resulting from PKC action). **(B)** Phosphorylation of β-adducin prevents its interaction with actin and spectrin and destabilizes cortical cytoskeleton. Picture modified from Engmann et al 2015.

Furthermore, Collinet and collaborators used HeLa cells to phenotypically profile genes involved in the clathrin-mediated endocytosis of both EGFR and TFR1, the prototype tyrosine kinase receptors of endocytosis. By means of a whole genome silencing approach they identified more than 4000 genes involved in the clathrin-mediated endocytosis; among them, I retrieved *PPP1R1B.* The silencing of *PPP1R1B* results in the selective upregulation of TFR1 endocytosis and notably it does not affect EGFR endocytosis (Collinet et al., 2010). This data suggest a possible link between DARPP-32 and iron metabolism through the transferrin /transferrin receptor endocytosis.

Regarding t-DARPP-32, it presents calcium-binding activity that activates PKA upon phosphorylation by CdK1 or CdK5 at Thr39 (analogous to Thr75 in DARPP-32) (Momand et al., 2017; Theile, Geng, Denny, Momand, & Kane, 2017). In addition, t-DARPP-32 also forms a complex with insulin-like growth factor 1 receptor (IGF1R), resulting in increased glucose uptake, glucose catabolism, and robust signaling through the AKT anti-apoptosis pathway (Lenz et al., 2018). It is hypothesized that this mechanism leads to cell survival in cancer cells.

1.7.5. Mouse knockout model of the *Ppp1r1b* gene

In contrast to other molecules, for which specific pharmacological agonists and antagonists are available, no such agents exist for DARPP-32 (Fienberg & Greengard, 2000). Thus, Fienberg and collaborators developed a transgenic mouse with a disruption in the translational start site in exon 1 of Darpp-32. Darpp-32 mutant mice present significant reduction in neurotransmitter release (Fienberg & Greengard, 2000), in concordance with Darpp-32 playing an important role in neuronal vesicle trafficking. The DARPP-32 knockout mice were severely impaired in reacquisition of the discriminated operant task (Heyser, Fienberg, Greengard, & Gold, 2000) and they are generally more sensitive to drugs of abuse such as cocaine (Fienberg & Greengard, 2000).

Different authors agree that DARPP-32 has a growth inhibitory effect on cells and t-DARPP-32 has the opposite effect promoting cell proliferation (Christenson & Kane, 2014; Ebihara et al., 2004; Hansen, Greengard, Nairn, Andersson, & Vogel, 2006; Hansen et al., 2009; Pimenta et al., 2007; Televantou et al., 2013). Interestingly, Darpp-32 KO mice do not present increased spontaneous tumorigenesis versus wild type mice suggesting that Darpp-32 does not contribute to early tumor onset. Indeed, the net rate of tumor growth in darpp-32 KO mice is minor (Christenson & Kane, 2014). These data suggest that Darpp-32 and t-Darpp-32 play a role in enhancing tumor growth rather than cancer initiation (Avanes et al., 2019; Christenson & Kane, 2014). Unfortunately, in KO Darpp-32 mice hematological and systemic iron balance parameters were not characterized in those mice. The KO Darpp-32 mice were generated more than 20 years ago and nowadays only embryonic stem cells (ESC) are available.

2. Hypotheses

Due to the central role of the post-transcriptional IRP/IRE regulatory system in iron homeostasis, we hypothesized that novel not yet discovered mRNAs could be controlled by that system. Our results (see section 5) reveal that this is the case as we have identified *Ppp1r1b* as a new gene with a 5' IRE in its mRNA regulated by IRPs and iron cellular levels.

In addition, we wanted to contribute to extend the implication of IREs in human diseases, in particularly characterizing new cases of the human disease HHCS (see section 5.1.) and by studying the role in iron homeostasis of the 3' IRE of Dmt1 (*Slc11a2* gene) in a mouse model (see section 5.2.).

Overall, this thesis contributes to a better understanding of the IRP/IRE regulatory system and provides relevant data for the iron metabolism field and for iron-related diseases.

3. Objectives

Iron responsive elements (IRE) are cis-regulatory elements present in mRNAs that encode for proteins involved in iron metabolism. These IREs are regulated by iron regulatory proteins 1 and 2 (IRP1 and IRP2) in a post-transcriptional regulatory manner. The dysregulation of the IRP/IRE system is involved in human diseases such as Hereditary Hyperferritinemia with Cataract Syndrome (HHCS) and mRNAs containing IREs are involved in human diseases such as *Slc11a2* mRNA (Dmt1 protein) that is responsible for Anemia Hypochromic Microcytic, with Iron Overload 1 (AHMIO1).

Taking into consideration the importance of the IRP/IRE regulatory system in cellular iron homeostasis and human diseases, the objectives of this thesis are:

1) The characterization of new human cases of Hereditary Hyperferritinemia with Cataract Syndrome (HHCS), an autosomal dominant (AD) disease characterized by mutations in the 5' IRE of *FTL* gene.

2) The characterization of the role of the 3' IRE in the *Slc11a2* gene (encoding Dmt1 protein) in a murine model (Collaboration with Dr. Bruno Galy, Heidelberg, Germany).

3) The study of *Ppp1r1b* as a novel mRNA interacting with iron regulatory proteins (IRPs) and its regulation by iron.

4. Materials and Methods

4.1.Materials

4.1.1. Chemicals and Reagents

Reagent	Company
Acrylamide	Sigma
Agarose	Condalab
Aminoallyl-ATTO680-UTP	Jena Bioscience
Ammonium persulfate – APS	Sigma
Bio-Rad Protein Assay Dye Reagent Concentrate	Bio-Rad
Bovine Serum Albumin – BSA	Roche
Bromophenol Blue – BPB	Sigma
Chloroform	PanReac
cOmplete EDTA-freee Protease Inhibitor Cocktail Tablets	Roche
Deferoxamine mesylate – DFO	Sigma
Deoxynucleotides set – dNTPs	Labclinics
Dimethil Sulfoxide – DMSO	Sigma
Dithiothreitol – DTT	Sigma
DMEM high glucose with pyruvate, without L-glutamine	Sigma
EMEM	ATCC
Ethanol absolute	Panreac
Ethidium bromide	Inno-train
Ethylenediaminetetraacetic acid – EDTA	PanReac
Ferric Amonium Citrate – FAC	Sigma
Fetal Bovine Serum	Quimigen
Glycerol	VWR

Glycine	Sigma
Glycogen	ThermoFisher
Heparin sodium	Sigma
Hydrochloric acid 37% - HCl	VWR
L-glutamine	Labclinics
Lipofectamine	Invitrogen
Luminata	Sigma
MEGAscript kit	Ambion
Methanol	VWR
NNNN-Tetramethylethylenediamine – TEMED	Sigma
NP40	Sigma
NucleoBond Xtra Maxi	Macherey-Nagel
Nucleospin plasmid mini DNA purification kit	Macherey-Nagel
Opti-MEM	Gibco
Phenol-Chloroform-isoamyl alcohol mixture (25:24:1)	Sigma
Potassium chloride – KCl	VWR
PureYield Plasmid Midiprep System	Macherey-Nagel
Random Primers	Promega
Sodium acetate - CH_3COONa	PanReac
Sodium cloride – NaCl	VWR
Sodium dodecyl sulphate – SDS	Bio-Rad
TRIReagent	Ambion
TRIS base	Sigma
Tris-Borate-EDTA (TBE) buffer (5X)	Thermo Fisher
Tris/Glycine/SDS Buffer (10X)	Bio-Rad
Triton X100	Sigma
Tween 20	Sigma

β-Mercaptoethanol	Sigma

4.1.2. Antibodies and Enzymes

Antobodies used for Western blotting:

Primary	Source	Dilution	Secondary	Company	Dilution
Ferritin (both FTH and FTL)	Abcam	1:3000	α-rabbit-HRP conjugated	Jackson Immunoresearch	1:5000
PPP1R1B	Abcam	1:3000	α-rabbit-HRP conjugated	Jackson Immunoresearch	1:5000
β-actin	Sigma	1:50.000	α-mouse-HRP conjugated	Jackson Immunoresearch	1:50.000

Enzymes used in this study:

Enzyme	Company
HindIII	New England Biolabs
KpnI	New England Biolabs
Pfu DNA polymerase	EMBL Heidelberg core facility
Quick Ligation kit (T4 DNA ligase)	New England Biolabs
RNasin Ribonuclease Inhibitor	EMBL Heidelberg core facility
T7 RNA polymerase	EMBL Heidelberg core facility
XbaI	New England Biolabs

4.1.3. Buffers and solutions

All solutions are prepared with MilliQ water (Millipore).

Buffer	Composition
Cytoplasmic lysis buffer (CLB) - for EMSA	25mM TRIS/HCl pH 7.4
	40mM KCl
	1% Triton X100
	1x cOmplete, EDTA free protease inhibitor cocktail
Luria Bertani broth (LB) pH 7.0 - bacterial culture medium	10g tryptone
	5g yeast extract

	10g NaCl adjust pH to 7.0 and autoclave (1.5% agar - added for plates) cool down to -50ºC and add 100 µg/ml ampicillin or 30 µg/ml kanamycin
TLL	20mM TRIS pH 7.4 5mM EDTA 150mM NaCl
TBS buffer	50mM TRIS/HCl pH 7.4 150mM NaCl
TBST buffer pH 8.0 - 8.4 (10x)	0.6M TRIS/HCl pH 7.4 1.5M NaCl 20% Tween 20

4.1.4. Instruments

Instrument	Company
Centrifuge	Eppendorf
Eletrophoresis power supply	Bio-Rad
Transfer iBlot2	Invitrogen
Minispin	DLAB
Nanodrop	ThermoFisher
Thermomixer	Eppendorf
Odyssey Infrared Imaging System	LI-COR

4.1.5. Primers

All primers are purchased in IDT and diluted to 100µM with H_2O following manufacturer instructions.

Table 4.1: Primer sequences.

Gene	Specie	Sequence (5' → 3')	Use
Ppp1r1b	Mm	CcctgggtgcggggacagtgctcctcctcctccT	cloning
Ppp1r1b	Mm	CTAGAggaggaggaggagcactgtccccgcacccaggGGTAC	cloning
Ppp1r1b	Mm	CcctgggtgcggggaagtgctcctcctcctccT	cloning
Ppp1r1b	Mm	CTAGAggaggaggaggagcacttccccgcacccaggGGTAC	cloning
PPP1R1B	Hs	CgagggagcgaggcacagacctggctcagcgT	cloning
PPP1R1B	Hs	CgagggagcgaggacagacctggctcagcgT	cloning
PPP1R1B	Hs	CcctgggtgcggggaagtgctcctcctcctccT	cloning
PPP1R1B	Hs	CTAGAggaggaggaggagcacttccccgcacccaggGGTAC	cloning
Fth1	Mm	TGGAACTGCACAAACTGGCTACT ATGGATTTCACCTGTTCACTCAGATAA	qPCR
Tfrc	Mm	CCCATGACGTTGAATTGAACCT GTAGTCTCCACGAGCGGAATA	qPCR

Epas1	Mm	ACCCCGAGGAGCTACTTGGA GTTTGGCTAGCATCCGGTACTG	qPCR
Ppp1r1b	Mm	TATACGCCCCCATCACTGAAA GTACCCAAGCTCCCGAAGCT	qPCR
Slc40a1	Mm	GGGTGGATAAGAATGCCAGACTT GTCAGGAGCTCATTCTTGTGTAGGA	qPCR
Gox	Mm	GTGTTCAAGATGTCCTCGAGATATTG CAAGTAATCCACGCTGGAAAAAA	qPCR
Slc11a2 – IRE	Mm	AGCTAGGGCATGTGGCACTCT ATGTTGCCACCGCTGGTATC	qPCR
Slc11a2 – non IRE	Mm	GTGGTGGCTGCAGTGGTTAGCG GCGGTCAGTCCCAGGCGGTACG	qPCR
Gapdh	Mm	GTGGAGATTGTTGCCATCAACGA CCCATTCTCGGCCTTGACTGT	qPCR
FTL	Hs	GGGCTGAGACTCCTATGTGC GCAGCTGGAGGAAATTAGGG	Sanger

4.1.6. Plasmid constructs

Table 4.2: Plasmid vectors.

Insert	Gene	Specie	Backbone	Use
FTH1 IRE WT	*FTH1*	Hs	pI12-CAT (Gray et al., 1993)	EMSA
FTH1 IRE MUT ΔC apical loop	*FTH1*	Hs	pI12-CAT (Gray et al., 1993)	EMSA
Ppp1r1b IRE WT	*Ppp1r1b*	Mm	pI12-CAT (Gray et al., 1993)	EMSA
Ppp1r1b IRE MUT ΔC apical loop	*Ppp1r1b*	Mm	pI12-CAT (Gray et al., 1993)	EMSA
PPP1R1B IRE WT	*PPP1R1B*	Hs	pI12-CAT (Gray et al., 1993)	EMSA
PPP1R1B IRE MUT ΔC apical loop	*PPP1R1B*	Hs	pI12-CAT (Gray et al., 1993)	EMSA
Dmt1 IRE WT	*Slc11a2*	Mm	PCR Blunt II TOPO (Invitrogen)	EMSA
Dmt1 IRE MUT	*Slc11a2*	Mm	PCR Blunt II TOPO (Invitrogen)	EMSA

4.2.Methods

4.2.1. Cell biology

4.2.1.1. Cell culture

Cells were cultured with DMEM Dulbecco's Modified Eagle Medium (HeLa and U-118 MG) and EMEM Eagle's Minimal Essential Medium (HuTu-80) supplemented with 2mM L-Glutamine, 10% Fetal Bovine Serum and 1% of Penicillin - Streptomycin.

Cells were seeded at a density of $1.5x10^5$ cells per well in 6-well plates. The next day, they were treated with 200μM of deferoxamine (DFO) as an iron chelator or 200μM of Ferric Ammonium Citrate (FAC) as an iron source overnight (16 hours).

4.2.1.2. Transfections

HuTu-80 cells were transcient transfected with IRP1 and IRP2 siRNA using Lipofectamine 3000 and OptiMEM following the manufacturer instructions. Luciferase siRNA was used as control. 4-5 hours after transfection the medium was changed for

complete culture medium. The day after transfection different wells were treated with DFO to stimulate the IRPs pathway.

4.2.2. Molecular biology and biochemistry

4.2.2.1. RNA extraction

Total RNA was extracted using 1mL of TRIReagent by resuspension of cell pellets in Eppendorf tubes which were incubated 10 minutes at room temperature. Then, 200µL of chloroform was added, vortexed and incubated 10 minutes at room temperature. The tubes were centrifuged at 12000 G for 15 minutes at 4ºC. Aqueous phase was extracted into another tube and RNA was precipitated with 500 µL of isopropanol and 60 minutes of incubation at -20ºC. The samples were centrifuged to pellet RNA at 12000 G for 30 minutes at 4ºC. The supernatant was removed and the pellet was washed with 75% ethanol, air dried and re-suspended in MilliQ water. The purity and concentration of RNA was determined measuring the absorbance at 260nm and 280nm using a Nanodrop 1000 (Thermo Scientific). Finally, samples were stored at -80ºC.

4.2.2.2. cDNA synthesis

1 µg of total RNA was reverse transcribed with Random Primers (Life Technologies) and GoScript Reverse Transcriptase (Promega) following the manufacturer's instructions. It was added a negative control reaction without enzyme (reverse transcriptase) to each experiment to evaluate possible DNA contamination. cDNA obtained was stored at -20ºC.

4.2.2.3. Polymerase chain reaction (PCR)

The PCR reaction was performed on a T100 Thermal Cycler (Bio-Rad) with the following conditions: 95ºC 5min, (95ºC 30s, 60ºC 30s, 72ºC 30s) x 30 cycles and 72ºC 7min.The number of cycles and annealing temperature were optimized for each reaction. Primers are listed on Table 4.1. PCR was performed in final volume of 25µL with 1x PCR buffer, 0.3mM dNTPs mix (Fisher Scientific), 0.5µM of forward and reverse primers and 0.1µL of high fidelity Pfu DNA Polymerase (EMBL Heidelberg core facility) and 50ng of DNA template.

4.2.2.4. Quantitative polymerase chain reaction (qPCR)

The cDNA produced in reverse transcription was diluted 1:4. 1µL of this DNA was mixed with iTaq Universal SYBR Green Supermix 2x (Bio-Rad) and 0,3µM of forward and reverse primers. The qPCR conditions were: 95ºC 2 min, (95ºC 15s, 60ºC 1min) x 40 cycles. The run was performed in C1000 Touch Thermal Cycler (Bio-Rad). The expression level of the gene was calculated as the average of the triplicates normalized against housekeeping β-actin.

4.2.2.5. Restriction digestion of DNA

Enzyme restriction was used for linearization of plasmid vectors used in EMSA and cloning strategies. 1µg of DNA was incubated with the appropriate 1x restriction buffer and 10 units of restriction enzyme and incubated at 37ºC overnight. Restriction enzymes used are listed in section 4.1.2. Digestion efficiency was checked by electrophoresis with agarose gel. Linearized DNA was purified with

phenol:chloroform:isoamyl alcohol extraction. It was precipitated using 1:10 volume of 3M NaOAc and 2.5 volumes of ethanol absolute and quantified with Nanodrop 1000 (Thermo Scientific).

4.2.2.6. Agarose DNA electrophoresis

Agarose gels were used at different percentage depending on DNA size. Normally, 1% agarose gel was used for plasmid DNA quality control or for check restriction digestion efficiency, while 2% agarose gel was used for separation of PCR product. The desired amount of agarose was diluted in TAE buffer applying heat and posteriorly cooled down. Ethidium bromide solution was added (0.5µg/mL) and allowed to solidify in a horizontal electrophoresis chamber. DNA was prepared with 1x Loading Buffer and separated at 90V during 45min. Molecular weight markers of 100bp or 1kb were used depending on DNA size. The gel mage was obtained with Gene Flash Bio-imaging (Syngene).

4.2.2.7. Cloning strategies

The cloning of different inserts into the plasmid vector was performed using two restriction enzymes linearizing the vector. Primers are designed with tails containing a restriction site for the restriction enzymes used to linearize the vector (one site in the forward primer and the second one in the reverse). Ligation was performed using Quick Ligation kit (New England Biolabs) according to the manufacturer's instructions. Finally, the ligation product was transformed into competent 5DHα competent E.coli cells by heat-shock. Transformed bacteria were seeded onto LB plates with 100µg/mL of Ampicillin. Selected colonies were grown in LB broth with same antibiotic concentration and plasmid DNA was extracted with Nucleospin plasmid mini DNA purification kit (Macherey-Nagel). 1mL of grown cells was stored at -80ºC with 10% glycerol as cryopreserving. DNA extracted with above mentioned kit was sequenced by Sanger (Macrogen) to verify the cloning success. If the sequence was OK high volume DNA extraction was performed with NucleoBond Xtra Maxi (Macherey-Nagel) from glycerol stock.

4.2.2.8. *In vitro* Transcription

In vitro transcription was used to synthesize RNA probes for EMSA. XbaI-linearized I12CAT plasmid with a T7 promoter followed by the IRE sequence was used as a template. For each reaction, 2µg of linearized DNA was used with 1x *in vitro* transcription buffer, 0.33mM of rATP, rCTP, rGTP, 3.3µM of rUTP (Invitrogen), 20µM of aminoallyl-ATTO680-rUTP (Jena Bioscience), 0.33mM DTT, 20 units of RNasin Ribonuclease Inhibitor (EMBL Heidelberg core facility) and 1µL of T7 RNA Polymerase (EMBL Heidelberg core facility). Mix was incubated for 4 hours at 37ºC. Non-labelled competitors corresponding to competitive EMSA assays were *in vitro* transcribed with MEGAscript T7 kit (Invitrogen) following the manufacturer's instructions.

The RNA synthetized was purified with phenol:chloroform:isoamyl alcohol extraction. It was precipitated using 1:10 volume of 3M NaOAc and 2.5 volumes of ethanol absolute. The concentration of newly RNA was measured with Nanodrop 1000 (Thermo Scientific).

4.2.2.9. Non- Radioactive Electrophoretic Mobility Shift Assay (EMSA)

Direct EMSA was used to assess *in vitro* binding between RNA sequences and recombinant IRPs. Competitive EMSA is a more stringent assay than a direct EMSA. Classical EMSA were done by means of radioactivity, but a non-radioactive version was developed in our laboratory based on Köhn and colleagues paper (Köhn, Lederer, Wächter, & Hüttelmaier, 2010).

In direct EMSAs, fluorescent-labeled probe (ATTO-UTP label) was incubated with recombinant IRP1 or IRP2 diluted in CLB buffer. If a signal band appears it means that there is a binding between RNA and the protein. While in the competitive EMSA, the fluorescent labeled probe corresponds to the FTH1-IRE sequence, which was incubated with recombinant IRP1 or IRP2 diluted in CLB buffer and competes with increasing amounts of non-labeled competitor sequence. If the non-labeled sequence binds with IRPs we will see that the intensity of the FTH1 IRE-IRP shift is reduced due to the competition.

For direct EMSAs, 50ng of labeled probe was heated at 95ºC for 2 minutes and cooled down on ice. FTH1-IRE and a mutant version of it lacking the first C of the IRE apical loop named FTH1-ΔCIRE, which does not interacts with IRPs (Gray, Pantopoulos, Dandekar, Ackrell, & Hentze, 1996), were used as positive and negative control, respectively. For competitive EMSAs, 50ng of FTH1-IRE labeled probe were mixed with increasing molar excess (1x, 5x, 10x, 20x, 40x, 80x) of unlabeled competitors. The mixture was also heated at 95ºC for 2min and cooled down on ice. Then, 200ng of IRP1 or 1250ng of IRP2 on direct EMSAs, and 300ng of IRP1 or 750ng of IRP2 on competitive EMSAs were incubated with the probes during 15 minutes at room temperature for binding. 50µg of heparin was added and incubated during 10 min to avoid unspecific interactions. Finally, 1µL of glycerol 80% was added as loading buffer. The mixture was loaded on a 5% native acrylamide (60:1 acrylamide:bisacrylamide) gel and ran at 100V during 1 hour in a Mini-PROTEAN (Bio-Rad). Gels were scanned directly inside the glass plates using the Odyssey Infrared Imaging System (LI-COR) and images were analyzed with Image Studio Lite v5.2.

4.2.2.10. Total protein extraction from cultured cells

Cells grow adhered to the bottom of the well. Medium was removed by aspiration and cells were washed with PBS. Trypsin was used to detach cells and then, medium has added to avoid trypsin toxicity. Cells were transferred to an Eppendorf tube and centrifuged 3 minutes at 13000 rpm. Supernatant was removed and cell pellet was re-suspended with 20µL of TLL buffer and sonicated. Protein extract was quantified by Bradford assay using BSA as protein standard.

4.2.2.11. Western blotting

20µg of protein extracts was prepared with SDS loading buffer at final concentration of 1x. Protein samples were denaturalized with heat at 95ºC for 5 minutes. Protein extract was loaded on 12% SDS-PAGE gel. Proteins were transferred to polyvinylidene fluoride (PVDF) membranes using the iBlot™ 2 Transfer Device (ThermoFisher Scientific, MA, USA). Transfer of proteins was verified by staining the membranes with Ponceau S (Sigma-Aldrich, St. Louis, MO, USA). Immunoblots were incubated with

blocking solution (5% skim milk in TBST) a minimum of 45 minutes at room temperature. Primary antibody incubation was performed overnight (16h) at 4°C in blocking solution. The day after, the membrane was washed 3 times with 1x TBST and incubated with appropriate secondary antibody coupled to horseradish peroxidase in blocking solution for 1h at room temperature. Primary and secondary antibodies used and respective dilutions were indicated in section 4.1.2. After secondary antibody treatment, the membrane was washed 3 times again with 1x TBST. Then, the membrane was treated with Luminata Forte Western HRP substrate (Millipore) during 1 minute. Images were acquired with ChemiDoc™ MP Imaging System (Bio-Rad) and analyzed with Image Lab software (Bio-Rad). Ferritin was used as a positive control for the treatment and β-actin as housekeeping.

4.2.3. Genetics

4.2.3.1. Sanger sequencing

Genomic DNA was extracted from peripheral blood using the FlexiGene DNA kit (Qiagen, Hilden, Germany) according to manufacturer's instructions. The *FTL* gene was amplified using 50 ng of genomic DNA. Primers used for sequencing are listed in Table 4.1. The resulting amplification products were verified on a 2% ethidium bromide agarose gel. The purified PCR products were sequenced using a conventional Sanger method. Sequencing results were analyzed using Mutation Surveyor software (SoftGenetics LLC, State College, PA, USA).

4.2.3.2. Targeted NGS panels

NGS panel #10010 (BloodGenetics) was used for the patient B-IV.1 diagnosis, described in this thesis. The NGS gene panel (v15) for hereditary hemochromatosis and hyper/hypoferritinaemia include the following nine genes: *HFE*, *HFE2*, *HAMP*, *TFR2*, *SLC40A1*, *BMP6*, *FTL*, *FTH1*, and *GNPAT*. The performed NGS panel follows a protocol reported previously for a different panel (Vila Cuenca et al., 2020)

4.2.4. Statistical analysis

Statistical analysis was done using two-tailed unpaired Student's t test with GraphPad Prism software. Data are shown as mean values ± SD. Statistical signification is considered when p-values < 0.05 and represented with asterisks.

P-value < 0.05*, P-value < 0.01**, P-value < 0.001***.

5. Results and Discussion

5.1. New patients in Hereditary Hyperferritinemia-Cataract Syndrome (HHCS)

The results here exposed were published in the peer-reviewed journal named International journal of Molecular Science (Q1 journal) with impact factor 5.923 (see Annex I).

Int J Mol Sci. 2021 May 21;22(11):5451. doi: 10.3390/ijms22115451. PMID: 34064225

"Hereditary Hyperferritinemia Cataract Syndrome: Ferritin L Gene and Physiopathology behind the Disease-Report of New Cases"

Ferran Celma Nos, Gonzalo Hernández, Xènia Ferrer-Cortès, Ines Hernandez-Rodriguez, Begoña Navarro-Almenzar, José Luis Fuster, Mar Bermúdez Cortés, Santiago Pérez-Montero, Cristian Tornador, Mayka Sanchez

This manuscript is part of a Special Issue focused on Molecular and Genetic Mechanism of Cataracts.

See section 1.6.2.1. for an introduction of HHCS. In brief, HHCS is an autosomal dominant (AD) disease due to mutations in the 5' IRE of the *FTL* gene.

5.1.1. Clinical data of two families with HHCS

I have studied two independent families where probands present the typical clinical features of HHCS of high serum ferritin levels and congenital bilateral cataracts.

Family A

Proband A-III.2 from family A (Figure 5.1) is a 38-year-old woman referred to the Hematology Service at the University Hospital Germans Trias i Pujol (HGTiP) in Barcelona due to unexplained hyperferritinemia. Serum ferritin levels were high (1143 ng/mL), while serum iron and transferrin saturation levels were normal. For this patient, the main biochemical and hematological parameters are listed in Table 5.1. The mother (A-II.3) and the maternal uncle (A-II.2) have reported cataracts and hyperferritinemia. In addition, a first cousin of the mother (A-II.1) has hyperferritinemia. In the proband, genetic studies of Hereditary Hemochromatosis (HH) were negative with no pathogenic mutation found in any of the HH-related genes. Liver magnetic resonance showed normal levels of hepatic iron. Interestingly, but not related to HHCS, three family members died at a young age as a result of ischemic events (cerebral vascular accident or acute myocardial infarction) as reflected in the pedigree, so the proband is also currently under study for thrombophilia.

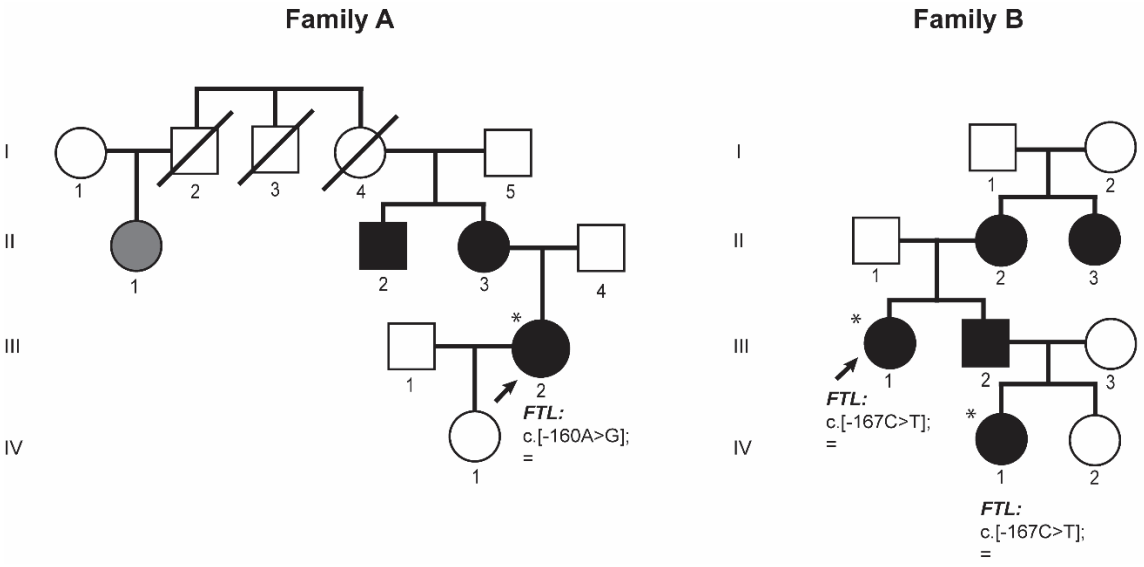

Figure 5.1: Pedigrees of the two studied families affected by HHCS pedigrees. Circles indicate females, and squares, males; slashed symbols indicate deceased individuals. Probands are pointed with an arrow. Filled symbols indicate affected individuals by genetically confirmed HHCS or by the presence of hyperferritinemia and cataracts; grey filled symbol denotes an individual where only hyperferritinemia has been reported. Asterisks indicate subjects with genetic studies done at BloodGenetics SL. Mutations are named according to the HGVS nomenclature.

Table 5.1: Biochemical and hematological data of the two families affected with HHCS. The nomenclature of the mutations follows the HGVS guidelines. Abbreviations meaning: Hb, hemoglobin; MCV, mean corpuscular volume; TF sat, transferrin saturation; F, female; M, male; n.a., not available data.

Case	Family A	Family B	Family B	Reference Values
Patient	III.1	III.1	IV.1	-
Gender	F	F	F	-
Age at diagnosis (years)	38	44	11	-
Hb (g/dL)	13.3	12.7	14	13.5-17.5 (M) 12.1-15.1 (F)
MCV (fL)	83.3	87.9	82.6	80-95
Ferritin (ng/mL)	**1143**	**919**	**931**	12-300 (M) 12-200 (F)
TF sat (%)	23.0	21.9	14.7	25-50
Iron (µg/dL)	66.45	116	n.a.	49-226
***FTL* Mutation (NM_00146.3)**	c.-160 A>C	c.-167 C>T	c.-167 C>T	-

Family B

Proband III.1 from family B (Figure 5.1) is a 44-year-old woman presenting hyperferritinemia since 8-years old, and was referred to the Hematology Service in the University Hospital Virgen de la Arrixaca in Murcia. The patient also had endometriosis. Her serum ferritin level was high (919 ng/mL) while serum iron and transferrin saturation levels were normal (Table 5.1). She was tested for hereditary hemochromatosis *HFE* gene mutation, and she was found to be a carrier of the H63D variant in *HFE* gene (this genetic finding could not explain her hyperferritinemia). Magnetic resonance imaging showed normal liver iron deposits (<20 µmol/g) as expected for a HHCS case. During anamnesis, the patient reported having visual problems, so she was directed to an ophthalmology service, where she was diagnosed with cataracts and underwent cataract surgery at the age of 44 years. At that moment, she was interrogated about her family history. Proband's mother (B-II.2) also has the HFE H63D variant in heterozygous state and had hyperferritinemia too, resulting in a misdiagnose as HH and treated with phlebotomies. Proband's mother (B-II.2) had also undergone cataract surgery when she was younger. Proband's maternal aunt (B-II.3) has hyperferritinemia and cataracts but she has not undergone cataract surgery. The proband also has a brother (B-III.2) with hyperferritinemia and already corrected congenital cataracts and two nieces, one had normal ferritin levels and no cataracts (B-IV.2) and an older niece (B-IV.1) who was also genetically studied because of hyperferritinemia and she was operated for congenital cataracts. For the proband and her older niece, the main biochemical and hematological data are listed in Table 5.1.

The patient B-IV.1 is the niece of the proband (B-III.1) (Figure 5.1), she was 10-year-old when she attended the hematology service due to hyperferritinemia. Her serum ferritin levels were elevated (931 ng/mL) and transferrin saturation was normal. She was diagnosed with cataracts at the age of 10-years old.

5.1.2. Genetic studies

Three members of these two families (Family A-III.2, Family B-III.1 and Family B-IV.1) where genetically studied. The genetic studies revealed the presence of two different but previously described mutations in the *FTL* gene.

Family A

Genetic test by Sanger sequencing performed on the proband (A-III.2) revealed the presence of a heterozygous point mutation c.-160A>G located in the 5′ *FTL* IRE. This mutation consists of a substitution in the conserved apical hexanucleotide loop (CAGUGU) (Figure 5.1). This mutation was indeed the first pathogenic alteration reported for HHCS and described by Beaumont in 1995; the traditional nomenclature referred to it as +40A>G Paris1 mutation.

Family B

After genetic testing by Sanger sequencing of the *FTL* gene on the proband B-III.1 and by a targeted next generation sequencing panel on the patient B-IV.1 from the same family, both patients were found to be heterozygous for the NM_00146.3:c.[-

167C>T];[=] mutation in *FTL* gene. This pathogenic mutation is located in the C-bulge of the *FTL* IRE (Figure 5.1), which is a critical residue for IRP-IRE interaction (see section 1.4.2.). This mutation is also known as the +33C>T Madrid/Philadelphia pathological variant (following the traditional nomenclature) that was reported for the first time by Balas and collaborators (Balas, Aviles, Garcia-Sanchez, & Vicario, 1999).

5.1.3. Discussion

Overall, our clinical and genetic studies revealed a genetic diagnosis for HHCS in these two families. Since it was discovered in 1995, different authors have reported several mutations that affect the *FTL* IRE causing HHCS. We did a literature review of all mutations reported for this disease that can be found in appendix section 8.1.4.1 (Supplementary data Table S1). This exhaustive revision is important as complete lists of mutation in regulatory regions are not fully well reported in databases such as ClinVar. Therefore, a complete list of mutations described in the 5' IRE of the *FTL* gene is an important tool for geneticist and for the accurate diagnostic of these cases.

The only clinical manifestation of patients with HHCS is the presence of cataracts and high serum ferritin levels. A genetic test in patients with hyperferritinemia is crucial to avoid a misdiagnosis with hereditary hemochromatosis (HH) that could lead to the implementation of phlebotomies as treatment. Phlebotomies are not needed in HHCS cases and actually can be counterproductives because it could result in the development of anemia in the HHCS patient. Ophthalmologists should test serum ferritin levels routinely while investigating cataracts especially in pediatric cases. On the other hand, hematologists should refer patients with unexplained hyperferritinemia for ophthalmological assessment, as cataracts may be asymptomatic but lead to a correct diagnosis of HHCS.

5.2. Characterizing the role of the 3' IRE in a mouse model of divalent metal transporter 1 (Dmt1) with an IRE deletion.

We collaborated with the group of Dr. Bruno Galy (German Cancer Research Center (DKFZ), Heidelberg, Germany) assisting with protocols in the characterization of *Dmt1* mutant mice. Results here exposed were published in the peer-reviewed journal named HemaSphere (see Annex II). This journal (HemaSphere) has not yet an impact factor because it is a new journal from the Haematologica group.

Specifically in this work we contributed by testing the 3' Dmt1 IRE disruption by doing competitive EMSAs.

HemaSphere. 2020 Oct; 4(5): e459. doi: 10.1097/HS9.0000000000000459
PMID: 33062942

"Control of Systemic Iron Homeostasis by the 3' Iron-Responsive Element of Divalent Metal Transporter 1 in Mice"

Elisabeth Tybl, Hiromi Gunshin, Sanjay Gupta, Tomasa Barrientos, Michael Bonadonna, Ferran Celma Nos, Gael Palais, Zoubida Karim, Mayka Sanchez, Nancy C. Andrews, and Bruno Galy

See section 1.6.2.2. for an introduction of DMT1 and its mutations.

5.2.1. Test of 3' *Dmt1* IRE disruption by EMSA

The knock-in mouse model *Dmt1*, which has a partial IRE deletion (*Dmt1* ΔIRE), was created in Dr. Galy's group through homologous recombination with a targeting construct in mouse embryonic stem cells. The structure of the murine *Dmt1* IRE stem-loop and the introduced mutation in the *Dmt1* ΔIRE mouse is represented in Figure 5.2.

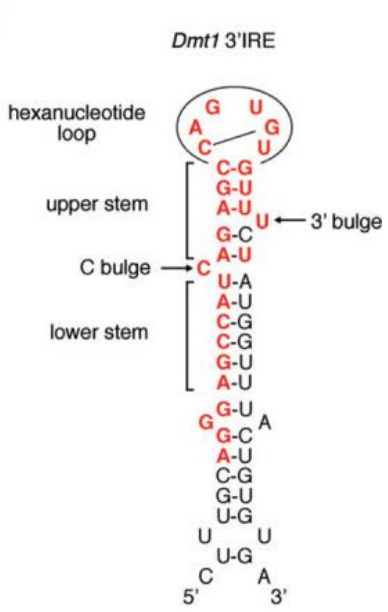

Figure 5.2: Schematic representation of murine *Dmt1* 3' IRE. Bases in red were deleted in the *Dmt1*$^{\Delta IRE}$ knock-in mouse. Picture from Tybl et al. 2020.

In order to determinate if the IRP binding capability of the *Dmt1*$^{\Delta IRE}$ allele was impaired, we performed a competitive non-radioactive EMSA (see methods section 4.2.2.9.). The *Dmt1*^{IRE} and *Dmt1*$^{\Delta IRE}$ sequences were cloned into the plasmid vector pCR-BluntII-TOPO, which has a T7 promoter, for *in vitro* transcription and subsequently we did competitive EMSA. The assay consists in determining if the IRE is functional and able to compete for the binding to the IRPs versus a canonical and strong IRE such as *FTH* IRE. The competition, and the IRE functionality, will result in a reduction of the fluorescent signal (Figure 5.3A). As expected, the wild-type *Dmt1* RNA (Dmt1 WT) competes efficiently, but not the RNA from *Dmt1*$^{\Delta IRE}$ mice (Dmt1 ΔIRE), confirming the loss of functionality and the efficient disruption of the *Dmt1* 3'IRE (Figure 5.3). As controls we used the IRE of *Fth1* wt and a negative competitor *Fth1* mut which consists in a deletion of the first C of the apical loop competing with the labeled *Fth1* wt probe (see section 4.2.2.9.).

5.2.2. Discussion

Our competitive EMSAs experiments confirm the binding between IRP1 and wild type *Dmt1* 3' IRE and the impairment of this coupling with the mutated transcript (*Dmt1* 3' ΔIRE), despite the Dmt1 IRE exhibits a weaker affinity for IRPs than other canonical IREs (Figure 5.3). In agreement with Connell and collaborators, this work confirms that the 3'IRE of *Dmt1* plays a role in controlling DMT1 expression and systemic iron homeostasis (Connell, Danial, & Haastruthers, 2018).

Furthermore, additional experiments for this work shows that Dmt1 3' IRE may play a role in controlling duodenal iron absorption through DMT1 expression throughout mouse life. During postnatal growth, the *Dmt1* 3'IRE secures iron acquisition by promoting intestinal DMT1 expression whereas; in adulthood, it suppresses DMT1 to prevent systemic iron overload. The *Dmt1* IRE seems to influence RNA abundance and stability during early life and mRNA translation in adulthood in the intestine (Tybl et al., 2020). We attribute this age-dependent switch in *Dmt1* IRE to maintain iron homeostasis of immature intestinal absorption early in life, whereas, the 3'IRE may help to fine-tune DMT1 expression to avoid excessive iron assimilation in adulthood (Tybl et al., 2020).

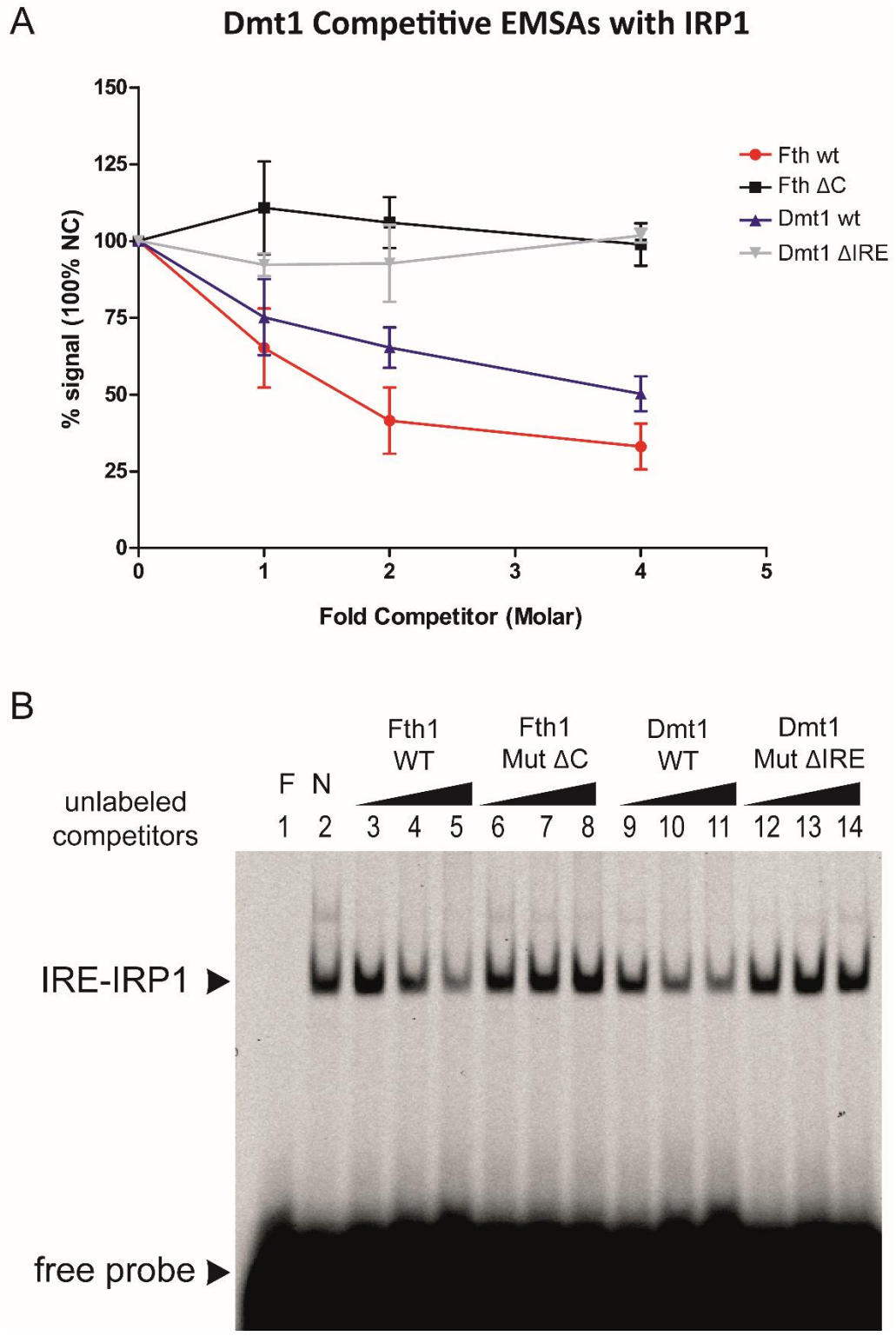

Figure 5.3: Competitive EMSAs with mouse *Dmt1* IRE. (A) Dose-dependent loss of signal and competition of *Dmt1* with recombinant IRP1. Fluorescent labeled *FTH* IRE was incubated with increasing molar excess (1X, 5X, 10X, 20X, 40X and 80X) of unlabeled competitors (WT and ΔC *FTH*, WT and ΔIRE *Dmt1*). **(B)** Representative EMSA gel image where loss of signal show the competition between fluorescent labeled *FTH* IRE and non-labeled *Dmt1* IRE.

5.3.PPP1R1B: a novel IRP-target mRNA

The results exposed here are not yet published.

5.3.1. Ppp1r1b immunoprecipitates together with IRP1 and IRP2

Previously, my supervisor Mayka Sanchez, identified several IRP1 and IRP2 target mRNAs using a high throughput genome-wide approach (Sanchez et al., 2011) (see section 1.7). In that new pool of IRP-interacting mRNAs we find *Ppp1r1b* mRNA. *Ppp1r1b* was selected for further studies since 3 independent Affymetrix microarray probes corresponding to *Ppp1r1b* mRNA were positively detected after RNA immunoprecipitation with IRP1 and IRP2 in duodenum and brain tissues (Figure 1.12). The lack of detection of *Ppp1r1b* in other tested tissues used for immunoprecipitation with IRP1 and IRP2 agree with the selective mouse tissue expression (Figure 1.15).

We further validated the Affymetrix data by qPCR analysis in brain samples where IRP1 mRNPs complexes were immunoprecipitated (Figure 5.4). The qPCR showed that *Ppp1r1b* mRNA was enriched 48 times over the immunoprecipitating control where IRP1 antibody was omitted. Control mRNAs (including *Fth, Tfrc, Slc40a1, Gox* and *Slc11a2*-IRE) were also enriched, while negative controls (including *Slc11a2*-non IRE variant and *Gapdh*) were not enriched.

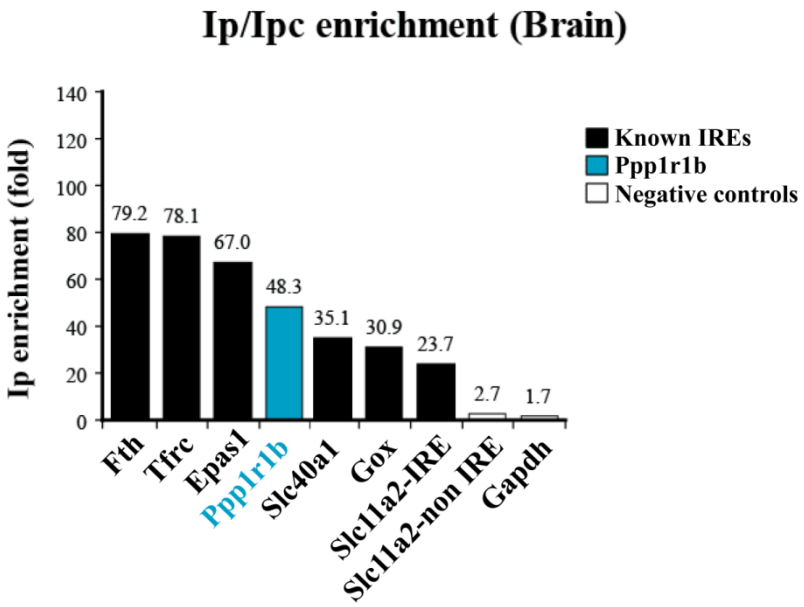

Figure 5.4: Specific enrichment of *Ppp1r1b* mRNA in IRP1 immunoprecipitated fractions. The IRE mRNA-protein complexes (mRNPs) were isolated using anti-IRP1 antibody, recombinant IRP1 and mRNAs from mouse brain (Sanchez et al., 2011). The specificity of IRP1/IRE mRNPs isolation was tested by qPCR analysis of immunoprecipitated (IP) brain samples versus mock IP reactions (no recombinant IRP1 added). Fold enrichment is indicated for Ppp1r1b mRNA as well as for positive IRE containing mRNA controls (*Fth1*, *Tfrc*, *Epas*, *Slc40a1*, *Gox* and the IRE isoform of *Slc11a2*) and negative non-IRE containing mRNAs (*Gapdh* and the non-IRE isoform of *Slc11a2*). qPCR absolute quantification values are reported as means ± SD

5.3.2. Ppp1r1b has a functional 5' Iron Responsive Element (IRE)

A canonical motif-containing 5' IRE was predicted in mouse *Ppp1r1b* (nucleotides 574-605 in NM_144828.2) using the in-house bioinformatics tool (SIREs (http://ccbg.imppc.org/sires/) and the Vienna RNAfold Web Server (http://rna.tbi.univie.ac.at/)) in the mRNA transcript variant 1 encoding the full-length of the Darpp-32 protein. The predicted IRE is in exon 1a (Figure 1.12) and it is not present in other transcripts which encode t-Darpp-32 protein (Figure 5.5A). As in other canonical IREs, mouse *Ppp1r1b* 5' IRE have a 6 nucleotide apical loop (CAGUGC), 5-paired upper stem and an unpaired C bulge at the 5' side of the stem (Figure 5.5C). On the contrary, same bioinformatics tools did not find an IRE in the human *PPP1R1B* homologous sequence (Figure 5.5). Consistent with SIREs and Vienna RNAfold software, the human aligned and homologous sequence to the mouse predicted IRE present with different and non-conserved nucleotides that lead to an altered IRE in several positions. In the homologous human sequence of the mouse Ppp1r1b IRE, there is no pairing between the 1^{st} and 5^{th} position of the hexanucleotide sequence and the upper stem is opened in two positions. Additionally, the lower stem is opened in several positions too (Figure 5.5C). These features indicate that the homologous human sequence to the mouse predicted IRE might not form a structure considered to be a good IRE. In this situation, an additional human sequence (see later) could be the one working as a functional IRE. Therefore, we look for a better human IRE using Vienna RNAflod Web Server software.

In human *PPP1R1B* 5' UTR, RNAfold WebServer (ViennaRNA Web Services, Institute for Theoretical Chemistry, University of Vienna) predicts a sequence that folds forming a hairpin structure (Figure 5.6A) depicted in red at positions 176-205 in NM_032192.4 (Figure 5.6B) that could resemble an IRE. However, this hairpin structure also lacks some of the typical IRE structure components. While the hexanucleotide apical loop of mouse *Ppp1r1b* 5' IRE (CAGUGC) follows a canonical IRE sequence (CAGHGN, see section 1.4.2), the predicted human *PPP1R1B* hairpin loop (CACAGA) is different with a C instead of a G at the third position. However, the first and the fifth nucleotides of the apical loop still could pair allowing the formation of an ACA pseudotriloop. In addition, human *PPP1R1B* hairpin lacks a C-bulge present in canonical IREs. The presence of an atypical apical loop (CACAGA) and the absence of the c-bulge makes that the bioinformatic predictor SIREs does not recognize this as a predicted IRE. ClustalO, EMBL-EBI Web Service reveals that this motif is well conserved in primates (Figure 5.6C). Interestingly, this hairpin motif is only present in the mRNA coding for DARPP-32 but not in the t-DARPP-32 transcripts because it is encoded in exon 1a in a similar way to what happens in the mouse IRE sequence (Figure 1.12). To test the functionality as a potential IRE of this human predicted hairpin loop we performed EMSA experiments as described below.

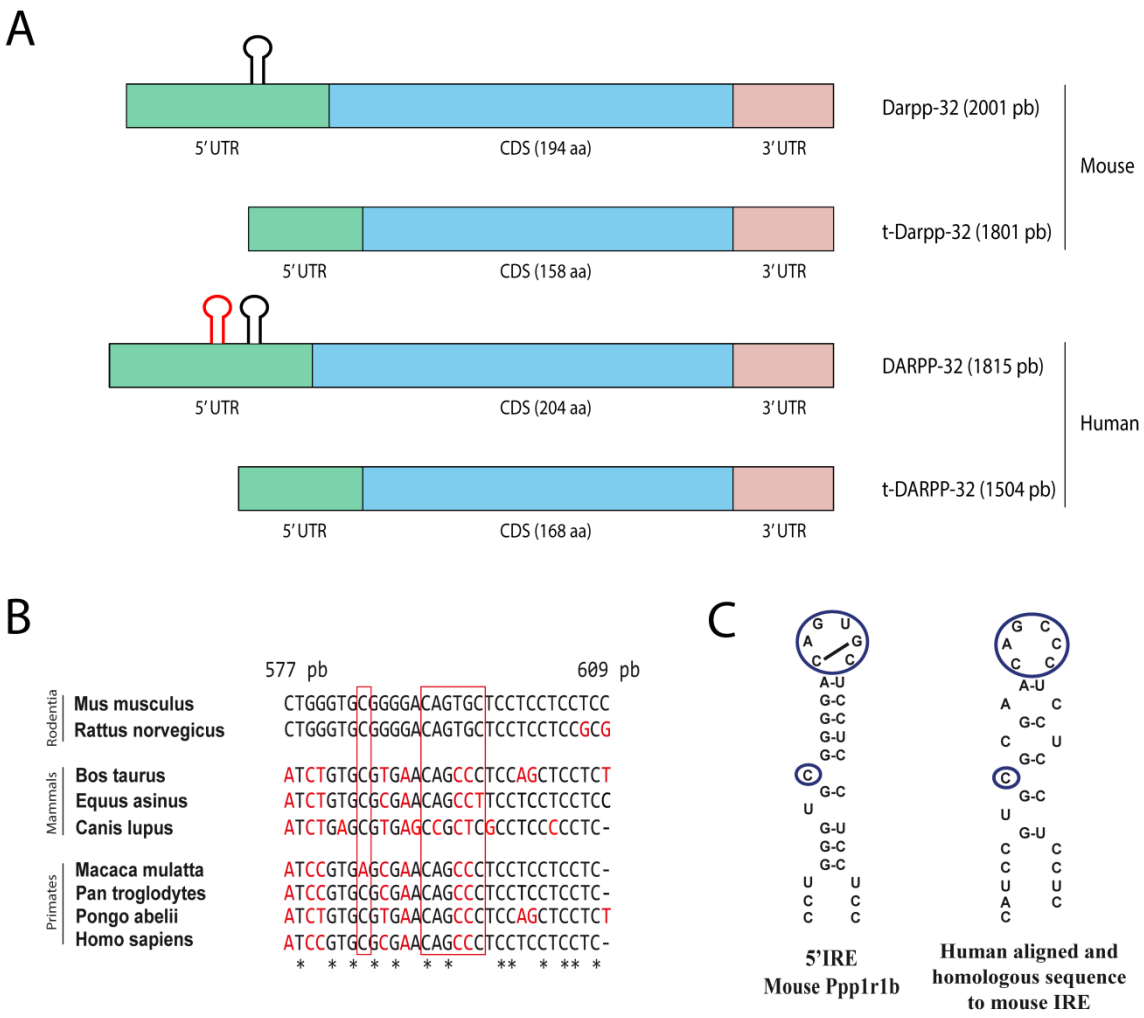

Figure 5.5: *Ppp1r1b* Iron Responsive Element location and comparison. (A) Schematic representation of the mouse and human Darpp-32 protein isoforms: Darpp-32 and t-Darpp-32. The 5'UTR is in green color, CDS in blue and 3'UTR in red. We can see that the CDS of the Darpp-32 is bigger than the t-Darpp-32. The predicted mouse IRE and its human homologous sequence are only located in the 5'UTR of the Darpp-32 isoform in black color. The human hairpin predicted by Vienna RNAfold WebServer is in the 5'UTR of human DARPP-32 in red color. **(B)** Sequence alignment of the mouse IRE motif with other species (including human, *Homo sapiens*). 100% conserved residues are in black, while different residues are in red. The putative IRE and the c-bulge are marked into a red box. Asterisk mark equal nucleotides in the different sequences. The alignment was made following the bases located between the positions 577 and 609 of mouse *Ppp1r1b* transcript. **(C)** Comparison of the mouse IRE motif and the human homologous sequence mRNAs. The c-bulge and the hexanucleotide apical loop are marked with a blue circle.

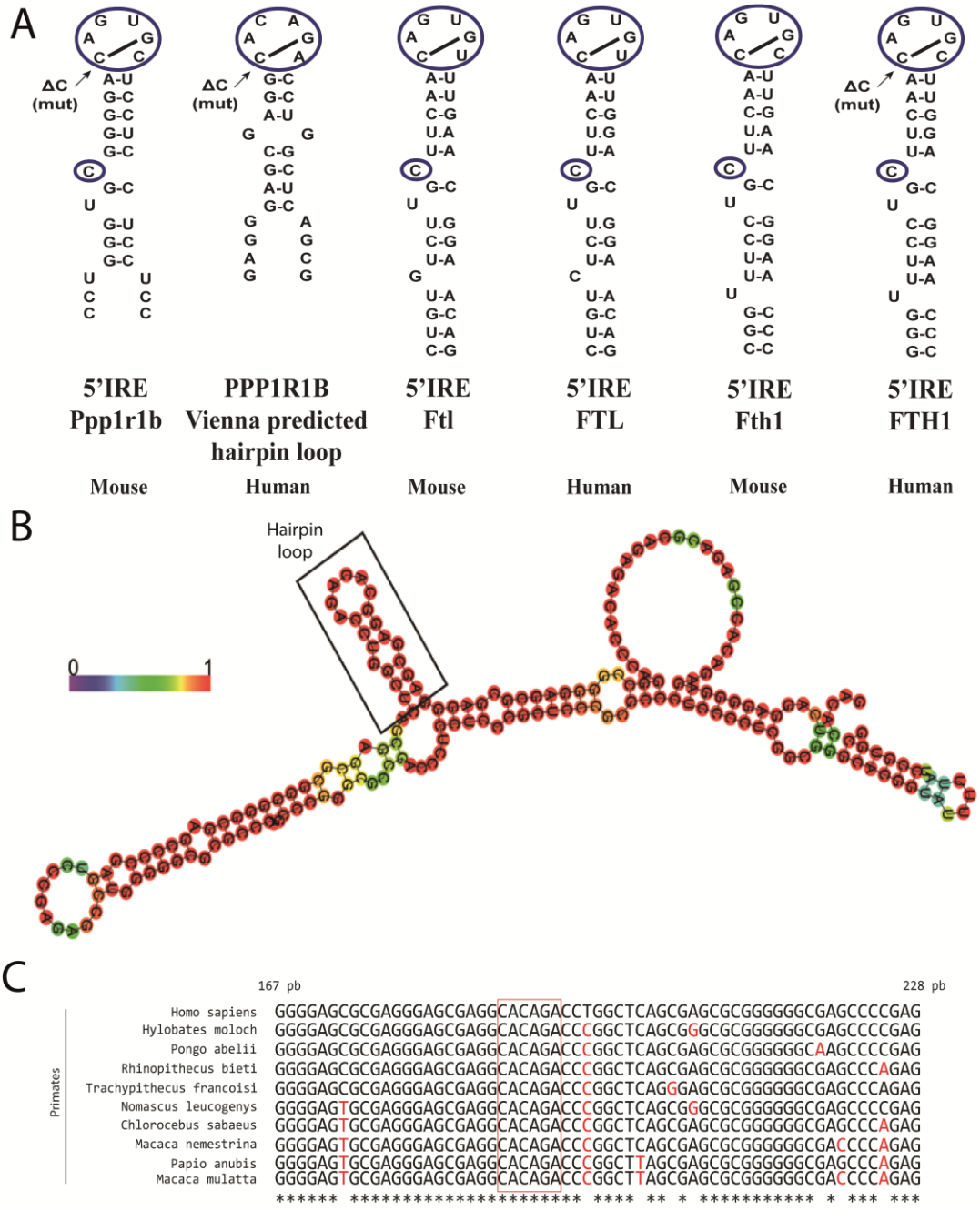

Figure 5.6: *PPP1R1B* predicted hairpin loop. (A) Comparison of the mouse and human 5' IRE motifs in PPP1R1B and ferritins (L and H) mRNAs. Arrows indicate the deletion of the first cytosine (ΔC mut) of the apical loop, used as mutant construct. **(B)** Folding prediction of human fragment of PPP1R1B using RNAfold WebServer (ViennaRNA Web Services, Institute for Theorical Chemistry, University of Vienna). Color indicates the probability of base pairing from 0 (blue, low) to 1 (red, high). The IRE like motif detected in PPP1R1B is boxed. **(C)** Sequence alignment showing phylogenic conservation of PPP1R1B IRE among primates. 100% conserved residues are in black, while different residues are in red. The putative IRE is marked into a red box. The alignment was made following the bases located between the positions 167 and 228 of human PPP1R1B transcript Asterisks mark equal nucleotides.

Ppp1r1b mouse IRE and human *PPP1R1B* Vienna predicted hairpin structure sequences were cloned into pI12 vector, linearized, *in vitro* transcribed and used as labeled probe in a direct EMSA to check the binding capacity between recombinant IRPs and these structures (Figure 5.7). In our *in vitro* direct EMSA using short probes of the mouse and human motif we could detect a binding between mouse *Ppp1r1b* IRE and recombinant IRP1. However, it was not possible to detect a binding between the same probe and recombinant IRP2. This result differs from Sanchez *et al.* 2011 where it was observed that mouse *Ppp1r1b* IRE binds with IRP1 and IRP2 by immunoprecipitation. Therefore, while immunoprecipitation experiments were positive in showing IRP2 – *Ppp1r1b* mouse mRNA binding, in vitro EMSAs were not able to show this interaction. This could be due to a weak interaction between IRP2 and the *Ppp1r1b* mouse mRNA or because of this binding requires physiological conditions for binding that differ from the ones in an *in vitro* EMSAs (i.e. a longer probe or full length RNA could be needed for an efficient binding to IRP2).

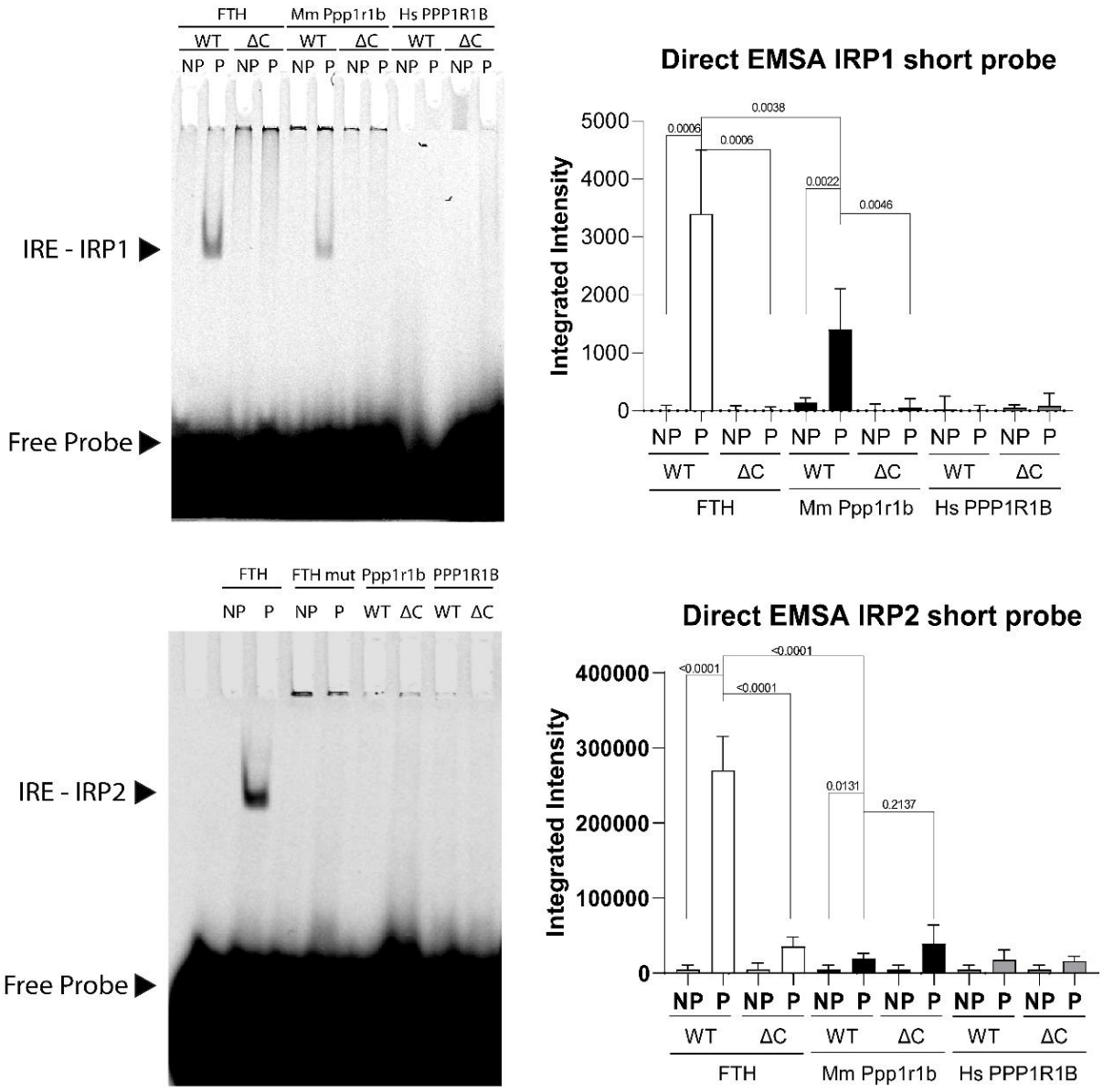

Figure 5.7: Direct EMSAs with mouse and human *PPP1R1B* IRE. Binding between recombinant IRP1 (top) and IRP2 (bottom) with fluorescently-labeled mouse (nucleotides 574-605 in NM_144828.2) and human (nucleotides 176-205 in NM_032192.4) *PPP1R1B* hairpin loop sequence and their respective mutants (lacking the first C of the apical loop). Wild type and mutant human ferritin H have been used as positive and negative control respectively. The images were acquired by Odyssey Infrared Imaging System (LI-CORE Bioscience) and analyzed with Image Studio (LI-CORE Bioscience). NP means no protein; P means protein, with no competitor.

For the human Vienna predicted hairpin structure short probe, we could not detect any binding neither with recombinant IRP1 nor with recombinant IRP2. As positive control for binding we used the original pI12 vector which contains the *FTH* IRE. To confirm that the binding is via the IRE, we created mutant IREs lacking the first cytosine of the apical loop (ΔC mut) of each sequence (Figure 5.6A). All mutants IREs show no IRP1/2 binding in direct EMSA experiments (Figure 5.7). As mentioned before, the human hairpin structure predicted by Vienna fold does not represent a canonical IRE structure and this could be the reason why it does not bind with the IRPs, at least in the conditions we tested by EMSA experiments. Alternative the binding could be very weak and not possible to be detected by *in vitro* direct EMSAs in the tested conditions.

To further study the IRE functionality of these mouse and human sequences, we performed a competitive EMSA against a fluorescent labeled *FTH* mRNA probe using the mouse/human sequences as non-labeled competitor probes (Figure 5.8). In the *in vitro* competitive EMSAs using short probes of the mouse IRE and human hairpin structure motifs, we detected a reduction of the *FTH*-IRP1 signal in mouse *Ppp1r1b* IRE, produced by the competition between both probes, indicating the *in vitro* functionality of the mouse *Ppp1r1b* IRE for binding IRP1 (Figure 5.8A). However, in agreement with direct EMSAs, it was not possible to detect a competition between the probes when we used recombinant IRP2 (Figure 5.8B). For the human hairpin structure short probe we could not detect any competition neither with recombinant IRP1 nor IRP2 (Figure 5.8). As positive control for binding we used the original pI12 vector which contains the *FTH* IRE to compete with the *FTH* labeled probe. As with the direct EMSAs, we used mutant IREs lacking the first cytosine of the apical loop (ΔC mut) of each sequence and they do not show competition as expected (Figure 5.8).

In summary, we conclude that there is a functional 5' IRE that can bind to recombinant IRP1, at least for the mouse Ppp1r1b mRNA in our in vitro direct and competitive EMSA experiments. Binding to recombinant IRP2 was no detected in contrast to immunoprecipitation experiments previously reported (Sanchez et al., 2011). This could be for instance due to a weaker interaction between *Ppp1r1b*-IRE and IRP2 or the necessity of longer probes for detecting the interaction with recombinant IRP2.

As for the predicted human hairpin loop experiments, both direct and competitive EMSAs were unable to show any in vitro binding of the predicted hairpin to both IRP1 and IRP2. Two conclusions can be drawn from these negative results. Either the human hairpin loop is not a *bona fide* IRE (as it is lacking the C-bulge) or the interactions between the human hairpin and the IRPs are too weak to be detected in these *in vitro* assays. It is possible that the probes used are not long enough to detect the interaction because they cannot fold correctly to form the required secondary RNA structure.

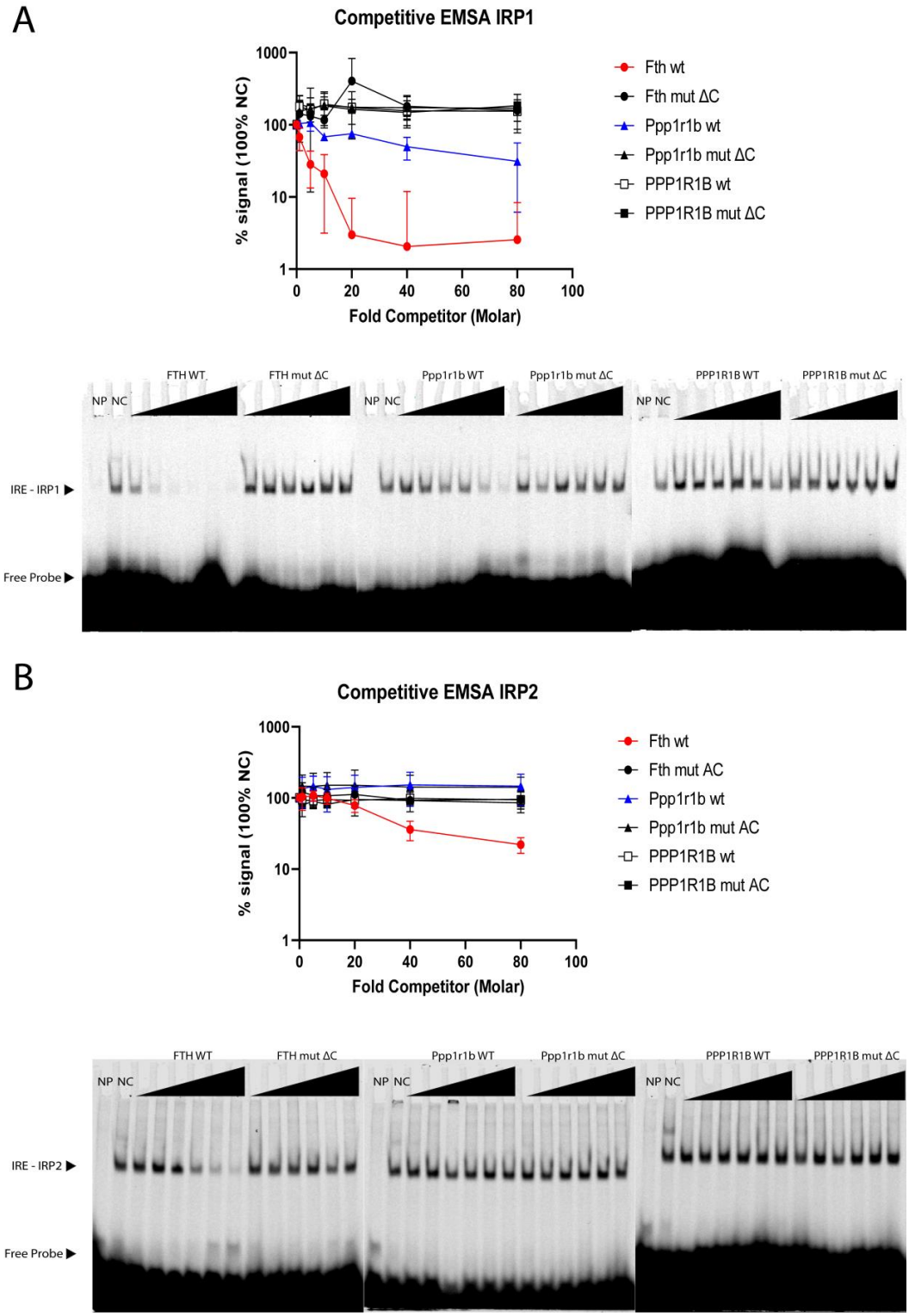

Figure 5.8: Competitive EMSAs with mouse and human *PPP1R1B* IRE. (A) Dose dependent competition of *PPP1R1B* with recombinant IRP1. Fluorescent labeled *FTH* IRE was incubated with increasing molar excess (1X, 5X, 10X, 20X, 40X and 80X) of unlabeled competitors (WT and ΔC *FTH*, WT and ΔC *Ppp1r1b* and WT and ΔC *PPP1R1B*). **(B)** Dose dependent competition of *PPP1R1B* with recombinant IRP2. Fluorescent labeled *FTH* IRE was incubated with increasing molar excess (1X, 5X, 10X, 20X, 40X and 80X) of unlabeled competitors (WT and ΔC *FTH*, WT and ΔC *Ppp1r1b* and WT and ΔC *PPP1R1B*). NP means no protein; P means protein, with no competitor.

5.3.3. Iron modulation of DARPP-32 in human cell lines

It is known that mRNAs containing 5' IREs such as ferritins are modulated post-transcriptionally by iron cell content via the IRPs. For this reason, we next studied whether if iron levels can alter the protein levels of DARPP-32 or not. Two human cell lines were treated overnight (16h) with ferric ammonium citrate (FAC) as an iron source or deferoxamine (DFO) as iron chelator or left untreated (NT – non treated) (Figure 5.9). Human ferritins (both FTH and FTL) were measured in parallel as positive control for iron via IRP/IRE regulation. We used HuTu-80 (human duodenal cells, from an adenocarcinoma) and U-118 MG (human neuronal cells, from a glioblastoma) cells, as *PPP1R1B* is highly expressed in those two tissues according to GTEx web page (Figure 1.14).

In HuTu-80 duodenal cells, western blot results showed that ferritins were, as expected, downregulated by the iron chelation DFO and upregulated by iron supplementation with FAC. Interestingly, DARPP-32 showed a similar regulation pattern that was statistically significant when it is compared with non-treated cells (Figure 5.9). DARPP-32 protein levels are 1.8-fold upregulated in the presence of an iron donor (FAC) and are 3-fold downregulated in the presence of an iron chelator (DFO).

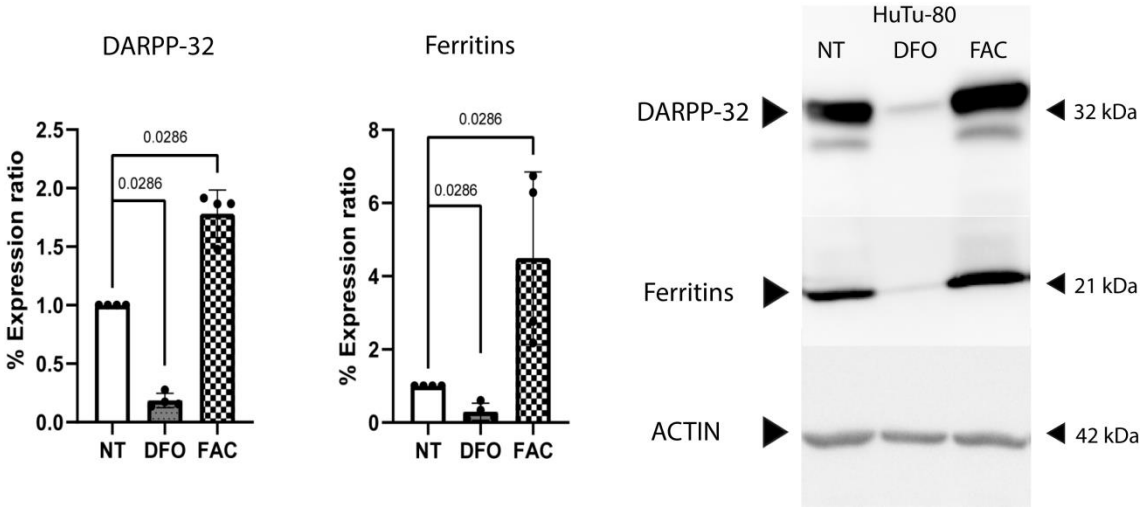

Figure 5.9: DARPP-32 protein levels in HuTu-80 cells after iron treatments. HuTu-80 cells were treated overnight (16h) with DFO 200µM, FAC 200µM or left untreated (NT). Protein levels of DARPP-32 (left) and both ferritins (right) were analyzed by Western blotting. Ferritins were used as positive control. β-actin protein levels were used for normalization. The intensity bands signal was quantified using ImageLab software (Bio-Rad). Data were normalized to the signal of not treated cells, set as 1. Values are means ± SD of 4 experiments.

Additionally, we studied DARPP-32 expression in U-118 MG cells by western blot. In those experiments, we have identified the same pattern as in duodenal cells. Despite the DFO treatment downregulates DARPP-32 expression we do not see statistical significance, probably due to the standard deviation, but FAC treatment upregulates 4-fold the DARPP-32 expression, similarly as occurs with ferritin, the positive control.

These results are statistically significant compared with the non-treated group (Figure 5.10).

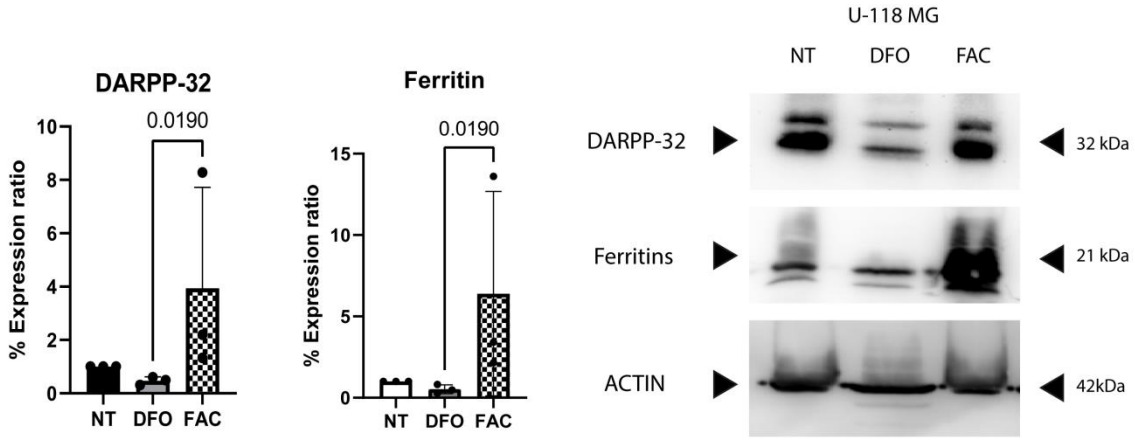

Figure 5.10: DARPP-32 protein levels in U-118 MG cells after iron treatments. U-118 MG cells were treated overnight (16h) with DFO 200µM, FAC 200µM or left untreated (NT). Protein levels of DARPP-32 (left) and both ferritins (right) were analyzed by Western blotting. Ferritins were used as positive control. β-actin protein levels were used for normalization. The intensity bands signal was quantified using ImageLab software (Bio-Rad). Data were normalized to the signal of not treated cells, set as 1. Values are means ± SD of 3 experiments.

Therefore, with these experiments we demonstrate that human DARPP-32 protein is regulated in two human cell lines by iron similarly as what it is expected for genes containing a functional 5' IRE. Although our *in vitro* EMSA data fail to show human *PPP1R1B* interaction with recombinant IRPs (using short probe), in cell culture data is pointing to an iron modulation compatible with an IRP/IRE post-transcriptional regulation. This contradiction could be because in the EMSA experiments we used only a short probe which contains only the putative IRE and additional mRNA sequences could be needed to allow IRP binding. In addition, we cannot exclude that another IRE-like motif, not detected bioinformatically, is present in another part of the 5'UTR of human *PPP1R1B*. We could not use a longer probe containing a full *PPP1R1B* mRNA because the impossibility of cloning the complete 5' UTR of *PPP1R1B* due to the high G-C percentage (we tried several times). On the other hand, *in vitro* EMSA experiments are performed in conditions that are not the ones found in a physiological context, therefore, the binding may only occur under physiological conditions and only seen in tissue culture experiments as we observe.

5.3.4. Discussion

IRP/IRE post transcriptional regulatory system plays a crucial role in the regulation of cellular iron homeostasis by coordinating iron uptake, utilization, storage and export. In addition to the classical mRNA-containing IREs, in the last decade several studies have reported other IREs or IRE-like structures in genes that are directly related or not with iron metabolism. Our laboratory identified in the past novel IRP-target mRNAs detected with a genome wide screening approach aimed to identify mRNAs that can bind with recombinant IRP1 and/or IRP2 (Sanchez et al., 2011), such as CDC14A (Sanchez et al., 2006), Hif2a (Sanchez et al., 2007) and Pfn2 (Luscieti et al., 2017).

We had identified an IRE-like structure in the 5' UTR of mouse *Ppp1r1b* gene using bioinformatics tools. Mouse *Ppp1r1b* IRE presents a classical IRE structure with an unpaired cytosine (C-bulge) and a canonical hexanucleotide apical loop sequence (CAGUGC) (Figure 5.5A).

On the other hand, the human homologous sequence to mouse IRE is not well conserved and it is not bioinformatically predicted as a good IRE (Figure 5.5). However, human *PPP1R1B* 5' UTR presents another predicted hairpin structure that does not have a C-bulge and present an atypical hexanucleotide apical loop (CACAGA) features that differ from the classical IREs.

We demonstrated the positive interaction between mouse *Ppp1r1b* IRE and IRP1 with direct and competitive EMSAs. Despite Sanchez and collaborators showed immunoprecipitation of full length mouse *Ppp1r1b* mRNA with recombinant IRP2, our *in vitro* EMSAs using short probes failed to show that interaction, this could be because longer probes are needed for such interaction or because the interaction is too weak to be detected in the *in vitro* conditions of the EMSA assay.

In vitro EMSA tests with a 5' hairpin loop present in the mRNA of human *PPP1R1B* failed to show interaction neither with recombinant IRP1 nor with recombinant IRP2. This could be because we used short probes that maybe are not fully recapitulating an *in vivo* situation compared with a full length mRNA, i.e. may the short probe folding is suboptimal or not optimal at all to produce a secondary structure able to bind to the IRPs while *in vivo* a longer mRNA is able to bind them. Further experiments testing longer human *PPP1R1B* probes could solve this issue. However, we cannot rule out the possibility that the bioinformatically identified sequence by Vienna Software is not the responsible mRNA element that interacts with IRPs, and there is another, not yet identified sequence in human *PPP1R1B* mRNA, responsible for this interaction. The full length human PPP1R1B 5'UTR sequence was not possible to get neither commercially nor cloned by PCR. We attribute this to the high percentage of G-C that contains the sequence and the elevated number of repetitions.

We demonstrated in our *in vivo* experiments in two human cell lines (HuTu-80 and U-118 MG) that human DARPP-32 protein is regulated by iron levels in the same way as expected for a gene regulated by IRPs with a 5'UTR. DARPP-32 protein levels are upregulated by iron supplementation with FAC and reduced by iron chelation by DFO. The results were consistent with a 5' IRE/IRP post-transcriptional regulation, similarly to ferritin protein expression regulation, used as positive control.

5.3.5. Future line of research with Ppp1r1b

Further experiments are required to complete our understanding of the iron-mediated PPP1R1B regulation and, as mentioned in section 1.7.4, the possible PPP1R1B-mediated iron regulation.

To complete our understanding of the iron-mediated *PPP1R1B* regulation, the post-transcriptional regulation of *PPP1R1B*'s mRNA will be studied by qPCR in human cells after DFO or FAC treatments. With the regulation observed at the protein level (see

section 5.3.3.), we expect no change in mRNA levels in any of the treatments since a 5'UTR IRE affects mRNA translation rather than mRNA stability.

The fact that the IRE is only present in one of the transcript variants (Figure 5.5) means we need specific primers for this mRNA. The design of these primers has proven difficult, since the sequence differences between the IRE and non-IRE variants are small, limiting the options to design primer sequences to. Moreover, the region that we want to amplify presents a high percentage of G-C and a big number of repetitions. Therefore, we cannot design functional primers.

Additionally, since the link between IRPs and *PPP1R1B* was originally stablished in mouse (Figure 1.12; Figure 5.4), it would be of interest to replicate the experiments at the protein and mRNA levels in murine cell lines. The experimental design would be the same as the one presented in section 5.3.3 but using murine cell lines where Darpp-32 is expressed (Figure 1.15).

As mentioned in section 1.7.4, Collinet and collaborators pointed to a possible PPP1R1B-mediated iron regulation. In their high throughput work to study genes affecting clathrin-mediated endocytosis in HeLa cells, they showed that PPP1R1B silencing led to a specific increase in transferrin receptor endocytosis. We aim to validate this data by silencing *PPP1R1B* in both human and murine cell lines and to study transferrin receptor uptake. If *PPP1R1B* is directly modulating iron intake, changes in the levels of cellular iron are expected to be observed when overexpressing DARPP-32. We contacted with Dr. Lucía Gutierrez from Universidad de Zaragoza and Dr. Maria del Puerto Morales from Institute of Material Science in Madrid (ICMM/CSIC) to establish a collaboration to assess the total cellular iron content by atomic absorption in *PPP1R1B* overexpressed murine and human cell lines.

Adding in vivo data to our work would increase the impact of this work and increase the possibility to publish it in a high-ranking journal. For this reason, we have contacted Dr. Albert Quintana's group at the Institute of Neuroscience (INc) at Universitat Autonoma de Barcelona. Unfortunately, the *Ppp1r1b* KO mouse strain is not available, but after discussing the alternatives with Dr. Albert Quintana and Dr. Elisenda Sanz, a set of alternative approaches have been proposed. One course of action would be generating a tissue-specific *Ppp1r1b* silencing using viral vector to later study iron accumulation/depletion in the affected tissues. Another approach would be performing a brain intraventricular iron injection to test the modulation of *Ppp1r1b* expression *in vivo*. Finally, we could perform a *in vivo* ribosomal profiling taking advantage of the system generated by Dr. Elisenda Sanz. The technique consists in tissue-specific ribosome isolation and the subsequent identification of the mRNAs that are translating at the moment (Sanz et al., 2009). By this technique we expect an increase of *Ppp1r1b* translation when mice are treated with an iron source and reduction when they are treated with an iron chelator.

Proving this PPP1R1B-mediated iron regulation would validate our working hypothesis of the PPP1R1B-iron system depicted in Figure 5.11. In this model, in high Fe conditions, DARPP-32 protein binds adducin and impedes the formation of the actin

filaments required for clathrin-mediated endocytosis of TF/TFR1, resulting in a halt in the iron-uptake. Moreover, in that conditions the IRPs will not bind with TFRC IREs and the TFRC mRNA will be degraded by endonucleases such Regnase-1 and Roquin-1 (Corral, Schultz, Eisenstein, & Connell, 2021; Yoshinaga et al., 2017). On the other hand, when the cellular iron levels are low, IRPs will bind the 5'UTR in the PPP1R1B gene, reducing DARPP-32 protein levels. In this scenario, adducins will be able to form the actin filaments required to induce transferrin endocytosis, increasing iron-uptake.

Answering these questions would allow us to deep into the role of *PPP1R1B* in iron homeostasis.

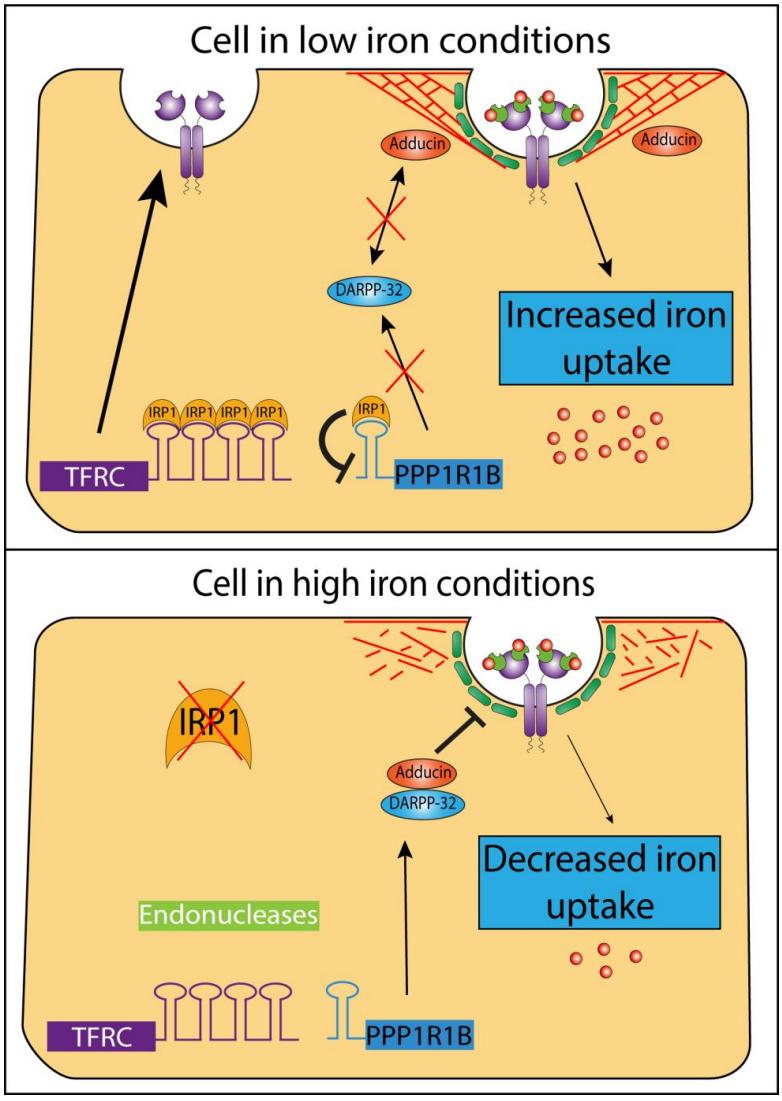

Figure 5.11: Proposed model for DARPP-32 iron role. Adducins are needed for actin-spectrin network formation, and this complex is required for TF-TFRC endocytosis. We propose that DARPP-32 indirectly regulates the transferrin receptor endocytosis by binding to adducin and also by promoting adducin phosphorylation. This proposed new mechanism agrees with the presence of an IRE-like structure in the PPP1R1B 5' UTR. In low iron conditions, PPP1R1B translation will be repressed, allowing adducin to form the actin cytoskeleton and inducing TF-TFRC complex internalization. On the contrary, in high iron conditions, IRPs are not active and the TFRC mRNA is degraded by endonucleases, PPP1R1B will be actively translated and DARPP-32 will block adducin-induced actin cytoskeleton formation needed for endocytosis of the TF/TFR1 complex. Overall decreasing iron uptake and restoring iron balance.

6. Conclusions

6.1. New cases in Hereditary Hyperferritinemia-Cataract Syndrome (HHCS)

6.1.1. We have identified members of two Spanish families affected with HHCS (Figure 5.1). Three patients (A-III.2, B-III.1 and B-IV.1) were clinically and genetically characterized (Table 5.1).

6.1.2. We identified the Paris1 mutation (NM_00146.3:c.[-160A>G];[=]) in the *FTL* gene in Family A and the Madrid/Philadelphia mutation (NM_00146.3:c.[-167C>T];[=]) in the *FTL* gene in Family B.

6.1.3. Mutations in the 5' IRE of *FTL* gene cause HHCS. In these patients the genetic, biochemical data and the presence of cataracts are in line with this diagnostic.

6.1.4. We pointed to the importance of an early and differential diagnosis in HHCS to avoid unnecessary/dangerous treatments.

6.1.5. We did an extensive revision of all literature reporting 5' IRE *FTL* mutations. This is an important genetic list of mutations that will help in the genetic diagnosis of HHCS cases as variants in regulatory regions are not always well reported in human mutation databases such as ClinVar or HGMD.

6.1.6. This work was published at the International journal of Molecular Science (IJMS): Celma Nos, F., Hernández, G., Ferrer-Cortès, X., Hernandez-Rodriguez, I., Navarro-Almenzar, B., Fuster, J. L., Bermúdez Cortés, M., Pérez-Montero, S., Tornador, C., & Sanchez, M. (2021). Hereditary Hyperferritinemia Cataract Syndrome: Ferritin L Gene and Physiopathology behind the Disease-Report of New Cases. International journal of molecular sciences, 22(11), 5451. https://doi.org/10.3390/ijms22115451 impact factor 5.923 in year 2020.

6.2. Characterizing the role of the 3' IRE in a mouse model of divalent metal transporter 1 (*Dmt1*) with an IRE deletion

6.2.1. We confirmed by EMSA that murine *Dmt1* has a functional 3' IRE.

6.2.2. The disruption of the murine *Dmt1* 3' IRE impedes the binding between *Dmt1* mRNA and IRP1.

6.2.3. The IRE of *Dmt1* 3' plays a role in controlling duodenal iron absorption through DMT1 expression. The *Dmt1* 3'IRE secures iron sufficiency by promoting intestinal DMT1 expression during postnatal growth and; in adulthood, suppresses DMT1 preventing systemic iron loading.

6.2.4. Our EMSA experiments are included in the supplementary data of a published letter in HemaSphere journal: Tybl, Elisabeth; Gunshin, Hiromi; Gupta, Sanjay; Barrientos, Tomasa; Bonadonna, Michael; Celma Nos, Ferran; Palais, Gael; Karim,

Zoubida; Sanchez, Mayka; Andrews, Nancy C.; Galy, Bruno. (2020). Control of Systemic Iron Homeostasis by the 3' Iron-Responsive Element of Divalent Metal Transporter 1 in Mice. HemaSphere: October 2020 - Volume 4 - Issue 5 - p e459 doi: 10.1097/HS9.0000000000000459. It has not yet an IF because it is a novel journal of Haematologica group.

6.3.PPP1R1B a novel IRP-target mRNA

6.3.1. Mouse *Ppp1r1b* mRNA immunoprecipitates together with IRP1 and IRP2 in brain (shown by microarray data and qPCR) and in duodenum (shown by microarray data).

6.3.2. *In vitro* EMSA experiments (direct and competitive) using short probes show that mouse *Ppp1r1b* has a functional 5' IRE that binds with recombinant IRP1.

6.3.3. One tested human *PPP1R1B* hairpin structure similar to IREs with EMSA experiments fail to show interaction with IRP1 and IRP2. The failure could be due to:

a) The tested mRNA element is not a truly IRE and there is another sequence in the 5' UTR not yet tested doing this function.
b) The tested human mRNA element is a very weak IRE and *in vitro* EMSA experiments are not sensitive enough to show the interaction and/or competition as longer probes might be needed to detect an interaction with IRPs.

6.3.4. Despite the negative results in *in vitro* human EMSAs, tissue culture experiments, using two human cell lines (HuTu-80 and U-118 MG), show that DARPP-32 protein levels are upregulated by iron supplementation with FAC and downregulated by the iron chelator DFO. This behavior is compatible with a regulation done by the IRP/IRE post-transcriptional system, as this is how a 5' IRE is regulated by the IRPs at protein level.

6.3.5. Further *in vivo* studies will be done to complete our understanding of the role of PPP1R1B in iron metabolism.

7. Bibliography

References

Abboud, S., & Haile, D. J. (2000). A novel mammalian iron-regulated protein involved in intracellular iron metabolism. *The Journal of Biological Chemistry, 275*(26), 19906-19912. doi:10.1074/jbc.M000713200

Addess, K. J., Basilion, J. P., Klausner, R. D., Rouault, T. A., & Pardi, A. (1997). Structure and dynamics of the iron responsive element RNA: Implications for binding of the RNA by iron regulatory binding proteins. *Journal of Molecular Biology, 274*(1), 72-83. doi:10.1006/jmbi.1997.1377

Agar, J. N., Krebs, C., Frazzon, J., Huynh, B. H., Dean, D. R., & Johnson, M. K. (2000). IscU as a scaffold for Iron−Sulfur cluster biosynthesis: Sequential assembly of [2Fe-2S] and [4Fe-4S] clusters in IscU. *Biochemistry, 39*(27), 7856-7862. doi:10.1021/bi000931n

Alam, S. K., Astone, M., Liu, P., Hall, S. R., Coyle, A. M., Dankert, E. N., . . . Hoeppner, L. H. (2018). DARPP-32 and t-DARPP promote non-small cell lung cancer growth through regulation of IKKα-dependent cell migration. *Communications Biology, 1*(1), 1-15. doi:10.1038/s42003-018-0050-6

Allerson, C. R., Cazzola, M., & Rouault, T. A. (1999). Clinical severity and thermodynamic effects of iron-responsive element mutations in hereditary hyperferritinemia-cataract syndrome. *The Journal of Biological Chemistry, 274*(37), 26439-26447. doi:10.1074/jbc.274.37.26439

Allikmets, R., Raskind, W. H., Hutchinson, A., Schueck, N. D., Dean, M., & Koeller, D. M. (1999). Mutation of a putative mitochondrial iron transporter gene (ABC7) in X-linked sideroblastic anemia and ataxia (XLSA/A). *Human Molecular Genetics, 8*(5), 743-749. doi:10.1093/hmg/8.5.743

Álvarez-Coca-González, J., Moreno-Carralero, M., Martínez-Pérez, J., Méndez, M., García-Ros, M., & Morán-Jiménez, M. (2010). The hereditary hyperferritinemia-cataract syndrome: A family study. *European Journal of Pediatrics, 169*(12), 1553-1555. doi:10.1007/s00431-010-1251-2

Anderson, C. P., Shen, M., Eisenstein, R. S., & Leibold, E. A. (2012). Mammalian iron metabolism and its control by iron regulatory proteins. *Biochimica Et Biophysica Acta, 1823*(9), 1468-1483. doi:10.1016/j.bbamcr.2012.05.010

Anderson, G. J., & Frazer, D. M. (2017). Current understanding of iron homeostasis. *The American Journal of Clinical Nutrition, 106*(Suppl 6), 1559S-1566S. doi:10.3945/ajcn.117.155804

Anderson, S. A., Nizzi, C. P., Chang, Y., Deck, K. M., Schmidt, P. J., Galy, B., . . . Eisenstein, R. S. (2013a). The IRP1-HIF-2α axis coordinates iron and oxygen sensing with erythropoiesis and iron absorption. *Cell Metabolism, 17*(2), 282-290. doi:10.1016/j.cmet.2013.01.007

Anderson, S. A., Nizzi, C. P., Chang, Y., Deck, K. M., Schmidt, P. J., Galy, B., . . . Eisenstein, R. S. (2013b). The IRP1-HIF-2α axis coordinates iron and oxygen sensing with erythropoiesis and iron absorption. *Cell Metabolism, 17*(2), 282-290. doi:10.1016/j.cmet.2013.01.007

Arezes, J., Costa, M., Vieira, I., Dias, V., Kong, X. L., Fernandes, R., . . . Pinto, J. P. (2013). Non-transferrin-bound iron (NTBI) uptake by T lymphocytes: Evidence for the selective acquisition of oligomeric ferric citrate species. *PloS One, 8*(11), e79870. doi:10.1371/journal.pone.0079870

Armitage, A. E., Eddowes, L. A., Gileadi, U., Cole, S., Spottiswoode, N., Selvakumar, T. A., . . . Drakesmith, H. (2011). Hepcidin regulation by innate immune and infectious stimuli. *Blood, 118*(15), 4129-4139. doi:10.1182/blood-2011-04-351957

Arosio, C., Fossati, L., Viganò, M., Trombini, P., Cazzaniga, G., & Piperno, A. (1999). Hereditary hyperferritinemia cataract syndrome: A de novo mutation in the iron responsive element of the L-ferritin gene. *Haematologica, 84*(6), 560-561.

Arosio, P., Ingrassia, R., & Cavadini, P. (2009). Ferritins: A family of molecules for iron storage, antioxidation and more. *Biochimica Et Biophysica Acta (BBA) - General Subjects, 1790*(7), 589-599. doi:10.1016/j.bbagen.2008.09.004

Arosio, P., & Levi, S. (2010). Cytosolic and mitochondrial ferritins in the regulation of cellular iron homeostasis and oxidative damage. *Biochimica Et Biophysica Acta (BBA) - General Subjects, 1800*(8), 783-792. doi:10.1016/j.bbagen.2010.02.005

Avanes, A., Lenz, G., & Momand, J. (2019). Darpp-32 and t-darpp protein products of PPP1R1B: Old dogs with new tricks. *Biochemical Pharmacology, 160*, 71-79. doi:10.1016/j.bcp.2018.12.008

Balas, A., Aviles, M. J., Garcia-Sanchez, F., & Vicario, J. L. (1999). Description of a new mutation in the L-ferrin iron-responsive element associated with hereditary hyperferritinemia-cataract syndrome in a spanish family. *Blood, 93*(11), 4020-4021.

Balk, J., Pierik, A. J., Netz, D. J. A., Mühlenhoff, U., & Lill, R. (2004). The hydrogenase-like Nar1p is essential for maturation of cytosolic and nuclear iron–sulphur proteins. *The EMBO Journal, 23*(10), 2105-2115. doi:10.1038/sj.emboj.7600216

Bardou-Jacquet, E., Island, M., Jouanolle, A., Détivaud, L., Fatih, N., Ropert, M., . . . Loréal, O. (2011). A novel N491S mutation in the human SLC11A2 gene impairs protein trafficking and in association with the G212V mutation leads to microcytic anemia and liver iron overload. *Blood Cells, Molecules & Diseases, 47*(4), 243-248. doi:10.1016/j.bcmd.2011.07.004

Barrios, M., Moreno-Carralero, M., Cuadrado-Grande, N., Baro, M., Vivanco, J., & Morán-Jiménez, M. (2012). The homozygous mutation G75R in the human SLC11A2 gene leads to microcytic anaemia and iron overload. *British Journal of Haematology, 157*(4), 514-516. doi:10.1111/j.1365-2141.2012.09043.x

Beaumont, C., Leneuve, P., Devaux, I., Scoazec, J. Y., Berthier, M., Loiseau, M. N., . . . Bonneau, D. (1995). Mutation in the iron responsive element of the L ferritin mRNA in a family with dominant hyperferritinaemia and cataract. *Nature Genetics, 11*(4), 444-446. doi:10.1038/ng1295-444

Beaumont, C., Delaunay, J., Hetet, G., Grandchamp, B., de Montalembert, M., & Tchernia, G. (2006). Two new human DMT1 gene mutations in a patient with microcytic anemia, low ferritinemia, and liver iron overload. *Blood, 107*(10), 4168-4170. doi:10.1182/blood-2005-10-4269

Belkhiri, A., Zhu, S., & El-Rifai, W. (2016). DARPP-32: From neurotransmission to cancer. *Oncotarget, 7*(14), 17631-17640. doi:10.18632/oncotarget.7268

Berger, B., Febvret, A., Greengard, P., & Goldman-Rakic, P. S. (1990). DARPP-32, a phosphoprotein enriched in dopaminoceptive neurons bearing dopamine D1 receptors: Distribution in the cerebral cortex of the newborn and adult rhesus monkey. *The Journal of Comparative Neurology, 299*(3), 327-348. doi:10.1002/cne.902990306

Bibb, J. A., Snyder, G. L., Nishi, A., Yan, Z., Meijer, L., Fienberg, A. A., . . . Greengard, P. (1999). Phosphorylation of DARPP-32 by Cdk5 modulates dopamine signalling in neurons. *Nature, 402*(6762), 669-671. doi:10.1038/45251

Blanco, E., Kannengiesser, C., Grandchamp, B., Tasso, M., & Beaumont, C. (2009). Not all DMT1 mutations lead to iron overload. *Blood Cells, Molecules & Diseases, 43*(2), 199-201. doi:10.1016/j.bcmd.2009.05.003

Bonneau, D., Winter-Fuseau, I., Loiseau, M. N., Amati, P., Berthier, M., Oriot, D., & Beaumont, C. (1995). Bilateral cataract and high serum ferritin: A new dominant genetic disorder? *Journal of Medical Genetics, 32*(10), 778-779. doi:10.1136/jmg.32.10.778

Bradley, J., Le Brun, N., & Moore, G. (2016). Ferritins: Furnishing proteins with iron. *JBIC Journal of Biological Inorganic Chemistry, 21*(1), 13-28. doi:10.1007/s00775-016-1336-0

Brasse–Lagnel, C., Karim, Z., Letteron, P., Bekri, S., Bado, A., & Beaumont, C. (2011). Intestinal DMT1 cotransporter is down-regulated by hepcidin via proteasome internalization and degradation. *Gastroenterology, 140*(4), 1261-1271. doi:10.1053/j.gastro.2010.12.037

Brené, S., Hall, H., Lindefors, N., Karlsson, P., Halldin, C., & Sedvall, G. (1995). Distribution of messenger RNAs for D1 dopamine receptors and DARPP-32 in striatum and cerebral cortex of the cynomolgus monkey: Relationship to D1 dopamine receptors. *Neuroscience, 67*(1), 37-48. doi:10.1016/0306-4522(95)00037-j

Brené, S., Lindefors, N., Ehrlich, M., Taubes, T., Horiuchi, A., Kopp, J., . . . Persson, H. (1994). Expression of mRNAs encoding ARPP-16/19, ARPP-21, and DARPP-32 in human brain tissue. *The Journal of Neuroscience: The Official Journal of the Society for Neuroscience, 14*(3 Pt 1), 985-998.

Bulteau, A., O'Neill, H. A., Kennedy, M. C., Ikeda-Saito, M., Isaya, G., & Szweda, L. I. (2004). Frataxin acts as an iron chaperone protein to modulate mitochondrial aconitase activity. *Science (New York, N.Y.), 305*(5681), 242-245. doi:10.1126/science.1098991

Cadenas, B., Fita-Torró, J., Bermúdez-Cortés, M., Hernandez-Rodriguez, I., Fuster, J. L., Llinares, M. E., . . . Sanchez, M. (2019). L-ferritin: One gene, five diseases; from hereditary hyperferritinemia to Hypoferritinemia—Report of new cases. *Pharmaceuticals, 12*(1) doi:10.3390/ph12010017

Caltagirone, A., Weiss, G., & Pantopoulos, K. (2001). Modulation of cellular iron metabolism by hydrogen peroxide. effects of H2O2 on the expression and function of iron-responsive element-containing mRNAs in B6 fibroblasts. *The Journal of Biological Chemistry, 276*(23), 19738-19745. doi:10.1074/jbc.M100245200

Camaschella, C., Campanella, A., De Falco, L., Boschetto, L., Merlini, R., Silvestri, L., . . . Iolascon, A. (2007). The human counterpart of zebrafish shiraz shows sideroblastic-like microcytic anemia and iron overload. *Blood, 110*(4), 1353-1358. doi:10.1182/blood-2007-02-072520

Campillos, M., Cases, I., Hentze, M. W., & Sanchez, M. (2010). SIREs: Searching for iron-responsive elements. *Nucleic Acids Research, 38*(Web Server issue), 360. doi:10.1093/nar/gkq371

Campuzano, V., Montermini, L., Moltò, M. D., Pianese, L., Cossée, M., Cavalcanti, F., . . . Pandolfo, M. (1996). Friedreich's ataxia: Autosomal recessive disease caused by an intronic GAA triplet repeat expansion. *Science (New York, N.Y.), 271*(5254), 1423-1427. doi:10.1126/science.271.5254.1423

Cao, W., McMahon, M., Wang, B., O'Connor, R., & Clarkson, M. (2010). A case report of spontaneous mutation (C33>U) in the iron-responsive element of L-ferritin causing hyperferritinemia-cataract syndrome. *Blood Cells, Molecules & Diseases, 44*(1), 22-27. doi:10.1016/j.bcmd.2009.09.003

Cartwright, G. E., & Deiss, A. (1975). Sideroblasts, siderocytes, and sideroblastic anemia. *The New England Journal of Medicine, 292*(4), 185-193. doi:10.1056/NEJM197501232920405

Casale, M., Borriello, A., Scianguetta, S., Roberti, D., Caiazza, M., Bencivenga, D., . . . Perrotta, S. (2018). Hereditary hypochromic microcytic anemia associated with loss-of-function DMT1 gene mutations and absence of liver iron overload. *American Journal of Hematology, 93*(3), E58-E60. doi:10.1002/ajh.24988

Casey, J. L., Koeller, D. M., Ramin, V. C., Klausner, R. D., & Harford, J. B. (1989). Iron regulation of transferrin receptor mRNA levels requires iron-responsive elements and a rapid turnover determinant in the 3' untranslated region of the mRNA. *The EMBO Journal, 8*(12), 3693-3699.

Castro, L., Tórtora, V., Mansilla, S., & Radi, R. (2019). Aconitases: Non-redox iron-sulfur proteins sensitive to reactive species. *Accounts of Chemical Research, 52*(9), 2609-2619. doi:10.1021/acs.accounts.9b00150

Cavadini, P., O'Neill, H. A., Benada, O., & Isaya, G. (2002). Assembly and iron-binding properties of human frataxin, the protein deficient in friedreich ataxia. *Human Molecular Genetics, 11*(3), 217-227. doi:10.1093/hmg/11.3.217

Chen, O. S., Schalinske, K. L., & Eisenstein, R. S. (1997). Dietary iron intake modulates the activity of iron regulatory proteins and the abundance of ferritin and mitochondrial aconitase in rat liver. *The Journal of Nutrition, 127*(2), 238-248. doi:10.1093/jn/127.2.238

Christenson, J. L., & Kane, S. E. (2014). Darpp-32 and t-darpp are differentially expressed in normal and malignant mouse mammary tissue. *Molecular Cancer, 13*, 192. doi:10.1186/1476-4598-13-192

Clarke, S. L., Vasanthakumar, A., Anderson, S. A., Pondarré, C., Koh, C. M., Deck, K. M., . . . Eisenstein, R. S. (2006). Iron-responsive degradation of iron-regulatory protein 1 does not require the fe-S cluster. *The EMBO Journal, 25*(3), 544-553. doi:10.1038/sj.emboj.7600954

Collinet, C., Stöter, M., Bradshaw, C. R., Samusik, N., Rink, J. C., Kenski, D., . . . Zerial, M. (2010). Systems survey of endocytosis by multiparametric image analysis. *Nature, 464*(7286), 243-249. doi:10.1038/nature08779

Connell, G. J., Danial, J. S., & Haastruthers, C. X. (2018). Evaluation of the iron regulatory protein-1 interactome. *Biometals: An International Journal on the Role of Metal Ions in Biology, Biochemistry, and Medicine, 31*(1), 139-146. doi:10.1007/s10534-018-0076-8

Cooper, M. S., Stark, Z., Lunke, S., Zhao, T., & Amor, D. J. (2019). IREB2-associated neurodegeneration. *Brain: A Journal of Neurology, 142*(8), e40. doi:10.1093/brain/awz183

Cooperman, S. S., Meyron-Holtz, E. G., Olivierre-Wilson, H., Ghosh, M. C., McConnell, J. P., & Rouault, T. A. (2005). Microcytic anemia, erythropoietic protoporphyria, and neurodegeneration in mice with targeted deletion of iron-regulatory protein 2. *Blood, 106*(3), 1084-1091. doi:10.1182/blood-2004-12-4703

Corral, V. M., Schultz, E. R., Eisenstein, R. S., & Connell, G. J. (2021). Roquin is a major mediator of iron-regulated changes to transferrin receptor-1 mRNA stability. *iScience, 24*(4), 102360. doi:10.1016/j.isci.2021.102360

Costain, G., Ghosh, M. C., Maio, N., Carnevale, A., Si, Y. C., Rouault, T. A., & Yoon, G. (2019). Absence of iron-responsive element-binding protein 2 causes a novel neurodegenerative syndrome. *Brain (London, England : 1878), 142*(5), 1195-1202. doi:10.1093/brain/awz072

Cotter, P. D., Baumann, M., & Bishop, D. F. (1992). Enzymatic defect in "X-linked" sideroblastic anemia: Molecular evidence for erythroid delta-aminolevulinate synthase deficiency. *Proceedings of the National Academy of Sciences, 89*(9), 4028-4032.

Craig, J. E., Clark, J. B., McLeod, J. L., Kirkland, M. A., Grant, G., Elder, J. E., . . . Mackey, D. A. (2003). Hereditary hyperferritinemia-cataract syndrome: Prevalence, lens morphology, spectrum of mutations, and clinical presentations. *Archives of Ophthalmology (Chicago, Ill.: 1960), 121*(12), 1753-1761. doi:10.1001/archopht.121.12.1753

Crispin, A., Guo, C., Chen, C., Campagna, D. R., Schmidt, P. J., Lichtenstein, D., . . . Ducamp, S. (2020). Mutations in the iron-sulfur cluster biogenesis protein HSCB cause congenital sideroblastic anemia. *The Journal of Clinical Investigation, 130*(10), 5245-5256. doi:10.1172/JCI135479

Cullis, J. O., Fitzsimons, E. J., Griffiths, W. J., Tsochatzis, E., & Thomas, D. W. (2018). Investigation and management of a raised serum ferritin. *British Journal of Haematology, 181*(3), 331-340. doi:10.1111/bjh.15166

D'Alessio, F., Hentze, M. W., & Muckenthaler, M. U. (2012). The hemochromatosis proteins HFE, TfR2, and HJV form a membrane-associated protein complex for hepcidin regulation. *Journal of Hepatology, 57*(5), 1052-1060. doi:https://doi.org/10.1016/j.jhep.2012.06.015

Daher, R., Kannengiesser, C., Houamel, D., Lefebvre, T., Bardou-Jacquet, E., Ducrot, N., . . . Tchernitchko, D. (2016). Heterozygous mutations in BMP6 pro-peptide lead to inappropriate hepcidin synthesis and moderate iron overload in humans. *Gastroenterology, 150*(3), 672-683.e4. doi:10.1053/j.gastro.2015.10.049

Dautry-Varsat, A., Ciechanover, A., & Lodish, H. F. (1983). pH and the recycling of transferrin during receptor-mediated endocytosis. *Proceedings of the National Academy of Sciences, 80*(8), 2258-2262. Retrieved from https://www.pnas.org/content/80/8/2258.short

De Domenico, I., Ward, D. M., di Patti, Maria Carmela Bonaccorsi, Jeong, S. Y., David, S., Musci, G., & Kaplan, J. (2007). Ferroxidase activity is required for the stability of cell surface ferroportin in cells expressing GPI-ceruloplasmin. *The EMBO Journal, 26*(12), 2823-2831. doi:10.1038/sj.emboj.7601735

De Falco, L., Bruno, M., Andolfo, I., David, B. P., Girelli, D., Di Noce, F., . . . Iolascon, A. (2012). Identification and characterization of the first SLC11A2 isoform 1a mutation causing a defect in splicing process and an hypomorphic allele expression of the SLC11A2 gene. *British Journal of Haematology, 159*(4), 492-495. doi:10.1111/bjh.12062

Delatycki, M. B., Knight, M., Koenig, M., Cossée, M., Williamson, R., & Forrest, S. M. (1999). G130V, a common FRDA point mutation, appears to have arisen from a common founder. *Human Genetics, 105*(4), 343-346. doi:10.1007/s004399900142

Denny, E. C., & Kane, S. E. (2015). T-darpp promotes enhanced EGFR activation and new drug synergies in Her2-positive breast cancer cells. *PloS One, 10*(6), e0132267. doi:10.1371/journal.pone.0132267

Détivaud, L., Island, M., Jouanolle, A., Ropert, M., Bardou-Jacquet, E., Lan, C. L., . . . Loréal, O. (2013). Ferroportin diseases: Functional studies, a link between genetic

and clinical phenotype. *Human Mutation, 34*(11), 1529-1536. doi:10.1002/humu.22396

Dev, S., & Babitt, J. L. (2017). Overview of iron metabolism in health and disease. *Hemodialysis International. International Symposium on Home Hemodialysis, 21*(Suppl 1), S6-S20. doi:10.1111/hdi.12542

Donovan, A., Lima, C. A., Pinkus, J. L., Pinkus, G. S., Zon, L. I., Robine, S., & Andrews, N. C. (2005). The iron exporter ferroportin/Slc40a1 is essential for iron homeostasis. *Cell Metabolism, 1*(3), 191-200. doi:10.1016/j.cmet.2005.01.003

Drakesmith, H., Schimanski, L. M., Ormerod, E., Merryweather-Clarke, A. T., Viprakasit, V., Edwards, J. P., . . . Townsend, A. R. M. (2005). Resistance to hepcidin is conferred by hemochromatosis-associated mutations of ferroportin. *Blood, 106*(3), 1092-1097. doi:10.1182/blood-2005-02-0561

Ducamp, S., & Fleming, M. D. (2019). The molecular genetics of sideroblastic anemia. *Blood, 133*(1), 59-69. doi:10.1182/blood-2018-08-815951

Ducamp, S., Luscieti, S., Ferrer-Cortès, X., Nicolas, G., Manceau, H., Peoc'h, K., . . . Sanchez, M. (2021). A mutation in the iron-responsive element of ALAS2 is a modifier of disease severity in a patient suffering from CLPX associated erythropoietic protoporphyria. *Haematologica, 106*(7), 2030-2033. doi:10.3324/haematol.2020.272450

Ducamp, S., Schneider-Yin, X., de Rooij, F., Clayton, J., Fratz, E. J., Rudd, A., . . . Puy, H. (2013). Molecular and functional analysis of the C-terminal region of human erythroid-specific 5-aminolevulinic synthase associated with X-linked dominant protoporphyria (XLDPP). *Human Molecular Genetics, 22*(7), 1280-1288. doi:10.1093/hmg/dds531

Dupuy, J., Volbeda, A., Carpentier, P., Darnault, C., Moulis, J., & Fontecilla-Camps, J. C. (2006). Crystal structure of human iron regulatory protein 1 as cytosolic aconitase. *Structure, 14*(1), 129-139. doi:10.1016/j.str.2005.09.009

Ebihara, Y., Miyamoto, M., Fukunaga, A., Kato, K., Shichinohe, T., Kawarada, Y., . . . Katoh, H. (2004). DARPP-32 expression arises after a phase of dysplasia in oesophageal squamous cell carcinoma. *British Journal of Cancer, 91*(1), 119-123. doi:10.1038/sj.bjc.6601899

El-Rifai, W., Smith, M. F., Li, G., Beckler, A., Carl, V. S., Montgomery, E., . . . Powell, S. M. (2002). Gastric cancers overexpress DARPP-32 and a novel isoform, t-DARPP. *Cancer Research, 62*(14), 4061-4064.

Engmann, O., Giralt, A., Gervasi, N., Marion-Poll, L., Gasmi, L., Filhol, O., . . . Girault, J. (2015). DARPP-32 interaction with adducin may mediate rapid environmental effects on striatal neurons. *Nature Communications, 6*, 10099. doi:10.1038/ncomms10099

Fagerberg, L., Hallström, B. M., Oksvold, P., Kampf, C., Djureinovic, D., Odeberg, J., . . . Uhlén, M. (2014). Analysis of the human tissue-specific expression by genome-

wide integration of transcriptomics and antibody-based proteomics. *Molecular & Cellular Proteomics: MCP, 13*(2), 397-406. doi:10.1074/mcp.M113.035600

Ferreira, C., Bucchini, D., Martin, M. E., Levi, S., Arosio, P., Grandchamp, B., & Beaumont, C. (2000). Early embryonic lethality of H ferritin gene deletion in mice. *The Journal of Biological Chemistry, 275*(5), 3021-3024. doi:10.1074/jbc.275.5.3021

Ferring-Appel, D., Hentze, M. W., & Galy, B. (2009). Cell-autonomous and systemic context-dependent functions of iron regulatory protein 2 in mammalian iron metabolism. *Blood, 113*(3), 679-687. doi:10.1182/blood-2008-05-155093

Fienberg, A. A., & Greengard, P. (2000). The DARPP-32 knockout mouse. *Brain Research. Brain Research Reviews, 31*(2-3), 313-319. doi:10.1016/s0165-0173(99)00047-8

Finch, C. (1994). Regulators of iron balance in humans. *Blood, 84*(6), 1697-1702.

Fleming, M. D., Romano, M. A., Su, M. A., Garrick, L. M., Garrick, M. D., & Andrews, N. C. (1998). Nramp2 is mutated in the anemic belgrade (b) rat: Evidence of a role for Nramp2 in endosomal iron transport. *Proceedings of the National Academy of Sciences of the United States of America, 95*(3), 1148-1153. doi:10.1073/pnas.95.3.1148

Fleming, M. D. (2002). The genetics of inherited sideroblastic anemias. *Seminars in Hematology, 39*(4), 270-281. doi:10.1053/shem.2002.35637

Franke, K., Gassmann, M., & Wielockx, B. (2013). Erythrocytosis: The HIF pathway in control. *Blood, 122*(7), 1122-1128. doi:10.1182/blood-2013-01-478065

Galy, B., Ferring, D., & Hentze, M. W. (2005). Generation of conditional alleles of the murine iron regulatory protein (IRP)-1 and -2 genes. *Genesis (New York, N.Y.: 2000), 43*(4), 181-188. doi:10.1002/gene.20169

Galy, B., Ferring, D., Minana, B., Bell, O., Janser, H. G., Muckenthaler, M., . . . Hentze, M. W. (2005). Altered body iron distribution and microcytosis in mice deficient in iron regulatory protein 2 (IRP2). *Blood, 106*(7), 2580-2589. doi:10.1182/blood-2005-04-1365

Galy, B., Ferring-Appel, D., Becker, C., Gretz, N., Gröne, H., Schümann, K., & Hentze, M. W. (2013). Iron regulatory proteins control a mucosal block to intestinal iron absorption. *Cell Reports, 3*(3), 844-857. doi:10.1016/j.celrep.2013.02.026

Galy, B., Ferring-Appel, D., Kaden, S., Gröne, H., & Hentze, M. W. (2008). Iron regulatory proteins are essential for intestinal function and control key iron absorption molecules in the duodenum. *Cell Metabolism, 7*(1), 79-85. doi:10.1016/j.cmet.2007.10.006

Galy, B., Ferring-Appel, D., Sauer, S. W., Kaden, S., Lyoumi, S., Puy, H., . . . Hentze, M. W. (2010). Iron regulatory proteins secure mitochondrial iron sufficiency and function. *Cell Metabolism, 12*(2), 194-201. doi:10.1016/j.cmet.2010.06.007

Gerber, J., Mühlenhoff, U., & Lill, R. (2003). An interaction between frataxin and Isu1/Nfs1 that is crucial for fe/S cluster synthesis on Isu1. *EMBO Reports, 4*(9), 906-911. doi:10.1038/sj.embor.embor918

Ghosh, M. C., Tong, W., Zhang, D., Ollivierre-Wilson, H., Singh, A., Krishna, M. C., . . . Rouault, T. A. (2008). Tempol-mediated activation of latent iron regulatory protein activity prevents symptoms of neurodegenerative disease in IRP2 knockout mice. *Proceedings of the National Academy of Sciences of the United States of America, 105*(33), 12028-12033. doi:10.1073/pnas.0805361105

Ghosh, M. C., Zhang, D., Jeong, S. Y., Kovtunovych, G., Ollivierre-Wilson, H., Noguchi, A., . . . Rouault, T. A. (2013). Deletion of iron regulatory protein 1 causes polycythemia and pulmonary hypertension in mice through translational derepression of HIF2α. *Cell Metabolism, 17*(2), 271-281. doi:10.1016/j.cmet.2012.12.016

Giansily-Blaizot, M., Cunat, S., Moulis, G., Schved, J., & Aguilar-Martinez, P. (2013). Homozygous mutation of the 5'UTR region of the L-ferritin gene in the hereditary hyperferritinemia cataract syndrome and its impact on the phenotype. *Haematologica, 98*(4), 42. doi:10.3324/haematol.2012.077198

Girelli, D., Bozzini, C., Zecchina, G., Tinazzi, E., Bosio, S., Piperno, A., . . . Corrocher, R. (2001). Clinical, biochemical and molecular findings in a series of families with hereditary hyperferritinaemia-cataract syndrome. *British Journal of Haematology, 115*(2), 334-340. doi:10.1046/j.1365-2141.2001.03116.x

Girelli, D., Corrocher, R., Bisceglia, L., Olivieri, O., De Franceschi, L., Zelante, L., & Gasparini, P. (1995). Molecular basis for the recently described hereditary hyperferritinemia-cataract syndrome: A mutation in the iron-responsive element of ferritin L-subunit gene (the "verona mutation"). *Blood, 86*(11), 4050-4053.

Gkouvatsos, K., Papanikolaou, G., & Pantopoulos, K. (2012). Regulation of iron transport and the role of transferrin. *Biochimica Et Biophysica Acta, 1820*(3), 188-202. doi:10.1016/j.bbagen.2011.10.013

Goldwurm, S., Casati, C., Venturi, N., Strada, S., Santambrogio, P., Indraccolo, S., . . . Biondi, A. (2000). Biochemical and genetic defects underlying human congenital hypotransferrinemia. *The Hematology Journal : The Official Journal of the European Haematology Association, 1*(6), 390-398. doi:10.1038/sj.thj.6200063

Graham, R., Chua, A. -., Herbison, C., Olynyk, J., & Trinder, D. (2007). Liver iron transport. *World Journal of Gastroenterology, 13*(35), 4725-4736. doi:10.3748/wjg.v13.i35.4725

Gray, N. K., Pantopoulos, K., Dandekar, T., Ackrell, B. A., & Hentze, M. W. (1996). Translational regulation of mammalian and drosophila citric acid cycle enzymes via iron-responsive elements. *Proceedings of the National Academy of Sciences of the United States of America, 93*(10), 4925-4930. doi:10.1073/pnas.93.10.4925

Gray, N. K., Quick, S., Goossen, B., Constable, A., Hirling, H., Kühn, L. C., & Hentze, M. W. (1993). Recombinant iron-regulatory factor functions as an iron-responsive-element-binding protein, a translational repressor and an aconitase. A functional

assay for translational repression and direct demonstration of the iron switch. *European Journal of Biochemistry, 218*(2), 657-667. doi:10.1111/j.1432-1033.1993.tb18420.x

Green, R., Charlton, R., Seftel, H., Bothwell, T., Mayet, F., Adams, B., . . . Layrisse, M. (1968). Body iron excretion in man: A collaborative study. *The American Journal of Medicine, 45*(3), 336-353. doi:10.1016/0002-9343(68)90069-7

Gulhar, R., Ashraf, M. A., & Jialal, I. (2021). Physiology, acute phase reactants. *StatPearls* (). Treasure Island (FL): StatPearls Publishing. Retrieved from http://www.ncbi.nlm.nih.gov/books/NBK519570/

Gunshin, H., Mackenzie, B., Berger, U. V., Gunshin, Y., Romero, M. F., Boron, W. F., . . . Hediger, M. A. (1997). Cloning and characterization of a mammalian proton-coupled metal-ion transporter. *Nature, 388*(6641), 482-488. doi:10.1038/41343

Guo, B., Yu, Y., & Leibold, E. A. (1994). Iron regulates cytoplasmic levels of a novel iron-responsive element-binding protein without aconitase activity. *Journal of Biological Chemistry, 269*(39), 24252-24260. Retrieved from http://www.jbc.org/content/269/39/24252

Haile, D. J., Rouault, T. A., Harford, J. B., Kennedy, M. C., Blondin, G. A., Beinert, H., & Klausner, R. D. (1992). Cellular regulation of the iron-responsive element binding protein: Disassembly of the cubane iron-sulfur cluster results in high-affinity RNA binding. *Proceedings of the National Academy of Sciences, 89*(24), 11735-11739. Retrieved from https://www.pnas.org/content/89/24/11735.short

Halpain, S., Girault, J. A., & Greengard, P. (1990). Activation of NMDA receptors induces dephosphorylation of DARPP-32 in rat striatal slices. *Nature, 343*(6256), 369-372. doi:10.1038/343369a0

Hamdi, A., Roshan, T. M., Kahawita, T. M., Mason, A. B., Sheftel, A. D., & Ponka, P. (2016). Erythroid cell mitochondria receive endosomal iron by a "kiss-and-run" mechanism. *Biochimica Et Biophysica Acta, 1863*(12), 2859-2867. doi:10.1016/j.bbamcr.2016.09.008

Hansen, C., Greengard, P., Nairn, A. C., Andersson, T., & Vogel, W. F. (2006). Phosphorylation of DARPP-32 regulates breast cancer cell migration downstream of the receptor tyrosine kinase DDR1. *Experimental Cell Research, 312*(20), 4011-4018. doi:10.1016/j.yexcr.2006.09.003

Hansen, C., Howlin, J., Tengholm, A., Dyachok, O., Vogel, W. F., Nairn, A. C., . . . Andersson, T. (2009). Wnt-5a-induced phosphorylation of DARPP-32 inhibits breast cancer cell migration in a CREB-dependent manner. *The Journal of Biological Chemistry, 284*(40), 27533-27543. doi:10.1074/jbc.M109.048884

Hemmings, H. C., Williams, K. R., Konigsberg, W. H., & Greengard, P. (1984). DARPP-32, a dopamine- and adenosine 3':5'-monophosphate-regulated neuronal phosphoprotein. I. amino acid sequence around the phosphorylated threonine. *The Journal of Biological Chemistry, 259*(23), 14486-14490.

Hentze, M. W., Muckenthaler, M. U., Galy, B., & Camaschella, C. (2010). Two to tango: Regulation of mammalian iron metabolism. *Cell, 142*(1), 24-38. doi:10.1016/j.cell.2010.06.028

Hernández Martín, D., Cervera Bravo, A., & Balas Pérez, A. (2008). [Hereditary hyperferritinemia and cataract syndrome: A de novo mutation]. *Anales De Pediatria (Barcelona, Spain: 2003), 68*(4), 408-410. doi:10.1157/13117721

Hetet, G., Devaux, I., Soufir, N., Grandchamp, B., & Beaumont, C. (2003). Molecular analyses of patients with hyperferritinemia and normal serum iron values reveal both L ferritin IRE and 3 new ferroportin (slc11A3) mutations. *Blood, 102*(5), 1904-1910. doi:10.1182/blood-2003-02-0439

Heyser, C. J., Fienberg, A. A., Greengard, P., & Gold, L. H. (2000). DARPP-32 knockout mice exhibit impaired reversal learning in a discriminated operant task. *Brain Research, 867*(1), 122-130. doi:10.1016/S0006-8993(00)02272-1

Hubert, N., & Hentze, M. W. (2002). Previously uncharacterized isoforms of divalent metal transporter (DMT)-1: Implications for regulation and cellular function. *Proceedings of the National Academy of Sciences of the United States of America, 99*(19), 12345-12350. doi:10.1073/pnas.192423399

Iolascon, A., d'Apolito, M., Servedio, V., Cimmino, F., Piga, A., & Camaschella, C. (2006). Microcytic anemia and hepatic iron overload in a child with compound heterozygous mutations in DMT1 (SCL11A2). *Blood, 107*(1), 349-354. doi:10.1182/blood-2005-06-2477

Iolascon, A., De Falco, L., & Beaumont, C. (2009). Molecular basis of inherited microcytic anemia due to defects in iron acquisition or heme synthesis. *Haematologica, 94*(3), 395-408. doi:10.3324/haematol.13619

Iwai, K., Klausner, R. D., & Rouault, T. A. (1995). Requirements for iron-regulated degradation of the RNA binding protein, iron regulatory protein 2. *The EMBO Journal, 14*(21), 5350-5357.

Jabara, H. H., Boyden, S. E., Chou, J., Ramesh, N., Massaad, M. J., Benson, H., . . . Geha, R. S. (2015). A missense mutation in TFRC, encoding transferrin receptor 1, causes combined immunodeficiency. *Nature Genetics, 48*(1), 74-78. doi:10.1038/ng.3465.

Jeong, S. Y., Crooks, D. R., Wilson-Ollivierre, H., Ghosh, M. C., Sougrat, R., Lee, J., . . . Rouault, T. A. (2011). Iron insufficiency compromises motor neurons and their mitochondrial function in Irp2-null mice. *PloS One, 6*(10), e25404. doi:10.1371/journal.pone.0025404

Johnson, N. B., Deck, K. M., Nizzi, C. P., & Eisenstein, R. S. (2017). A synergistic role of IRP1 and FBXL5 proteins in coordinating iron metabolism during cell proliferation. *The Journal of Biological Chemistry, 292*(38), 15976-15989. doi:10.1074/jbc.M117.785741

Kato, J., Fujikawa, K., Kanda, M., Fukuda, N., Sasaki, K., Takayama, T., . . . Niitsu, Y. (2001). A mutation, in the iron-responsive element of H ferritin mRNA, causing autosomal dominant iron overload. *American Journal of Human Genetics, 69*(1), 191-197. doi:10.1086/321261

Keel, S. B., Doty, R. T., Yang, Z., Quigley, J. G., Chen, J., Knoblaugh, S., . . . Abkowitz, J. L. (2008). A heme export protein is required for red blood cell differentiation and iron homeostasis. *Science (New York, N.Y.), 319*(5864), 825-828. doi:10.1126/science.1151133

Kernan, K. F., & Carcillo, J. A. (2017). Hyperferritinemia and inflammation. *International Immunology, 29*(9), 401-409. doi:10.1093/intimm/dxx031

Kiang, K. M., & Leung, G. K. (2018). A review on adducin from functional to pathological mechanisms: Future direction in cancer. *BioMed Research International, 2018*, 3465929. doi:10.1155/2018/3465929

Kidane, T. Z., Sauble, E., & Linder, M. C. (2006). Release of iron from ferritin requires lysosomal activity. *American Journal of Physiology. Cell Physiology, 291*(3), 445-455. doi:10.1152/ajpcell.00505.2005

Kispal, G., Csere, P., Guiard, B., & Lill, R. (1997). The ABC transporter Atm1p is required for mitochondrial iron homeostasis. *FEBS Letters, 418*(3), 346-350. doi:10.1016/S0014-5793(97)01414-2

Köhn, M., Lederer, M., Wächter, K., & Hüttelmaier, S. (2010). Near-infrared (NIR) dye-labeled RNAs identify binding of ZBP1 to the noncoding Y3-RNA. *RNA (New York, N.Y.), 16*(7), 1420-1428. doi:10.1261/rna.2152710

Krause, A., Neitz, S., Mägert, H. J., Schulz, A., Forssmann, W. G., Schulz-Knappe, P., & Adermann, K. (2000). LEAP-1, a novel highly disulfide-bonded human peptide, exhibits antimicrobial activity. *FEBS Letters, 480*(2-3), 147-150. doi:10.1016/s0014-5793(00)01920-7

Kühn, L. C. (2015). Iron regulatory proteins and their role in controlling iron metabolism. *Metallomics: Integrated Biometal Science, 7*(2), 232-243. doi:10.1039/c4mt00164h

Kulaksiz, H., Theilig, F., Bachmann, S., Gehrke, S. G., Rost, D., Janetzko, A., . . . Stremmel, W. (2005). The iron-regulatory peptide hormone hepcidin: Expression and cellular localization in the mammalian kidney. *The Journal of Endocrinology, 184*(2), 361-370. doi:10.1677/joe.1.05729

Kulaksiz, H., Fein, E., Redecker, P., Stremmel, W., Adler, G., & Cetin, Y. (2008). Pancreatic beta-cells express hepcidin, an iron-uptake regulatory peptide. *The Journal of Endocrinology, 197*(2), 241-249. doi:10.1677/JOE-07-0528

Kunii, Y., Ikemoto, K., Wada, A., Yang, Q., Kusakabe, T., Suzuki, T., & Niwa, S. (2011). Detailed DARPP-32 expression profiles in postmortem brains from patients with schizophrenia: An immunohistochemical study. *Medical Molecular Morphology, 44*(4), 190-199. doi:10.1007/s00795-010-0524-1

Lamoril, J., Boulechfar, S., de Verneuil, H., Grandchamp, B., Nordmann, Y., & Deybach, J. (1991). Human erythropoietic protoporphyria: Two point mutations in the ferrochelatase gene. *Biochemical and Biophysical Research Communications, 181*(2), 594-599. doi:10.1016/0006-291X(91)91231-Z

Lane, D. J. R., Merlot, A. M., Huang, M. L. -., Bae, D. -., Jansson, P. J., Sahni, S., . . . Richardson, D. R. (2015). Cellular iron uptake, trafficking and metabolism: Key molecules and mechanisms and their roles in disease. *Biochimica Et Biophysica Acta, 1853*(5), 1130-1144. doi:10.1016/j.bbamcr.2015.01.021

LaVaute, T., Smith, S., Cooperman, S., Iwai, K., Land, W., Meyron-Holtz, E., . . . Rouault, T. A. (2001). Targeted deletion of the gene encoding iron regulatory protein-2 causes misregulation of iron metabolism and neurodegenerative disease in mice. *Nature Genetics, 27*(2), 209-214. doi:10.1038/84859

Leidgens, S., Bullough, K. Z., Shi, H., Li, F., Shakoury-Elizeh, M., Yabe, T., . . . Philpott, C. C. (2013). Each member of the poly-r(C)-binding protein 1 (PCBP) family exhibits iron chaperone activity toward ferritin. *The Journal of Biological Chemistry, 288*(24), 17791-17802. doi:10.1074/jbc.M113.460253

Leimberg, M. J., Prus, E., Konijn, A. M., & Fibach, E. (2008). Macrophages function as a ferritin iron source for cultured human erythroid precursors. *Journal of Cellular Biochemistry, 103*(4), 1211-1218. doi:10.1002/jcb.21499

Lenz, G., Hamilton, A., Geng, S., Hong, T., Kalkum, M., Momand, J., . . . Huss, J. M. (2018). T-darpp activates IGF-1R signaling to regulate glucose metabolism in trastuzumab-resistant breast cancer cells. *Clinical Cancer Research: An Official Journal of the American Association for Cancer Research, 24*(5), 1216-1226. doi:10.1158/1078-0432.CCR-17-0824

Levy, J. E., Jin, O., Fujiwara, Y., Kuo, F., & Andrews, N. C. (1999). Transferrin receptor is necessary for development of erythrocytes and the nervous system. *Nature Genetics, 21*(4), 396-399. doi:10.1038/7727

Li, K., Besse, E. K., Ha, D., Kovtunovych, G., & Rouault, T. A. (2008). Iron-dependent regulation of frataxin expression: Implications for treatment of friedreich ataxia. *Human Molecular Genetics, 17*(15), 2265-2273. doi:10.1093/hmg/ddn127

Li, Q., & Kang, C. (2017). Chapter one - erythropoietin receptor structural domains. *Vitamins and Hormones, 105*, 1-17. doi:https://doi.org/10.1016/bs.vh.2017.02.005

Lill, R., & Mühlenhoff, U. (2008). Maturation of iron-sulfur proteins in eukaryotes: Mechanisms, connected processes, and diseases. *Annual Review of Biochemistry, 77*(1), 669-700. doi:10.1146/annurev.biochem.76.052705.162653

Liu, G., Guo, S., Anderson, G. J., Camaschella, C., Han, B., & Nie, G. (2014). Heterozygous missense mutations in the GLRX5 gene cause sideroblastic anemia in a chinese patient. *Blood, 124*(17), 2750-2751. doi:10.1182/blood-2014-08-598508

Liu, W., Shimomura, S., Imanishi, H., Iwamoto, Y., Ikeda, N., Saito, M., . . . Hada, T. (2005). Hemochromatosis with mutation of the ferroportin 1 (IREG1) gene. *Internal Medicine (Tokyo, Japan), 44*(4), 285-289. doi:10.2169/internalmedicine.44.285

Lopez, A., Cacoub, P., Macdougall, I. C., & Peyrin-Biroulet, L. (2016). Iron deficiency anaemia. *Lancet (London, England), 387*(10021), 907-916. doi:10.1016/S0140-6736(15)60865-0

Luscieti, S., Galy, B., Gutierrez, L., Reinke, M., Couso, J., Shvartsman, M., . . . Sanchez, M. (2017). The actin-binding protein profilin 2 is a novel regulator of iron homeostasis. *Blood, 130*(17), 1934-1945. doi:10.1182/blood-2016-11-754382

Luscieti, S., Tolle, G., Aranda, J., Campos, C. B., Risse, F., Morán, É, . . . Sánchez, M. (2013). Novel mutations in the ferritin-L iron-responsive element that only mildly impair IRP binding cause hereditary hyperferritinaemia cataract syndrome. *Orphanet Journal of Rare Diseases, 8*, 30. doi:10.1186/1750-1172-8-30

Maio, N., & Rouault, T. A. (2015). Iron-sulfur cluster biogenesis in mammalian cells: New insights into the molecular mechanisms of cluster delivery. *Biochimica Et Biophysica Acta, 1853*(6), 1493-1512. doi:10.1016/j.bbamcr.2014.09.009

Mastrogiannaki, M., Matak, P., Keith, B., Simon, M. C., Vaulont, S., & Peyssonnaux, C. (2009). HIF-2alpha, but not HIF-1alpha, promotes iron absorption in mice. *The Journal of Clinical Investigation, 119*(5), 1159-1166. doi:10.1172/JCI38499

McLeod, J. L., Craig, J., Gumley, S., Roberts, S., & Kirkland, M. A. (2002). Mutation spectrum in australian pedigrees with hereditary hyperferritinaemia-cataract syndrome reveals novel and de novo mutations. *British Journal of Haematology, 118*(4), 1179-1182. doi:10.1046/j.1365-2141.2002.03690.x

Merle, U., Fein, E., Gehrke, S. G., Stremmel, W., & Kulaksiz, H. (2007). The iron regulatory peptide hepcidin is expressed in the heart and regulated by hypoxia and inflammation. *Endocrinology, 148*(6), 2663-2668. doi:10.1210/en.2006-1331

Meyron-Holtz, E. G., Ghosh, M. C., Iwai, K., LaVaute, T., Brazzolotto, X., Berger, U. V., . . . Rouault, T. A. (2004). Genetic ablations of iron regulatory proteins 1 and 2 reveal why iron regulatory protein 2 dominates iron homeostasis. *The EMBO Journal, 23*(2), 386-395. doi:10.1038/sj.emboj.7600041

Mims, M. P., Guan, Y., Pospisilova, D., Priwitzerova, M., Indrak, K., Ponka, P., . . . Prchal, J. T. (2005). Identification of a human mutation of DMT1 in a patient with microcytic anemia and iron overload. *Blood, 105*(3), 1337-1342. doi:10.1182/blood-2004-07-2966

Mochel, F., Knight, M. A., Tong, W., Hernandez, D., Ayyad, K., Taivassalo, T., . . . Haller, R. G. (2008). Splice mutation in the iron-sulfur cluster scaffold protein ISCU causes myopathy with exercise intolerance. *American Journal of Human Genetics, 82*(3), 652-660. doi:10.1016/j.ajhg.2007.12.012

Mok, H., Jelinek, J., Pai, S., Cattanach, B. M., Prchal, J. T., Youssoufian, H., & Schumacher, A. (2004). Disruption of ferroportin 1 regulation causes dynamic

alterations in iron homeostasis and erythropoiesis in polycythaemia mice. *Development (Cambridge, England), 131*(8), 1859-1868. doi:10.1242/dev.01081

Momand, J., Magdziarz, P., Feng, Y., Jiang, D., Parga, E., Celis, A., . . . Zhou, F. (2017). T-darpp is an elongated monomer that binds calcium and is phosphorylated by cyclin-dependent kinases 1 and 5. *FEBS Open Bio, 7*(9), 1328-1337. doi:10.1002/2211-5463.12269

Montosi, G., Donovan, A., Totaro, A., Garuti, C., Pignatti, E., Cassanelli, S., . . . Pietrangelo, A. (2001). Autosomal-dominant hemochromatosis is associated with a mutation in the ferroportin (SLC11A3) gene. *The Journal of Clinical Investigation, 108*(4), 619-623. doi:10.1172/JCI13468

Moroishi, T., Nishiyama, M., Takeda, Y., Iwai, K., & Nakayama, K. (2011). The FBXL5-IRP2 axis is integral to control of iron metabolism in vivo. *Cell Metabolism, 14*(3), 339-351. doi:10.1016/j.cmet.2011.07.011

Muckenthaler, M., Gray, N. K., & Hentze, M. W. (1998). IRP-1 binding to ferritin mRNA prevents the recruitment of the small ribosomal subunit by the cap-binding complex eIF4F. *Molecular Cell, 2*(3), 383-388. doi:10.1016/S1097-2765(00)80282-8

Muckenthaler, M., Rivella, S., Hentze, M. W., & Galy, B. (2017). A red carpet for iron metabolism. *Cell, 168*(3), 344-361. doi:https://doi.org/10.1016/j.cell.2016.12.034

Muckenthaler, Galy, B., & Hentze, M. W. (2008). Systemic iron homeostasis and the iron-responsive element/iron-regulatory protein (IRE/IRP) regulatory network. *Annual Review of Nutrition, 28*, 197-213. doi:10.1146/annurev.nutr.28.061807.155521

Muckenthaler, Rivella, S., Hentze, M. W., & Galy, B. (2017). A red carpet for iron metabolism. *Cell, 168*(3), 344-361. doi:https://doi.org/10.1016/j.cell.2016.12.034

Muñoz-Muñoz, J., Cuadrado-Grande, N., Moreno-Carralero, M. -., Hoyos-Sanabria, B., Manubes-Guarch, A., González, A. -., . . . Morán-Jiménez, M. -. (2013). Hereditary hyperferritinemia cataract syndrome in four patients with mutations in the IRE of the FTL gene. *Clinical Genetics, 83*(5), 491-493. doi:10.1111/j.1399-0004.2012.01934.x

Nemeth, E., Tuttle, M. S., Powelson, J., Vaughn, M. B., Donovan, A., Ward, D. M., . . . Kaplan, J. (2004). Hepcidin regulates cellular iron efflux by binding to ferroportin and inducing its internalization. *Science (New York, N.Y.), 306*(5704), 2090-2093. doi:10.1126/science.1104742

Nicolas, G., Bennoun, M., Devaux, I., Beaumont, C., Grandchamp, B., Kahn, A., & Vaulont, S. (2001). Lack of hepcidin gene expression and severe tissue iron overload in upstream stimulatory factor 2 (USF2) knockout mice. *Proceedings of the National Academy of Sciences of the United States of America, 98*(15), 8780-8785. doi:10.1073/pnas.151179498

Njajou, O. T., Vaessen, N., Joosse, M., Berghuis, B., van Dongen, J. W., Breuning, M. H., . . . Heutink, P. (2001). A mutation in SLC11A3 is associated with autosomal dominant hemochromatosis. *Nature Genetics, 28*(3), 213-214. doi:10.1038/90038

Ohgami, R. S., Campagna, D. R., Greer, E. L., Antiochos, B., McDonald, A., Chen, J., . . . Fleming, M. D. (2005). Identification of a ferrireductase required for efficient transferrin-dependent iron uptake in erythroid cells. *Nature Genetics, 37*(11), 1264-1269. doi:10.1038/ng1658

Ohgami, R. S., Campagna, D. R., McDonald, A., & Fleming, M. D. (2006). The steap proteins are metalloreductases. *Blood, 108*(4), 1388-1394. doi:10.1182/blood-2006-02-003681

Olsson, A., Lind, L., Thornell, L., & Holmberg, M. (2008). Myopathy with lactic acidosis is linked to chromosome 12q23.3-24.11 and caused by an intron mutation in the ISCU gene resulting in a splicing defect. *Human Molecular Genetics, 17*(11), 1666-1672. doi:10.1093/hmg/ddn057

Oudit, G. Y., Sun, H., Trivieri, M. G., Koch, S. E., Dawood, F., Ackerley, C., . . . Backx, P. H. (2003). L-type ca 2+ channels provide a major pathway for iron entry into cardiomyocytes in iron-overload cardiomyopathy. *Nature Medicine, 9*(9), 1187-1194. doi:10.1038/nm920

Ouimet, C. C., Miller, P. E., Hemmings, H. C., Walaas, S. I., & Greengard, P. (1984). DARPP-32, a dopamine- and adenosine 3':5'-monophosphate-regulated phosphoprotein enriched in dopamine-innervated brain regions. III. immunocytochemical localization. *The Journal of Neuroscience: The Official Journal of the Society for Neuroscience, 4*(1), 111-124.

Pak, M., Lopez, M. A., Gabayan, V., Ganz, T., & Rivera, S. (2006). Suppression of hepcidin during anemia requires erythropoietic activity. *Blood, 108*(12), 3730-3735. doi:10.1182/blood-2006-06-028787

Pandey, A. K., Pain, J., Dancis, A., & Pain, D. (2019). Mitochondria export iron–sulfur and sulfur intermediates to the cytoplasm for iron–sulfur cluster assembly and tRNA thiolation in yeast. *The Journal of Biological Chemistry, 294*(24), 9489-9502. doi:10.1074/jbc.RA119.008600

Pandolfo, M., Arpa, J., Delatycki, M. B., Sang, Kim Hanh Le Quan, Mariotti, C., Munnich, A., . . . Tricta, F. (2014). Deferiprone in friedreich ataxia: A 6-month randomized controlled trial. *Annals of Neurology, 76*(4), 509-521. doi:10.1002/ana.24248

Paradkar, P. N., Zumbrennen, K. B., Paw, B. H., Ward, D. M., & Kaplan, J. (2009). Regulation of mitochondrial iron import through differential turnover of mitoferrin 1 and mitoferrin 2. *Molecular and Cellular Biology, 29*(4), 1007-1016. doi:10.1128/MCB.01685-08

Parkinson, M. H., Boesch, S., Nachbauer, W., Mariotti, C., & Giunti, P. (2013). Clinical features of friedreich's ataxia: Classical and atypical phenotypes. *Journal of Neurochemistry, 126 Suppl 1*, 103-117. doi:10.1111/jnc.12317

Patel, P. I., & Isaya, G. (2001). Friedreich ataxia: From GAA triplet-repeat expansion to frataxin deficiency. *American Journal of Human Genetics, 69*(1), 15-24. doi:10.1086/321283

Paul, B. T., Manz, D. H., Torti, F. M., & Torti, S. V. (2017). Mitochondria and iron: Current questions. *Expert Review of Hematology, 10*(1), 65-79. doi:10.1080/17474086.2016.1268047

Paulson, R. F., Ruan, B., Hao, S., & Chen, Y. (2020). Stress erythropoiesis is a key inflammatory response. *Cells, 9*(3) doi:10.3390/cells9030634

Percy, M. J., Furlow, P. W., Lucas, G. S., Li, X., Lappin, T. R. J., McMullin, M. F., & Lee, F. S. (2008). A gain-of-function mutation in the HIF2A gene in familial erythrocytosis. *The New England Journal of Medicine, 358*(2), 162-168. doi:10.1056/NEJMoa073123

Peto, T. E., Pippard, M. J., & Weatherall, D. J. (1983). Iron overload in mild sideroblastic anaemias. *Lancet (London, England), 1*(8321), 375-378. doi:10.1016/s0140-6736(83)91498-8

Petrat, F., Paluch, S., Dogruöz, E., Dörfler, P., Kirsch, M., Korth, H., . . . Groot, H. d. (2003). Reduction of fe(III) ions complexed to physiological ligands by lipoyl dehydrogenase and other flavoenzymes in vitro. IMPLICATIONS FOR AN ENZYMATIC REDUCTION OF fe(III) IONS OF THE LABILE IRON POOL. *Journal of Biological Chemistry, 278*(47), 46403-46413. doi:10.1074/jbc.M305291200

Peyssonnaux, C., Zinkernagel, A. S., Datta, V., Lauth, X., Johnson, R. S., & Nizet, V. (2006). TLR4-dependent hepcidin expression by myeloid cells in response to bacterial pathogens. *Blood, 107*(9), 3727-3732. doi:10.1182/blood-2005-06-2259

Peyssonnaux, C., Zinkernagel, A. S., Schuepbach, R. A., Rankin, E., Vaulont, S., Haase, V. H., . . . Johnson, R. S. (2007). Regulation of iron homeostasis by the hypoxia-inducible transcription factors (HIFs). *The Journal of Clinical Investigation, 117*(7), 1926-1932. doi:10.1172/JCI31370

Phillips, J. D. (2019). Heme biosynthesis and the porphyrias. *Molecular Genetics and Metabolism, 128*(3), 164-177. doi:10.1016/j.ymgme.2019.04.008

Pietrangelo, A., Montosi, G., Totaro, A., Garuti, C., Conte, D., Cassanelli, S., . . . Gasparini, P. (1999). Hereditary hemochromatosis in adults without pathogenic mutations in the hemochromatosis gene. *The New England Journal of Medicine, 341*(10), 725-732. doi:10.1056/NEJM199909023411003

Pigeon, C., Ilyin, G., Courselaud, B., Leroyer, P., Turlin, B., Brissot, P., & Loréal, O. (2001). A new mouse liver-specific gene, encoding a protein homologous to human antimicrobial peptide hepcidin, is overexpressed during iron overload. *The Journal of Biological Chemistry, 276*(11), 7811-7819. doi:10.1074/jbc.M008923200

Pimenta, F. J., Horta, M. C. R., Vidigal, P. V., De Souza, B. R., De Marco, L., Romano-Silva, M. A., & Gomez, R. S. (2007). Decreased expression of DARPP-32 in oral premalignant and malignant lesions. *Anticancer Research, 27*(4B), 2339-2343.

Pinilla-Tenas, J. J., Sparkman, B. K., Shawki, A., Illing, A. C., Mitchell, C. J., Zhao, N., . . . Mackenzie, B. (2011). Zip14 is a complex broad-scope metal-ion transporter whose functional properties support roles in the cellular uptake of zinc and nontransferrin-bound iron. *American Journal of Physiology. Cell Physiology, 301*(4), 862. doi:10.1152/ajpcell.00479.2010

Priwitzerova, M., Pospisilova, D., Prchal, J. T., Indrak, K., Hlobilkova, A., Mihal, V., . . . Divoky, V. (2004). Severe hypochromic microcytic anemia caused by a congenital defect of the iron transport pathway in erythroid cells. *Blood, 103*(10), 3991-3992. doi:10.1182/blood-2004-01-0225

Qiao, B., Sugianto, P., Fung, E., Del-Castillo-Rueda, A., Moran-Jimenez, M., Ganz, T., & Nemeth, E. (2012). Hepcidin-induced endocytosis of ferroportin is dependent on ferroportin ubiquitination. *Cell Metabolism, 15*(6), 918-924. doi:10.1016/j.cmet.2012.03.018

Richardson, D. R., Lane, D. J. R., Becker, E. M., Huang, M. L. -., Whitnall, M., Rahmanto, Y. S., . . . Ponka, P. (2010). Mitochondrial iron trafficking and the integration of iron metabolism between the mitochondrion and cytosol. *Proceedings of the National Academy of Sciences of the United States of America, 107*(24), 10775-10782. doi:10.1073/pnas.0912925107

Rouault, T. A., Haile, D. J., Downey, W. E., Philpott, C. C., Tang, C., Samaniego, F., . . . Harford, J. B. (1992). An iron-sulfur cluster plays a novel regulatory role in the iron-responsive element binding protein. *Biometals: An International Journal on the Role of Metal Ions in Biology, Biochemistry, and Medicine, 5*(3), 131-140. doi:10.1007/bf01061319

Ruiz, J. C., Walker, S. D., Anderson, S. A., Eisenstein, R. S., & Bruick, R. K. (2013). F-box and leucine-rich repeat protein 5 (FBXL5) is required for maintenance of cellular and systemic iron homeostasis. *The Journal of Biological Chemistry, 288*(1), 552-560. doi:10.1074/jbc.M112.426171

Salahudeen, A. A., Thompson, J. W., Ruiz, J. C., Ma, H., Kinch, L. N., Li, Q., . . . Bruick, R. K. (2009). An E3 ligase possessing an iron-responsive hemerythrin domain is a regulator of iron homeostasis. *Science, 326*(5953), 722-726. doi:10.1126/science.1176326

Sanchez, M., Galy, B., Dandekar, T., Bengert, P., Vainshtein, Y., Stolte, J., . . . Hentze, M. W. (2006). Iron regulation and the cell cycle: Identification of an iron-responsive element in the 3'-untranslated region of human cell division cycle 14A mRNA by a refined microarray-based screening strategy. *The Journal of Biological Chemistry, 281*(32), 22865-22874. doi:10.1074/jbc.M603876200

Sanchez, M., Galy, B., Muckenthaler, M. U., & Hentze, M. W. (2007). Iron-regulatory proteins limit hypoxia-inducible factor-2alpha expression in iron deficiency. *Nature Structural & Molecular Biology, 14*(5), 420-426. doi:10.1038/nsmb1222

Sanchez, M., Galy, B., Schwanhaeusser, B., Blake, J., Bähr-Ivacevic, T., Benes, V., . . . Hentze, M. W. (2011). Iron regulatory protein-1 and -2: Transcriptome-wide definition of binding mRNAs and shaping of the cellular proteome by iron regulatory proteins. *Blood, 118*(22), 168. doi:10.1182/blood-2011-04-343541

Santambrogio, P., Biasiotto, G., Sanvito, F., Olivieri, S., Arosio, P., & Levi, S. (2007). Mitochondrial ferritin expression in adult mouse tissues. *Journal of Histochemistry & Cytochemistry, 55*(11), 1129-1137. doi:10.1369/jhc.7A7273.2007

Sanz, E., Yang, L., Su, T., Morris, D. R., McKnight, G. S., & Amieux, P. S. (2009). Cell-type-specific isolation of ribosome-associated mRNA from complex tissues. *Proceedings of the National Academy of Sciences of the United States of America, 106*(33), 13939-13944. doi:10.1073/pnas.0907143106

Scheggi, S., De Montis, M. G., & Gambarana, C. (2018). DARPP-32 in the orchestration of responses to positive natural stimuli. *Journal of Neurochemistry, 147*(4), 439-453. doi:10.1111/jnc.14558

Schimanski, L. M., Drakesmith, H., Merryweather-Clarke, A. T., Viprakasit, V., Edwards, J. P., Sweetland, E., . . . Townsend, A. R. M. (2005). In vitro functional analysis of human ferroportin (FPN) and hemochromatosis-associated FPN mutations. *Blood, 105*(10), 4096-4102. doi:10.1182/blood-2004-11-4502

Schmitz-Abe, K., Ciesielski, S. J., Schmidt, P. J., Campagna, D. R., Rahimov, F., Schilke, B. A., . . . Fleming, M. D. (2015). Congenital sideroblastic anemia due to mutations in the mitochondrial HSP70 homologue HSPA9. *Blood, 126*(25), 2734-2738. doi:10.1182/blood-2015-09-659854

Schranzhofer, M., Schifrer, M., Cabrera, J. A., Kopp, S., Chiba, P., Beug, H., & Müllner, E. W. (2006). Remodeling the regulation of iron metabolism during erythroid differentiation to ensure efficient heme biosynthesis. *Blood, 107*(10), 4159-4167. doi:10.1182/blood-2005-05-1809

Sebastiani, G., Wilkinson, N., & Pantopoulos, K. (2016). Pharmacological targeting of the hepcidin/ferroportin axis. *Frontiers in Pharmacology, 7*, 160. doi:10.3389/fphar.2016.00160

Shah, Y. M., Matsubara, T., Ito, S., Yim, S., & Gonzalez, F. J. (2009). Intestinal hypoxia-inducible transcription factors are essential for iron absorption following iron deficiency. *Cell Metabolism, 9*(2), 152-164. doi:10.1016/j.cmet.2008.12.012

Shaw, G. C., Cope, J. J., Li, L., Corson, K., Hersey, C., Ackermann, G. E., . . . Paw, B. H. (2006). Mitoferrin is essential for erythroid iron assimilation. *Nature, 440*(7080), 96-100. doi:10.1038/nature04512

Sheftel, A., Stehling, O., & Lill, R. (2010). Iron–sulfur proteins in health and disease. *Trends in Endocrinology & Metabolism, 21*(5), 302-314. doi:10.1016/j.tem.2009.12.006

Shindo, M., Torimoto, Y., Saito, H., Motomura, W., Ikuta, K., Sato, K., . . . Kohgo, Y. (2006). Functional role of DMT1 in transferrin-independent iron uptake by human hepatocyte and hepatocellular carcinoma cell, HLF. *Hepatology Research: The Official Journal of the Japan Society of Hepatology, 35*(3), 152-162. doi:10.1016/j.hepres.2006.03.011

Smith, S. R., Cooperman, S., Lavaute, T., Tresser, N., Ghosh, M., Meyron-Holtz, E., . . . Rouault, T. A. (2004). Severity of neurodegeneration correlates with compromise of iron metabolism in mice with iron regulatory protein deficiencies. *Annals of the New York Academy of Sciences, 1012*, 65-83. doi:10.1196/annals.1306.006

Smith, S. R., Ghosh, M. C., Ollivierre-Wilson, H., Hang Tong, W., & Rouault, T. A. (2006). Complete loss of iron regulatory proteins 1 and 2 prevents viability of murine zygotes beyond the blastocyst stage of embryonic development. *Blood Cells, Molecules & Diseases, 36*(2), 283-287. doi:10.1016/j.bcmd.2005.12.006

Souza, J. S. D., Brunetto, E. L., & Nunes, M. T. (2016). Iron restriction increases myoglobin gene and protein expression in soleus muscle of rats. *Anais Da Academia Brasileira De Ciencias, 88*(4), 2277-2290. doi:10.1590/0001-3765201620160173

Svenningsson, P., Nishi, A., Fisone, G., Girault, J., Nairn, A. C., & Greengard, P. (2004). DARPP-32: An integrator of neurotransmission. *Annual Review of Pharmacology and Toxicology, 44*, 269-296. doi:10.1146/annurev.pharmtox.44.101802.121415

Taylor, M., Qu, A., Anderson, E. R., Matsubara, T., Martin, A., Gonzalez, F. J., & Shah, Y. M. (2011). Hypoxia-inducible factor-2α mediates the adaptive increase of intestinal ferroportin during iron deficiency in mice. *Gastroenterology, 140*(7), 2044-2055. doi:10.1053/j.gastro.2011.03.007

Televantou, D., Karkavelas, G., Hytiroglou, P., Lampaki, S., Iliadis, G., Selviaridis, P., . . . Kotoula, V. (2013). DARPP32, STAT5 and STAT3 mRNA expression ratios in glioblastomas are associated with patient outcome. *Pathology Oncology Research: POR, 19*(2), 329-343. doi:10.1007/s12253-012-9588-7

Theile, D., Geng, S., Denny, E. C., Momand, J., & Kane, S. E. (2017). T-darpp stimulates protein kinase A activity by forming a complex with its RI regulatory subunit. *Cellular Signalling, 40*, 53-61. doi:10.1016/j.cellsig.2017.08.012

Thorstensen, K., & Romslo, I. (1990). The role of transferrin in the mechanism of cellular iron uptake. *Biochemical Journal, 271*(1), 1-9. Retrieved from https://www.ncbi.nlm.nih.gov/pmc/articles/PMC1150207/

Torielli, L., Tivodar, S., Montella, R. C., Iacone, R., Padoani, G., Tarsini, P., . . . Zurzolo, C. (2008). Alpha-adducin mutations increase na/K pump activity in renal cells by affecting constitutive endocytosis: Implications for tubular na reabsorption. *American Journal of Physiology. Renal Physiology, 295*(2), 478. doi:10.1152/ajprenal.90226.2008

Torres, M., & Forman, H. J. (2000). Chapter 21 - nitric oxide, oxidative stress, and signal transduction. In L. J. Ignarro (Ed.), *Nitric oxide* (pp. 329-342). San Diego: Academic Press. doi:https://doi.org/10.1016/B978-012370420-7/50022-8 Retrieved from https://www.sciencedirect.com/science/article/pii/B9780123704207500228

Trenor, C. C., Campagna, D. R., Sellers, V. M., Andrews, N. C., & Fleming, M. D. (2000). The molecular defect in hypotransferrinemic mice. *Blood, 96*(3), 1113-1118.

Tybl, E., Gunshin, H., Gupta, S., Barrientos, T., Bonadonna, M., Celma Nos, F., . . . Galy, B. (2020). Control of systemic iron homeostasis by the 3' iron-responsive element of divalent metal transporter 1 in mice. *HemaSphere, 4*(5), e459. doi:10.1097/HS9.0000000000000459

Vangamudi, B., Peng, D., Cai, Q., El-Rifai, W., Zheng, W., & Belkhiri, A. (2010). T-DARPP regulates phosphatidylinositol-3-kinase-dependent cell growth in breast cancer. *Molecular Cancer, 9*, 240. doi:10.1186/1476-4598-9-240

Vanoaica, L., Darshan, D., Richman, L., Schümann, K., & Kühn, L. C. (2010). Intestinal ferritin H is required for an accurate control of iron absorption. *Cell Metabolism, 12*(3), 273-282. doi:10.1016/j.cmet.2010.08.003

Vashisht, A. A., Zumbrennen, K. B., Huang, X., Powers, D. N., Durazo, A., Sun, D., . . . Wohlschlegel, J. A. (2009). Control of iron homeostasis by an iron-regulated ubiquitin ligase. *Science, 326*(5953), 718-721. doi:10.1126/science.1176333

Vila Cuenca, M., Marchi, G., Barqué, A., Esteban-Jurado, C., Marchetto, A., Giorgetti, A., . . . Sanchez, M. (2020). Genetic and clinical heterogeneity in thirteen new cases with aceruloplasminemia. atypical anemia as a clue for an early diagnosis. *International Journal of Molecular Sciences, 21*(7) doi:10.3390/ijms21072374

Vogt, A. S., Arsiwala, T., Mohsen, M., Vogel, M., Manolova, V., & Bachmann, M. F. (2021). On iron metabolism and its regulation. *International Journal of Molecular Sciences, 22*(9) doi:10.3390/ijms22094591

Waheed, A., Parkkila, S., Saarnio, J., Fleming, R. E., Zhou, X. Y., Tomatsu, S., . . . Sly, W. S. (1999). Association of HFE protein with transferrin receptor in crypt enterocytes of human duodenum. *Proceedings of the National Academy of Sciences of the United States of America, 96*(4), 1579-1584. doi:10.1073/pnas.96.4.1579

Walaas, S. I., Aswad, D. W., & Greengard, P. (1983). A dopamine- and cyclic AMP-regulated phosphoprotein enriched in dopamine-innervated brain regions. *Nature, 301*(5895), 69-71. doi:10.1038/301069a0

Walaas, S. I., Hemmings, H. C., Greengard, P., & Nairn, A. C. (2011). Beyond the dopamine receptor: Regulation and roles of serine/threonine protein phosphatases. *Frontiers in Neuroanatomy, 5*, 50. doi:10.3389/fnana.2011.00050

Walden, W. E., Selezneva, A. I., Dupuy, J., Volbeda, A., Fontecilla-Camps, J. C., Theil, E. C., & Volz, K. (2006). Structure of dual function iron regulatory protein 1 complexed with ferritin IRE-RNA. *Science (New York, N.Y.), 314*(5807), 1903-1908. doi:10.1126/science.1133116

Wang, C., Jenkitkasemwong, S., Duarte, S., Sparkman, B. K., Shawki, A., Mackenzie, B., & Knutson, M. D. (2012). ZIP8 is an iron and zinc transporter whose cell-

surface expression is up-regulated by cellular iron loading. *The Journal of Biological Chemistry, 287*(41), 34032-34043. doi:10.1074/jbc.M112.367284

Wang, W., Knovich, M. A., Coffman, L. G., Torti, F. M., & Torti, S. V. (2010). Serum ferritin: Past, present and future. *Biochimica Et Biophysica Acta, 1800*(8), 760-769. doi:10.1016/j.bbagen.2010.03.011

Whatley, S. D., Ducamp, S., Gouya, L., Grandchamp, B., Beaumont, C., Badminton, M. N., . . . Puy, H. (2008). C-terminal deletions in the ALAS2 gene lead to gain of function and cause X-linked dominant protoporphyria without anemia or iron overload. *American Journal of Human Genetics, 83*(3), 408-414. doi:10.1016/j.ajhg.2008.08.003

Wilkinson, N., & Pantopoulos, K. (2013). IRP1 regulates erythropoiesis and systemic iron homeostasis by controlling HIF2α mRNA translation. *Blood, 122*(9), 1658-1668. doi:10.1182/blood-2013-03-492454

Wilkinson, N., & Pantopoulos, K. (2014). The IRP/IRE system in vivo: Insights from mouse models. *Frontiers in Pharmacology, 5*, 176. doi:10.3389/fphar.2014.00176

Wingert, R. A., Galloway, J. L., Barut, B., Foott, H., Fraenkel, P., Axe, J. L., . . . Zon, L. I. (2005). Deficiency of glutaredoxin 5 reveals fe-S clusters are required for vertebrate haem synthesis. *Nature, 436*(7053), 1035-1039. doi:10.1038/nature03887

Wolff, N. A., Garrick, L. M., Zhao, L., Garrick, M. D., & Thévenod, F. (2014). Mitochondria represent another locale for the divalent metal transporter 1 (DMT1). *Channels (Austin, Tex.), 8*(5), 458-466. doi:10.4161/19336950.2014.956564

Wolff, N. A., Ghio, A. J., Garrick, L. M., Garrick, M. D., Zhao, L., Fenton, R. A., & Thévenod, F. (2014). Evidence for mitochondrial localization of divalent metal transporter 1 (DMT1). *FASEB Journal: Official Publication of the Federation of American Societies for Experimental Biology, 28*(5), 2134-2145. doi:10.1096/fj.13-240564

Yanatori, I., Richardson, D. R., Dhekne, H. S., Toyokuni, S., & Kishi, F. (2021). CD63 is regulated by iron via the IRE-IRP system and is important for ferritin secretion by extracellular vesicles. *Blood, 138*(16), 1490-1503. doi:10.1182/blood.2021010995

Ye, H., Jeong, S. Y., Ghosh, M. C., Kovtunovych, G., Silvestri, L., Ortillo, D., . . . Rouault, T. A. (2010). Glutaredoxin 5 deficiency causes sideroblastic anemia by specifically impairing heme biosynthesis and depleting cytosolic iron in human erythroblasts. *The Journal of Clinical Investigation, 120*(5), 1749-1761. doi:10.1172/JCI40372

Yoshinaga, M., Nakatsuka, Y., Vandenbon, A., Ori, D., Uehata, T., Tsujimura, T., . . . Takeuchi, O. (2017). Regnase-1 maintains iron homeostasis via the degradation of transferrin receptor 1 and prolyl-hydroxylase-domain-containing protein 3 mRNAs. *Cell Reports, 19*(8), 1614-1630. doi:10.1016/j.celrep.2017.05.009

Zhang, D., Hughes, R. M., Ollivierre-Wilson, H., Ghosh, M. C., & Rouault, T. A. (2009). A ferroportin transcript that lacks an iron-responsive element enables duodenal and erythroid precursor cells to evade translational repression. *Cell Metabolism, 9*(5), 461-473. doi:10.1016/j.cmet.2009.03.006

Zhang, D., Meyron-Holtz, E., & Rouault, T. A. (2007). Renal iron metabolism: Transferrin iron delivery and the role of iron regulatory proteins. *Journal of the American Society of Nephrology: JASN, 18*(2), 401-406. doi:10.1681/ASN.2006080908

Zimelman, A. P., Zimmerman, H. J., McLean, R., & Weintraub, L. R. (1977). Effect of iron saturation of transferrin on hepatic iron uptake: An in vitro study. *Gastroenterology, 72*(1), 129-131.

Zimmer, M., Ebert, B. L., Neil, C., Brenner, K., Papaioannou, I., Melas, A., . . . Iliopoulos, O. (2008). Small-molecule inhibitors of HIF-2a translation link its 5'UTR iron-responsive element to oxygen sensing. *Molecular Cell, 32*(6), 838-848. doi:10.1016/j.molcel.2008.12.004

Zumbrennen, K. B., Wallander, M. L., Romney, S. J., & Leibold, E. A. (2009). Cysteine oxidation regulates the RNA-binding activity of iron regulatory protein 2. *Molecular and Cellular Biology, 29*(8), 2219-2229. doi:10.1128/MCB.00004-09

Zumbrennen-Bullough, K. B., Becker, L., Garrett, L., Hölter, S. M., Calzada-Wack, J., Mossbrugger, I., . . . Leibold, E. A. (2014). Abnormal brain iron metabolism in Irp2 deficient mice is associated with mild neurological and behavioral impairments. *PloS One, 9*(6), e98072. doi:10.1371/journal.pone.0098072

8. Appendix

8.1.International congresses and courses and other formation

8.1.1. Congress participation

"L-Ferritin: One Gene, Five Diseases; from Hereditary Hyperferritinemia to Hypoferritinemia—Report of New Cases"
8th Congress of the International BioIron Society, Heidelberg, 5-10 May 2019.
Poster presentation.

EMBL Italy: A brave new world of RNA, Online EMBL Alumni Meeting, Genoa, 20-21 May 2021.
Assistant

8.1.2. Formation and courses

"Biosecurity course"
UIC Campus Sant Cugat, 14 July 2020.

"Biostatistic course"
UIC Campus Sant Cugat, 28 September 2020.

"Software para el análisis de datos"
Subject of the Official Online Master in Bioinformatics and Biostatistics in Universitat Oberta de Catalunya (UOC), Barcelona, 15 January 2020 – 30 June 2020

"Inferencia Estadística"
Subject of the Official Online Master in Bioinformatics and Biostatistics in Universitat Oberta de Catalunya (UOC), Barcelona, 7 September 2020 – 25 January 2021

"Regresión, modelos y métodos"
Subject of the Official Online Master in Bioinformatics and Biostatistics in Universitat Oberta de Catalunya (UOC), Barcelona, 2 February 2021 – 15 June 2021

"Genómica computacional"
Subject of the Official Online Master in Bioinformatics and Biostatistics in Universitat Oberta de Catalunya (UOC), Barcelona, 15 October 2021 – 12 January 2022.

"Diseño y análisis de experimentos"
Subject of the Official Online Master in Bioinformatics and Biostatistics in Universitat Oberta de Catalunya (UOC), Barcelona, 15 January 2022 – 22 June 2022

8.1.3. Publications

Results presented in this thesis (Results and Discussion sections 5.1 and 5.2) are part of the following published manuscripts:

"HEREDITARY HYPERFERRITINEMIA CATARACT SYNDROME: FERRITIN L GENE AND PHYSIOPATHOLOGY BEHIND THE DISEASE-REPORT OF NEW CASES"

Ferran Celma Nos, Gonzalo Hernández, Xènia Ferrer-Cortès, Ines Hernandez-Rodriguez, Begoña Navarro-Almenzar, José Luis Fuster, Mar Bermúdez Cortés, Santiago Pérez-Montero, Cristian Tornador, Mayka Sanchez

Published in International Journal of Molecular Science (IJMS) 2021.
Impact factor in year 2020: 5.923
Quartile: Q1 category: Biochemistry & Molecular Biology
Citation 2 (date 04/05/2022) as reported by Scholar Google

(See Annex I)

*"*CONTROL OF SYSTEMIC IRON HOMEOSTASIS BY THE 3' IRON-RESPONSIVE ELEMENT OF DIVALENT METAL TRANSPORTER 1 IN MICE*"*

Elisabeth Tybl, Hiromi Gunshin, Sanjay Gupta, Tomasa Barrientos, Michael Bonadonna, **Ferran Celma Nos**, Gael Palais, Zoubida Karim, Mayka Sanchez, Nancy C. Andrews, and Bruno Galy

Published in HemaSphere Journal 2020.
First impact factor of this journal will be obtained in June 2022
Quartile: Q3 category: Hematology
Citation 5 (date 04/05/2022) as reported by Scholar Google

(See Annex II)

8.1.4. Annex I – Paper Celma-Nos *et al.* 2021 IJMS

Celma-Nos *et. al.* 2021 IJMS

International Journal of *Molecular Sciences*

MDPI

Case Report

Hereditary Hyperferritinemia Cataract Syndrome: Ferritin L Gene and Physiopathology behind the Disease—Report of New Cases

Ferran Celma Nos [1,†], Gonzalo Hernández [1,†], Xènia Ferrer-Cortès [1,2], Ines Hernandez-Rodriguez [3], Begoña Navarro-Almenzar [4], José Luis Fuster [5], Mar Bermúdez Cortés [5], Santiago Pérez-Montero [2], Cristian Tornador [2] and Mayka Sanchez [1,2,*]

1 Iron Metabolism: Regulation and Diseases, Department of Basic Sciences, Universitat Internacional de Catalunya (UIC), 08195 Sant Cugat del Vallès, Spain; fcelma@uic.es (F.C.N.); ghernandezv@uic.es (G.H.); xferrerc@uic.es (X.F.-C.)
2 BloodGenetics S.L. Diagnostics in Inherited Blood Diseases, 08950 Esplugues de Llobregat, Spain; sperez@bloodgenetics.com (S.P.-M.); Ctornador@bloodgenetics.com (C.T.)
3 Hematology Service, University Hospital Germans Trias i Pujol (HGTiP), Institut Català d'Oncología (ICO), 08916 Badalona, Spain; agnesrh@iconcologia.net
4 Hematology and Hemotherapy Service, Clinic University Hospital Virgen de la Arrixaca, Instituto Murciano de Investigación Biosanitaria (IMIB), 30120 Murcia, Spain; b.almenzar@gmail.com
5 Pediatric OncoHematology Service, Clinic University Hospital Virgen de la Arrixaca, Instituto Murciano de Investigación Biosanitaria (IMIB), 30120 Murcia, Spain; josel.fuster@carm.es (J.L.F.); mariam.bermudez2@carm.es (M.B.C.)
* Correspondence: msanchezfe@uic.es
† These authors contributed equally to this work.

Abstract: Hereditary hyperferritinemia-cataract syndrome (HHCS) is a rare disease characterized by high serum ferritin levels, congenital bilateral cataracts, and the absence of tissue iron overload. This disorder is produced by mutations in the iron responsive element (IRE) located in the 5′ untranslated regions (UTR) of the light ferritin (*FTL*) gene. A canonical IRE is a mRNA structure that interacts with the iron regulatory proteins (IRP1 and IRP2) to post-transcriptionally regulate the expression of proteins related to iron metabolism. Ferritin L and H are the proteins responsible for iron storage and intracellular distribution. Mutations in the FTL IRE abrogate the interaction of FTL mRNA with the IRPs, and de-repress the expression of FTL protein. Subsequently, there is an overproduction of ferritin that accumulates in serum (hyperferritinemia) and excess ferritin precipitates in the lens, producing cataracts. To illustrate this disease, we report two new families affected with hereditary hyperferritinemia-cataract syndrome with previous known mutations. In the diagnosis of congenital bilateral cataracts, HHCS should be taken into consideration and, therefore, it is important to test serum ferritin levels in patients with cataracts.

Keywords: hereditary hyperferritinemia cataract syndrome; HHCS; serum ferritin; *FTL* gene; cataracts; hyperferritinemia; IRE; IRP

check for updates

Citation: Celma Nos, F.; Hernández, G.; Ferrer-Cortès, X.; Hernandez-Rodriguez, I.; Navarro-Almenzar, B.; Fuster, J.L.; Bermúdez Cortés, M.; Pérez-Montero, S.; Tornador, C.; Sanchez, M. Hereditary Hyperferritinemia Cataract Syndrome: Ferritin L Gene and Physiopathology behind the Disease—Report of New Cases. *Int. J. Mol. Sci.* **2021**, *22*, 5451. https://doi.org/10.3390/ijms22115451

Academic Editor: Elena Vallespín

Received: 27 April 2021
Accepted: 19 May 2021
Published: 21 May 2021

1. Introduction

Hereditary hyperferritinemia-cataract syndrome (HHCS) (OMIM #600886) is a rare disease characterized by high serum ferritin levels, congenital bilateral cataracts, and the absence of tissue iron overload. It was first described in 1995 independently by two researcher teams in France and Italy as an autosomal dominant inherited disease [1,2]. These original manuscripts reported one and two families, respectively, with the previously mentioned clinical features. As no known disease could describe their patient's phenotype, they propose this new genetic disorder.

Beaumont described a three-generation family with visual acuity impairment since young age with deposits in all layers of both lens and an elevated level of circulating ferritin with no other hematological or biochemical abnormalities [2].

On the other hand, Girelli described two north Italian families: Family 1 presented congenital nuclear cataracts and high serum ferritin levels. The proband and his daughter were treated as hereditary hemochromatosis with phlebotomies until they developed microcytic anemia. In the second family, the proband presented bilateral cataracts; however, clinical doctors did not detect elevated serum ferritin levels until his third decade of life; this could be attributed to the fact that the patient was a blood donor [1].

The prevalence of the disease is 1 in 200,000 individuals. However, this number is probably underestimated because the disorder is often misdiagnosed as hereditary hemochromatosis due to hyperferritinemia, despite the absence of iron overload [3]. Actually, investigators often find out new cases with previously reported mutations, as in the case of Ferro and collaborators that described an Italian family [4]; for this reason, it is an important differential diagnosis.

2. Genetics of HHCS

HHCS is due to mutations in the iron responsive element (IRE) located in the 5′ UTR of the Ferritin L mRNA (FTL). At least 47 mutations have been described in *FTL* gene as causative of HHCS, including 36 single mutations, 9 deletions, and 2 insertion-deletions (Figure 1 and Supplementary Table S1). Some authors attempted to find out a relationship between the disease severity and the position of the mutation in the IRE structures [5–7]. Thus, Luscieti and collaborators correlated higher serum ferritin levels in patients with mutations located in the hexanucleotide loop or bulge C than in patients with mutations located in less critical regions as the upper or lower stems of the IRE. Most of the mutations causing HHCS are usually present in heterozygous state due to the dominant inheritance of the disease. However, there are few reported cases with mutations in homozygous state [7,8].

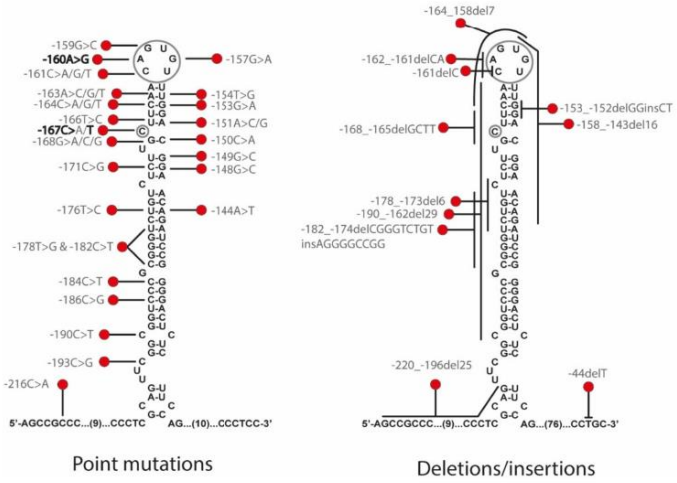

Figure 1. Summary of all reported mutations that cause HHCS. Point mutations are on the right and deletions/insertions are depicted on the left. A grey circle marks the C-bulge and the hexanucleotide loop. Mutations in the families from this study are marked in bold text (c.-160A>G family A and c.-167C>T family B). Genetic variants are reported following the official human genome variation sequence (HGVS) nomenclature. For more detailed information, see Supplementary Table S1.

Traditionally, the HHCS mutations were named following a nomenclature containing the name of the city where they have been described and the number of the mutational position counting from the transcription initiation site as +1; this is referred to as the traditional nomenclature (i.e., +40A>G Paris-1). The official HGVS nomenclature numbered the mutations considering +1 the A in the ATG of the starting codon (methionine 1, ATG), and thus mutations on the 5′ UTR have negative numbering (i.e., c.-160A>G is the same as the +40A>G Paris-1 mutation).

3. Molecular Mechanism behind HHCS

Ferritin is a highly conserved protein in evolution, and it is responsible for cellular iron storage. Cellular ferritin is composed of two different subunits, H-Ferritin and L-Ferritin, which are encoded by two different genes: *FTH* and *FTL* genes, respectively. A canonical ferritin is constituted by the assembly of 24 H- and L-ferritin subunits, forming a chest-like structure that can store thousands of iron atoms. H-Ferritin is the heavy subunit and presents ferroxidase activity converting ferrous iron (Fe^{+2}) into ferric iron (Fe^{+3}), allowing its storage. Whereas, L-Ferritin is part of the ferritin core and it is in charge of ferrous iron release when needed. Furthermore, serum ferritin is mainly constituted by L-ferritin and is partially glycosylated [9].

The expression of both ferritins is regulated post-transcriptionally by the iron regulatory proteins (IRP1 and IRP2) through its binding to the iron-responsive elements (IREs), a conserved hairpin-like motif, located in the 5′ untranslated region (UTR) of ferritin mRNAs [10]. A canonical IRE structure is composed of a six-nucleotide apical loop 5′-CAGUGN-3′ (N denotes A, C or U) on a stem of five paired nucleotides, a small asymmetrical bulge with an unpaired cytosine on the 5′ strand of the stem, and an additional lower stem of variable length [11].

In iron replete conditions, the IRP1 assembles Fe-S clusters and does not interact with IREs, while IRP2 is degraded. However, in iron-deficient conditions, IRPs bind with IREs to modify gene expression (Figure 2). Depending on the IRE location in the UTR, the binding with IRP has different effects. Thus, if the IRE is located in 3′ UTR, the IRP binding causes mRNA stabilization, but if the IRE is in the 5′ UTR, as in the case of *FTL* gene, the IRP binding produces protein translational repression. Mutations in the 5′ IRE of FTL mRNA lead to a loss of interaction between IRPs and the FTL IRE, and a loss of translation repression by them; consequently, an excessive level of ferritin is produced and can be detected in the serum (Figure 2).

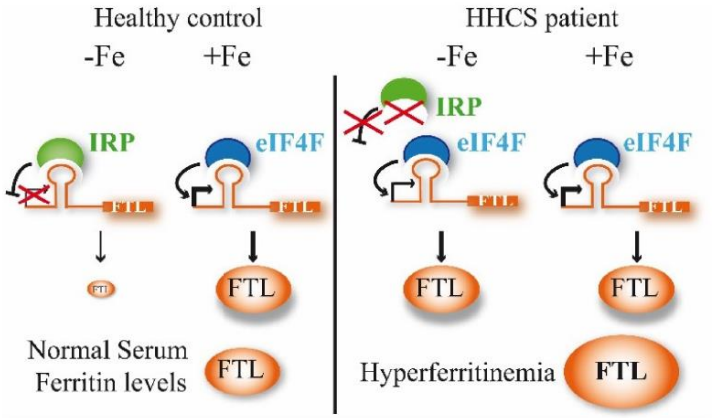

Figure 2. Regulation of *FTL* expression by the IRP/IRE post-transcriptional regulatory system and iron effect on *FTL* translation. IRPs can bind the IRE under low iron conditions (−Fe) forming a repressor complex for protein synthesis. Iron (+Fe) increases the binding of the translation factor eIF4F, forming an activator complex for protein synthesis. IRP and eIF4F compete for the IRE biding [12]. In patients with HHCS, mutations in the FTL IRE abrogate the IRP-IRE interaction, and overall, there is a loss of the post-transcriptional regulation, producing an excess of ferritin that can be detected in serum as hyperferritinemia.

4. Physiopathology of HHCS

Two main hypotheses have been postulated for the cause of the cataract formation in HHCS. The first hypothesis is related to iron homeostasis, and it is postulated that the overproduction of L-ferritin may increase free iron and reactive oxygen species (ROS) with concurrent oxidative damage to the lens that produces loss of transparency [13]. However, the facts that L-Ferritin does not directly bind iron and that the lens-diffracting crystals are iron-poor contradict this possible explanation [14].

The second and most accepted hypothesis refers to the loss of proper lens transparency due to the accumulation of large amounts of crystal deposits formed by aggregated and iron-poor L-ferritin, as demonstrated by Brooks and collaborators [14]

Uncontrolled production of serum ferritin due to the mutations in the L-ferritin IRE causes an excess of cellular ferritin that is secreted to the serum, where it is detected as hyperferritinemia. The excess of ferritin precipitates in the lens cortex, forming numerous small punctate, white breadcrumb-like opacities. The deposits are light-diffracting and impede the correct focus by the patient. In this disease, cataracts are bilateral and usually appear at early ages, however, the visual impairment is slight and patients may not need a surgical intervention until they reach adult age [14,15]. Moreover, the morphology of the HHCS cataracts is highly distinctive from other cataract types with scattered central and peripheral cystic flecks in the cortex and nucleus and small crystalline aggregates. Thus, some authors postulate the possibility of diagnosing HHCS, analyzing the cataract morphology as the main feature [3].

5. Treatment for HHCS

The HHCS patients have no clinical symptoms other than bilateral cataract. L-ferritin deposits in the lens are growing constantly but slowly, and patients diagnosed with HHCS are treated by undergoing surgical intervention when they suffer visual impairment due to the cataracts formation, usually in the adult stage. A suspicion of HHCS and a positive genetic testing will alert for ophthalmologists follow-up of the patient and would most

probably result in cataract early detection and therefore a possible intervention at an earlier age.

HHCS is usually misdiagnosed as hereditary hemochromatosis due to the detection of hyperferritinemia that is a common biochemical sign between both diseases. The importance of a differential diagnosis, including genetic diagnostic, is highlighted to avoid potential damage treatments as venesections or phlebotomies that are indeed counterproductive as it will end up causing iron-deficiency anemia in HHCS patients [8]. In the case of HHCS, phlebotomies are definitely not the proper treatment to apply as these patients do not have iron overload. Their hyperferritinemia does not reflect an excess of body iron but rather an impairment of L-ferritin post-transcriptional regulation.

6. Report of Two New Families with HHCS

6.1. Family A

Proband III.2 from family A (Figure 3 family A) is a 38-year-old woman referred to the Hematology Service at the University Hospital Germans Trias i Pujol (HGTiP) in Barcelona because of unexplained hyperferritinemia. Serum Ferritin levels were 1143 ng/mL, while serum iron and transferrin saturation levels were normal (Table 1). Additional biochemical and hematological data are listed in Table 1. Hereditary Hemochromatosis (HH) genetic studies were negative with no pathogenic mutation found in the HH-related genes. Liver magnetic resonance showed normal levels of hepatic iron. Other relatives, the mother and the maternal uncle, reported to have cataracts and hyperferritinemia; in addition, a first cousin of the mother has hyperferritinemia. Interestingly, three family members died at a young age as a result of ischemic events (cerebral vascular accident or acute myocardial infarction) as reflected in the pedigree, so the proband is currently under study for thrombophilia.

Genetic studies performed on proband (A-III.2) showed the presence of a heterozygous point mutation c.-160A>G located in the 5′ FTL IRE. This variant consists of a substitution in the conserved apical hexanucleotide loop (CAGUGU) (Figure 1). This mutation is indeed the first pathogenic alteration reported for HHCS and described by Beaumont in 1995; the traditional nomenclature referred to it as +40A>G Paris1 mutation.

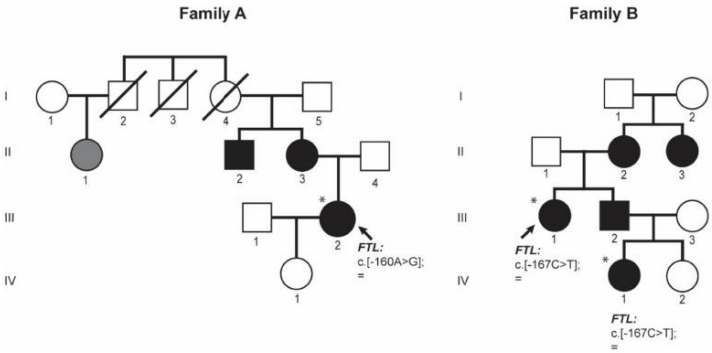

Figure 3. Pedigree trees for the two studied families affected by HHCS. Squares indicate males, and circles, females; slashed symbols indicate deceased individuals. Probands are pointed with an arrow. Filled symbols indicate affected individuals by genetically confirmed HHCS or by the presence of hyperferritinemia and cataracts; grey symbol denotes an individual where only hyperferritinemia has been reported. Asterisks indicate subjects with genetic studies done at BloodGenetics SL. Mutation is named according to the HGVS nomenclature.

Table 1. Biochemical and hematological data of the two studied families affected with HHCS.

Case	Family A	Family B	Family B	Reference Values
Patient	II.1	III.1	IV.1	-
Gender	F	F	F	-
Age at diagnosis (years)	38	44	11	-
Hb (g/dL)	13.3	12.7	14	13.5–17.5 (M) 12.1–15.1 (F)
MCV (fL)	83.3	87.9	82.6	80–95
Ferritin (ng/mL)	1143	919	931	12–300 (M) 12–200 (F)
TF sat (%)	23.0	21.9	14.7	25–50
Iron (µg/dL)	66.45	116	n.a.	49–226
FTL Mutation	c.-160 A>G	c.-167 C>T	c.-167 C>T	-

The following abbreviations were used: Hb, hemoglobin; MCV, mean corpuscular volume; TF sat, transferrin saturation; F, female; M, male; n.a., not available data. The mutation nomenclature used follows the HGVS guidelines.

6.2. Family B

Proband III.1 from family B (Figure 3) is a 44-year-old woman that has presented with hyperferritinemia since 8 years, so she was referred to the Hematology Service in the University Hospital Virgen de la Arrixaca in Murcia. The patient had no other significant clinical history but endometriosis. Her serum ferritin level was 919 ng/mL; serum iron and transferrin saturation levels were normal (Table 1). Additional biochemical and hematological data are listed in Table 1. She was tested for hereditary hemochromatosis HFE gene mutation, and she was found to be a carrier of the H63D variant in HFE gene (this genetic finding could not explain her hyperferritinemia). She had normal deposits of liver iron (<20 µmol/g) in magnetic resonance imaging. During anamnesis, the patient reported having visual problems, so she was directed to an ophthalmology service, where she was diagnosed with cataracts and underwent cataract surgery at the age of 44 years. At that moment, she was interrogated about her family history. Proband's mother (B-II.2) also was HFE H63D heterozygous and had hyperferritinemia, so she was misdiagnosed as HH and treated with phlebotomies. Proband's mother (B-II.2) had also undergone cataract surgery when she was younger. Proband's maternal aunt (B-II.3) has hyperferritinemia and cataracts but she has not undergone cataract surgery. The proband also has a brother (B-III.2) with hyperferritinemia and congenital cataracts that has been operated, and two nieces, one had normal ferritin levels and no cataracts (IV.2) and an older niece (IV.1) who was also genetically studied because of hyperferritinemia and operated congenital cataracts (see below).

In family B, patient IV.1 is the niece of the proband (B-III.1) (Figure 3 family B), she was 10 year old when she attended the hematology consult due to hyperferritinemia. Her serum ferritin levels were 931 ng/mL and transferrin saturation was normal. She was diagnosed with cataracts at the age of 10 years old. Additional biochemical and hematological data are listed in Table 1.

After genetic testing by Sanger sequencing of the *FTL* gene on the proband B-III.1 and by a NGS gene panel on the patient B-IV.1 from the same family, both patients were found to be heterozygous for the NM_00146.3:c.[-167C>T];[=] mutation in *FTL* gene, also known as the +33C>T Madrid/Philadelphia pathological variant that was reported for the first time by Balas and collaborators [16]. This pathogenic mutation is located in the C-bulge of the FTL IRE (Figure 1), and this is a critical residue for IRP-IRE interaction.

These two families (A and B, Figure 3) illustrate the clinical findings and the mode of inheritance (autosomal dominant) of hereditary hyperferritinemia-cataract syndrome (HHCS) and presented with mutations in the apical loop or the C-bulge of the FTL IRE, respectively.

7. Discussion

Hereditary hyperferritinemia-cataract syndrome (HHCS) was the first genetic disorder known to result from regulatory mutations affecting translation (Figure 2). As such, it

represents a novel mechanism for cataract formation. Since its discovery in 1995, different authors have reported mutations that affect the FTL IRE and cause HHCS (Supplementary Table S1 and Figure 1). Here, we describe two new families with several affected members, and identify previously reported mutations in *FTL* gene, the +40A>G Paris1 (c.-160A>G) [2] and the +33C>T Madrid/Philadelphia (c.-167C>T) [16] mutations, for family A and B, respectively. The +40A>G Paris1 mutation affected the IRE apical loop, while the +33C>T Madrid/Philadelphia mutation was located in the C-buge of the IRE. Both of these IRE positions are critical residues for IRP-IRE interaction [17]. In both families, the ferritin levels were substantially high (above 900 ng/mL), which is in agreement with the conclusions reported by Luscieti and collaborators, who demonstrated that despite all mutations in the FTL IRE increasing serum ferritin, mutations in the hexanucleotide loop or in the C-bulge lead to higher serum ferritin levels than mutations located in other IRE positions [7].

In patients with HHCS, the unique clinical abnormality is the presence of congenital cataracts. Thus, to improve the diagnosis of this disease, it is very relevant to increase awareness in ophthalmologists about the importance of testing serum ferritin levels routinely while investigating cataracts, especially in pediatric cases. On the other side, all unexplained hyperferritinemia should be referred for ophthalmological assessment, as cataracts may be asymptomatic but lead to a correct diagnosis of HHCS. The definitive confirmation of the disease will be achieved after a simple genetic test as all mutations leading to HHCS are concentrated in a concrete region comprising the 5′ UTR region of *FTL* gene.

8. Materials and Methods

8.1. Patients

All subjects gave their informed consent for inclusion in this study. The study was conducted in accordance with the Declaration of Helsinki, and the protocol was approved by the Ethics Committee of the Hospital General de Catalunya.

8.2. DNA Extraction, PCR Amplification and DNA Sequencing

Genomic DNA was extracted from peripheral blood using the FlexiGene DNA kit (Qiagen, Hilden, Germany) according to manufacturer's instructions.

Ferritin L (FTL) gene region was sequenced using the Sanger method or NGS by using a gene panel. For Sanger sequencing, the FTL gene was amplified using 50 ng of genomic DNA. Descriptions of the primers and conditions have been previously published elsewhere [18]. The resulting amplification products were verified on a 2% ethidium bromide agarose gel. The purified PCR products were sequenced using a conventional Sanger method. Sequencing results were analyzed using Mutation Surveyor software (SoftGenetics LLC, State College, PA, USA).

For NGS methods, patient B-IV.1 was analysed using a targeted NGS gene panel (v15) for hereditary hemochromatosis and hyper/hypoferritinaemia (BloodGenetics panel #10010) that included the following nine genes: HFE, HFE2, HAMP, TFR2, SLC40A1, BMP6, FTL, FTH1, and GNPAT, following a protocol reported previously for a different panel [19]. Data analysis was performed using Varsome clinical software [20]. Mutations detected by NGS were confirmed by conventional Sanger sequencing.

Genetic variants are reported following the official human genome variation sequence (HGVS) nomenclature and refer to NM_000146.3 for the Homo sapiens FTL transcript variant and NP_000137.2 for the Homo sapiens FTL protein.

Supplementary Materials: The following are available online at https://www.mdpi.com/article/10.3390/ijms22115451/s1, Table S1: Reported mutations in HHCS disease.

Author Contributions: Study concept and research design: M.S. Patients' clinics and management: I.H.-R., B.N.-A., J.L.F., M.B.C. Sequencing and mutation validation: X.F.-C. and F.C.N. Writing of the manuscript, table and figures: F.C.N., G.H. and M.S. Funding recruitment: M.S., S.P.-M., C.T. All

authors participated in data discussion. All authors have read and agreed to the published version of the manuscript.

Funding: This study was supported by the grant RTI-2018-101735-B-I100 (MCI/AEI/FEDER, EU) from Spanish Secretary of Research, Development and Innovation (MINECO) to M.S. F.C. held an FI-AGAUR predoctoral fellowship (2019FI-B00794) from Generalitat de Catalunya. G.H. is supported by funds provided by the APU and ADISCON Patient associations. X.F-C. is partially supported by funds provided by the grant RTI-2018-101735-B-I100 (MCI/AEI/FEDER, EU).

Institutional Review Board Statement: The study was conducted according to the guidelines of the Declaration of Helsinki, and approved by the Ethics Committee of the Hospital Universitari General de Catalunya (protocol code 2018/74-HEM_UIC-HUGC for A-IRON project date of approval 29 October 2018).

Informed Consent Statement: Informed consent was obtained from all subjects involved in this study.

Data Availability Statement: The data presented in this study are available on request from the corresponding author.

Acknowledgments: We are very grateful to all families who kindly contributed to this study. We thank Beatriz Cadenas for help with design of Figure 1.

Conflicts of Interest: The authors declare no conflict of interests.

References

1. Girelli, D.; Olivieri, O.; De Franceschi, L.; Corrocher, R.; Bergamaschi, G.; Cazzola, M. A linkage between hereditary hyperferritinaemia not related to iron overload and autosomal dominant congenital cataract. *Br. J. Haematol.* **1995**, *90*, 931–934. [CrossRef] [PubMed]
2. Beaumont, C.; Leneuve, P.; Devaux, I.; Scoazec, J.-Y.; Berthier, M.; Loiseau, M.-N.; Grandchamp, B.; Bonneau, D. Mutation in the iron responsive element of the L ferritin mRNA in a family with dominant hyperferritinaemia and cataract. *Nat. Genet.* **1995**, *11*, 444–446. [CrossRef] [PubMed]
3. Craig, J.E.; Clark, J.B.; McLeod, J.L.; Kirkland, M.A.; Grant, G.; Elder, J.E.; Toohey, M.G.; Kowal, L.; Savoia, H.F.; Chen, S.; et al. Hereditary hyperferritinemia-cataract syndrome: Prevalence, lens morphology, spectrum of mutations, and clinical presentations. *Arch. Ophthalmol.* **2003**, *121*, 1753–1761. [CrossRef] [PubMed]
4. Ferro, E.; Capra, A.P.; Zirilli, G.; Meduri, A.; Urso, M.; Briuglia, S.; La Rosa, M.A. FTL c.-168G>C Mutation in Hereditary Hyperferritinemia Cataract Syndrome: A New Italian Family. *Pediatr. Dev. Pathol.* **2018**, *21*, 456–460. [CrossRef] [PubMed]
5. Allerson, C.R.; Cazzola, M.; Rouault, T.A. Clinical severity and thermodynamic effects of iron-responsive element mutations in hereditary hyperferritinemia-cataract syndrome. *J. Biol. Chem.* **1999**, *274*, 26439–26447. [CrossRef] [PubMed]
6. Cazzola, M.; Bergamaschi, G.; Tonon, L.; Arbustini, E.; Grasso, M.; Vercesi, E.; Barosi, G.; Bianchi, P.E.; Cairo, G.; Arosio, P. Hereditary hyperferritinemia-cataract syndrome: Relationship between phenotypes and specific mutations in the iron-responsive element of ferritin light-chain mRNA. *Blood* **1997**, *90*, 814–821. [CrossRef] [PubMed]
7. Luscieti, S.; Tolle, G.; Aranda, J.; Campos, C.B.; Risse, F.; Morán, É.; Muckenthaler, M.U.; Sánchez, M. Novel mutations in the ferritin-L iron-responsive element that only mildly impair IRP binding cause hereditary hyperferritinaemia cataract syndrome. *Orphanet J. Rare Dis.* **2013**, *8*, 30. [CrossRef] [PubMed]
8. Giansily-Blaizot, M.; Cunat, S.; Moulis, G.; Schved, J.; Aguilar-Martinez, P. Homozygous mutation of the 5′UTR region of the L-Ferritin gene in the hereditary hyperferritinemia cataract syndrome and its impact on the phenotype. *Haematologica* **2013**, *98*, 42. [CrossRef] [PubMed]
9. Cohen, L.A.; Gutiérrez, L.; Weiss, A.; Leichtmann-Bardoogo, Y.; Zhang, D.-L.; Crooks, D.R.; Sougrat, R.; Morgenstern, A.; Galy, B.; Hentze, M.W.; et al. Serum ferritin is derived primarily from macrophages through a nonclassical secretory pathway. *Blood* **2010**, *116*, 1574–1584. [CrossRef] [PubMed]
10. Hentze, M.W.; Muckenthaler, M.U.; Andrews, N.C. Balancing acts: Molecular control of mammalian iron metabolism. *Cell* **2004**, *117*, 285–297. [CrossRef]
11. Wilkinson, N.; Pantopoulos, K. The IRP/IRE system in vivo: Insights from mouse models. *Front. Pharmacol.* **2014**, *5*, 176. [CrossRef] [PubMed]
12. Khan, M.A.; Domashevskiy, A.V. Iron enhances the binding rates and translational efficiency of iron responsive elements (IREs) mRNA with initiation factor eIF4F. *PLoS ONE* **2021**, *16*, e0250374. [CrossRef] [PubMed]
13. Levi, S.; Girelli, D.; Perrone, F.; Pasti, M.; Beaumont, C.; Corrocher, R.; Albertini, A.; Arosio, P. Analysis of ferritins in lymphoblastoid cell lines and in the lens of subjects with hereditary hyperferritinemia-cataract syndrome. *Blood* **1998**, *91*, 4180–4187. [CrossRef] [PubMed]
14. Brooks, D.G.; Manova-Todorova, K.; Farmer, J.; Lobmayr, L.; Wilson, R.B.; Eagle, R.C.; Pierre, T.G.S.; Stambolian, D. Ferritin crystal cataracts in hereditary hyperferritinemia cataract syndrome. *Invest. Ophthalmol. Vis. Sci.* **2002**, *43*, 1121–1126.

15. Moravikova, J.; Honzik, T.; Jadvidzakova, E.; Zdrahalova, K.; Kremlikova Pourova, R.; Korbasova, M.; Liskova, P.; Dudakova, L. Hereditary hyperferritinemia-cataract syndrome in three Czech families: Molecular genetic testing and clinical implications. *J. AAPOS* **2020**, *24*, 352.e1–352.e5. [CrossRef]
16. Balas, A.; Aviles, M.J.; Garcia-Sanchez, F.; Vicario, J.L. Description of a new mutation in the L-ferrin iron-responsive element associated with hereditary hyperferritinemia-cataract syndrome in a Spanish family. *Blood* **1999**, *93*, 4020–4021. [CrossRef] [PubMed]
17. Walden, W.E.; Selezneva, A.I.; Dupuy, J.; Volbeda, A.; Fontecilla-Camps, J.C.; Theil, E.C.; Volz, K.; Özcan, U.; Cao, Q.; Yilmaz, E.; et al. Structure of dual function iron regulatory protein 1 complexed with ferritin IRE-RNA. *Science* **2006**, *314*, 1903–1908. [CrossRef]
18. Cadenas, B.; Fita-Torró, J.; Bermúdez-Cortés, M.; Hernandez-Rodriguez, I.; Fuster, J.L.; Llinares, M.E.; Galera, A.M.; Romero, J.L.; Pérez-Montero, S.; Tornador, C.; et al. L-Ferritin: One Gene, Five Diseases; from Hereditary Hyperferritinemia to Hypoferritinemia-Report of New Cases. *Pharmaceuticals* **2019**, *12*, 17. [CrossRef] [PubMed]
19. Vila Cuenca, M.; Marchi, G.; Barqué, A.; Esteban-Jurado, C.; Marchetto, A.; Giorgetti, A.; Chelban, V.; Houlden, H.; Wood, N.W.; Piubelli, C.; et al. Genetic and Clinical Heterogeneity in Thirteen New Cases with Aceruloplasminemia. Atypical Anemia as a Clue for an Early Diagnosis. *Int. J. Mol. Sci.* **2020**, *21*, 2374. [CrossRef] [PubMed]
20. Kopanos, C.; Tsiolkas, V.; Kouris, A.; E Chapple, C.; Albarca Aguilera, M.; Meyer, R.; Massouras, A. VarSome: The human genomic variant search engine. *Bioinformatics* **2019**, *35*, 1978–1980. [CrossRef] [PubMed]

8.1.4.1. Annex I.I – Supplementary data Paper HHCS

Supplementary Table 1: Reported mutations in HHCS disease

Supplementary Table 1. Reported mutations in HHCS disease

N	HGVS nomenclature	Mutation type	Mutation position	First Publication	Old Nomenclature
1	c.-216C>A	IRE regulatory	Promoter *FTL*	(1)	NA
2	c.-193C>G + c.-160A>G	IRE regulatory	lower stem + hexanucleotide loop	(2)	+7C>G & +40A>G
3	c.-190C>T	IRE regulatory	lower stem	(3)	+10C>U
4	c.-186C>G	IRE regulatory	lower stem	(4)	+14C>G
5	c.-184C>T	IRE regulatory	lower stem	(3)	+16C>U
6	c.-182C>T + c.-178T>G	IRE regulatory	lower stem	(5)	Paiva-2 + 18C>U & 22U>G
7	c.-176T>C	IRE regulatory	lower stem	(6)	+24U>C
8	c.-171C>G	IRE regulatory	lower stem	(7)	Torino +29C>G
9	c.-168G>A	IRE regulatory	lower stem	(5)	Pavia-1 +32G>A
10	c.-168G>C	IRE regulatory	lower stem	(8)	Baltimore-1 +32G>C
11	c.-168G>T	IRE regulatory	lower stem	(9)	Paris-2 or Milano-1 +32G>U
12	c.-167C>A	IRE regulatory	C bulge	(10)	Paris +33C>A
13	c.-167C>T	IRE regulatory	C bulge	(11)	Madrid or Philadelphia +33C>U
14	c.-166T>C	IRE regulatory	upper stem	(12)	Paris +34U>C
15	c.-164C>A	IRE regulatory	upper stem	(13)	London-2 +36C>A
16	c.-164C>G	IRE regulatory	upper stem	(3)	Milano +36C>G
17	c.-164C>T	IRE regulatory	upper stem	(14)	Badalona +36C>U
18	c.-163A>C	IRE regulatory	upper stem	(15)	Pavia +37A>C
19	c.-163A>G	IRE regulatory	upper stem	(3)	Milano +37A>G
20	c.-163A>T	IRE regulatory	upper stem	(16)	Zaragoza +37A>U
21	c.-161C>A	IRE regulatory	hexanucleotide loop	(17)	Geelong +39C>A
22	c.-161C>G	IRE regulatory	hexanucleotide loop	(18)	Paris +39C>G
23	c.-161C>T	IRE regulatory	hexanucleotide loop	(13)	London-1 +39C>U
24	c.-160A>G	IRE regulatory	hexanucleotide loop	(19)	Paris-1 or Montpellier-1 +40A>G
25	c.-160A>G + c.-159G>C	IRE regulatory	hexanucleotide loop	(4)	Paris-1 or Montpellier-1 +40A>G & Verona-1 +41G>C
26	c.-159G>C	IRE regulatory	hexanucleotide loop	(20)	Verona-1 +41G>C
27	c.-157G>A	IRE regulatory	hexanucleotide loop	(21)	Salt Lake City +43G>A
28	c.-154T>G	IRE regulatory	upper stem	(22)	+46U>G
29	c.-153G>A	IRE regulatory	upper stem	(12)	Paris +47G>A
30	c.-151A>C	IRE regulatory	lower stem	(2)	+49A>C
31	c.-151A>G	IRE regulatory	lower stem	(23)	Ghent +49A > G
32	c.-150C>A	IRE regulatory	lower stem	(24)	+50C>A

33	c.-149G>C	IRE regulatory	lower stem	(25)	Torino +51G>C
34	c.-148G>C	IRE regulatory	lower stem	(14)	Heidelberg +52G>C
35	c.-144A>T	IRE regulatory	lower stem	(15)	Paris +56A>U
36	c.-110C>T	IRE regulatory	5′ UTR	(3)	+90C>U
37	c.-220_-196del25	IRE regulatory	new transcription starting site (resulting IRE lacks nt 1-24)	(26)	NA
38	c.-190-162del29	IRE regulatory	eliminating IRE	(27)	Verona-2 +10_38del29
39	c.-182_-174delCGGGTCTGTinsAGGGGCCGG $	IRE regulatory	eliminating part of lower stem	(28)	+18_+26 delCGGGTCTGTinsAGGGGCCGG
40	c.-178_-173del6	IRE regulatory	eliminating part of lower stem	(29)	+22_27del6
41	c.-168_-165delGCTT	IRE regulatory	eliminating C bulge	(30)	+32_35delGCTT
42	c.-164_158del7	IRE regulatory	eliminating part of hexanucleotide loop	(31)	Esplugues +36_42d
43	c.-161delC	IRE regulatory	eliminating IRE	(32)	+39delC
44	c.-162_-161delCA	IRE regulatory	eliminating part of hexanucleotide loop	(33)	+38_39del AC
45	c.-158_-143del16	IRE regulatory	eliminating part of hexanucleotide loop	(33)	+42_57del16
46	c.-153_-152delGGinsCT	IRE regulatory	eliminating part of upper stem	(34)	+47_48delGGinsCT
47	c.-44delT	IRE regulatory	eliminating IRE	(3)	+176delT

Supplementary table 1 references:

(1) Faniello MC, Di Sanzo M, Quaresima B, Nisticò A, Fregola A, Grosso M, et al. Bilateral cataract in a subject carrying a C to A transition in the L ferritin promoter region. Clin Biochem 2009 -06;42(9):911-914.

(2) Castiglioni E, Soriani N, Girelli D, Camaschella C, Spiga I, Della Porta MG, et al. High resolution melting for the identification of mutations in the iron responsive element of the ferritin light chain gene. Clin Chem Lab Med 2010 -10;48(10):1415-1418.

(3) Cremonesi L, Paroni R, Foglieni B, Galbiati S, Fermo I, Soriani N, et al. Scanning mutations of the 5'UTR regulatory sequence of L-ferritin by denaturing high-performance liquid chromatography: identification of new mutations. Br J Haematol 2003 -04;121(1):173-179.

(4) Cremonesi L, Fumagalli A, Soriani N, Ferrari M, Levi S, Belloli S, et al. Double-gradient denaturing gradient gel electrophoresis assay for identification of L-ferritin iron-responsive element mutations responsible for hereditary hyperferritinemia-cataract syndrome: identification of the new mutation C14G. Clin Chem 2001 -03;47(3):491-497.

(5) Cazzola M, Bergamaschi G, Tonon L, Arbustini E, Grasso M, Vercesi E, et al. Hereditary hyperferritinemia-cataract syndrome: relationship between phenotypes and specific mutations in the iron-responsive element of ferritin light-chain mRNA. Blood 1997 -07-15;90(2):814-821.

(6) Rüfer A, Howell JP, Lange AP, Yamamoto R, Heuscher J, Gregor M, et al. Hereditary hyperferritinemia-cataract syndrome (HHCS) presenting with iron deficiency anemia associated with a new mutation in the iron responsive element of the L ferritin gene in a Swiss family. Eur J Haematol 2011 -09;87(3):274-278.

(7) Bosio S, Campanella A, Gramaglia E, Porporato P, Longo F, Cremonesi L, et al. C29G in the iron-responsive element of L-ferritin: a new mutation associated with hyperferritinemia-cataract. Blood Cells Mol Dis 2004 Jul-Aug;33(1):31-34.

(8) L-ferritin-Baltmore-1: A novel mutation in the iron response element (C32G) as a cause of the hyperferritinemia-cataract syndrome. Blood: AMER SOC HEMATOLOGY 1200 19TH ST, NW, STE 300, WASHINGTON, DC 20036-2422 USA; 1999.

(9) Martin ME, Fargion S, Brissot P, Pellat B, Beaumont C. A point mutation in the bulge of the iron-responsive element of the L ferritin gene in two families with the hereditary hyperferritinemia-cataract syndrome. Blood 1998 -01-01;91(1):319-323.

(10) Durupt S, Durieu I, Salles B, Beaumont C, Hot A, Rousset H, et al. [A potential etiology of elevated ferritin: hyperferritinemia-cataract syndrome]. Rev Med Interne 2001 -01;22(1):83-85.

(11) Balas A, Aviles MJ, Garcia-Sanchez F, Vicario JL. Description of a new mutation in the L-ferrin iron-responsive element associated with hereditary hyperferritinemia-cataract syndrome in a Spanish family. Blood 1999 -06-01;93(11):4020-4021.

(12) Hetet G, Devaux I, Soufir N, Grandchamp B, Beaumont C. Molecular analyses of patients with hyperferritinemia and normal serum iron values reveal both L ferritin IRE and 3 new ferroportin (slc11A3) mutations. Blood 2003 -09-01;102(5):1904-1910.

(13) Mumford AD, Vulliamy T, Lindsay J, Watson A. Hereditary hyperferritinemia-cataract syndrome: two novel mutations in the L-ferritin iron-responsive element. Blood 1998 -01-01;91(1):367-368.

(14) Luscieti S, Tolle G, Aranda J, Campos CB, Risse F, Morán É, et al. Novel mutations in the ferritin-L iron-responsive element that only mildly impair IRP binding cause hereditary hyperferritinaemia cataract syndrome. Orphanet J Rare Dis 2013 -02-19;8:30.

(15) Ferrari F, Foglieni B, Arosio P, Camaschella C, Daraio F, Levi S, et al. Microelectronic DNA chip for hereditary hyperferritinemia cataract syndrome, a model for large-scale analysis of disorders of iron metabolism. Hum Mutat 2006 -02;27(2):201-208.

(16) García Erce JA, Cortés T, Cremonesi L, Cazzola M, Pérez-Lungmus G, Giralt M. [Hyperferritinemia-cataract syndrome associated to the HFE gene mutation. Two new Spanish families and a new mutation (A37T: "Zaragoza")]. Med Clin (Barc) 2006 -06-10;127(2):55-58.

(17) McLeod JL, Craig J, Gumley S, Roberts S, Kirkland MA. Mutation spectrum in Australian pedigrees with hereditary hyperferritinaemia-cataract syndrome reveals novel and de novo mutations. Br J Haematol 2002 -09;118(4):1179-1182.

(18) Garderet L, Hermelin B, Gorin NC, Rosmorduc O. Hereditary hyperferritinemia-cataract syndrome: a novel mutation in the iron-responsive element of the L-ferritin gene in a French family. Am J Med 2004 -07-15;117(2):138-139.

(19) Beaumont C, Leneuve P, Devaux I, Scoazec JY, Berthier M, Loiseau MN, et al. Mutation in the iron responsive element of the L ferritin mRNA in a family with dominant hyperferritinaemia and cataract. Nat Genet 1995 -12;11(4):444-446.

(20) Meneses FGA, Schnabel B, Silva, I. D. C. G., Alberto FL, Toma L, Nader HB, et al. Identification of the mutations associated with hereditary hyperferritinemia cataract syndrome and hemochromatosis in a Brazilian family. Clin Genet 2011 -02;79(2):189-192.

(21) Phillips JD, Warby CA, Kushner JP. Identification of a novel mutation in the L-ferritin IRE leading to hereditary hyperferritinemia-cataract syndrome. Am J Med Genet A 2005 -04-01;134A(1):77-79.

(22) Messa E, Pellegrino RM, Palmieri A, Carturan S, Cilloni D, Saglio G, et al. Identification of a novel mutation in the L ferritin iron-responsive element causing hereditary hyperferritinemia-cataract syndrome. Acta Haematol 2009;122(4):223-225.

(23) Van de Sompele S, Pécheux L, Couso J, Meunier A, Sanchez M, De Baere E. Functional characterization of a novel non-coding mutation "Ghent +49A > G" in the iron-responsive element of L-ferritin causing hereditary hyperferritinaemia-cataract syndrome. Sci Rep 2017 -12-21;7(1):18025.

(24) Gonzalez-Huerta L, Ramirez-Sanchez V, Rivera-Vega M, Messina-Baas O, Cuevas-Covarrubias S. A family with hereditary hyperferritinaemia cataract syndrome: evidence of incomplete penetrance and clinical heterogeneity. Br J Haematol 2008 -11;143(4):596-598.

(25) Camaschella C, Zecchina G, Lockitch G, Roetto A, Campanella A, Arosio P, et al. A new mutation (G51C) in the iron-responsive element (IRE) of L-ferritin associated with hyperferritinaemia-cataract syndrome decreases the binding affinity of the mutated IRE for iron-regulatory proteins. Br J Haematol 2000 -03;108(3):480-482.

(26) Burdon KP, Sharma S, Chen CS, Dimasi DP, Mackey DA, Craig JE. A novel deletion in the FTL gene causes hereditary hyperferritinemia cataract syndrome (HHCS) by alteration of the transcription start site. Hum Mutat 2007 -07;28(7):742.

(27) Girelli D, Corrocher R, Bisceglia L, Olivieri O, Zelante L, Panozzo G, et al. Hereditary hyperferritinemia-cataract syndrome caused by a 29-base pair deletion in the iron responsive element of ferritin L-subunit gene. Blood 1997 -09-01;90(5):2084-2088.

(28) Lenzhofer M, Schroedl F, Trost A, Kaser-Eichberger A, Wiedemann H, Strohmaier C, et al. Aqueous humor ferritin in hereditary hyperferritinemia cataract syndrome. Optom Vis Sci 2015 -04;92(4 Suppl 1):40.

(29) Cazzola M, Foglieni B, Bergamaschi G, Levi S, Lazzarino M, Arosio P. A novel deletion of the L-ferritin iron-responsive element responsible for severe hereditary hyperferritinaemia-cataract syndrome. Br J Haematol 2002 -03;116(3):667-670.

(30) Garber I, Pudek M. A novel deletion in the iron-response element of the L-ferritin gene, causing hyperferritinaemia cataract syndrome. Ann Clin Biochem 2014 November 1,;51(6):710-713.

(31) Cadenas B, Fita-Torró J, Bermúdez-Cortés M, Hernandez-Rodriguez I, Fuster JL, Llinares ME, et al. L-Ferritin: One Gene, Five Diseases; from Hereditary Hyperferritinemia to Hypoferritinemia—Report of New Cases. Pharmaceuticals (Basel) 2019 -1-23;12(1).

(32) Muñoz-Muñoz J, Cuadrado-Grande N, Moreno-Carralero M-, Hoyos-Sanabria B, Manubes-Guarch A, González A-, et al. Hereditary hyperferritinemia cataract syndrome in four patients with mutations in the IRE of the FTL gene. Clin Genet 2013 -05;83(5):491-493.

(33) Giansily M, Beaumont C, Desveaux C, Hetet G, Schved JF, Aguilar-Martinez P. Denaturing gradient gel electrophoresis screening for mutations in the hereditary hyperferritinaemia cataract syndrome. Br J Haematol 2001 -01;112(1):51-54.

(34) Mattila R, Sainio A, Järveläinen M, Pursiheimo J, Järveläinen H. A novel double nucleotide variant in the ferritin-L iron-responsive element in a Finnish patient with hereditary hyperferritinaemia-cataract syndrome. Acta Ophthalmol 2018 -02;96(1):95-99.

8.1.5. Annex II – Paper Tybl *et al.* 2020 HemaSphere

Tybl *et. al.* 2020 HemaSphere

HemaSphere
Powered by EHA

EHA EUROPEAN HEMATOLOGY ASSOCIATION

Letter
OPEN ACCESS

Control of Systemic Iron Homeostasis by the 3' Iron-Responsive Element of Divalent Metal Transporter 1 in Mice

Elisabeth Tybl[1], Hiromi Gunshin[2†], Sanjay Gupta[1], Tomasa Barrientos[3], Michael Bonadonna[1,4], Ferran Celma Nos[5], Gael Palais[1], Zoubida Karim[6], Mayka Sanchez[5], Nancy C. Andrews[7], Bruno Galy[1]

Correspondence: Bruno Galy (e-mail: b.galy@dkfz.de).

Tight control of intestinal iron absorption is required to avoid both iron insufficiency and excess.[1] Dietary nonheme iron is taken up by absorptive enterocytes via the apical iron transporter DMT1 (a.k.a. SLC11A2),[2–4] and transferred into the circulation by ferroportin (FPN, a.k.a. SLC40A1), with the help of a ferroxidase, hephaestin (HEPH).[1] FPN activity is controlled by the liver hormone hepcidin,[1] but DMT1 seems regulated locally via mechanisms operating within enterocytes.[5,6] *DMT1* messenger ribonucleic acid (mRNA) exists in four isoforms that differ in their 5' and 3' ends.[7] 3' end diversity results from alternative usage of splicing and polyadenylation sites and yields isoforms that either contain or lack a conserved iron responsive element (IRE) in their 3' untranslated region (UTR). IRE-containing isoforms are predominant in duodenal enterocytes.

IREs are stem-loop structures that interact with iron regulatory proteins (IRPs, a.k.a. ACO1 and IREB2) in iron-depleted cells.[1] IRP binding to multiple IREs in the 3'-UTR of the transferrin receptor 1 (*TFRC*) mRNA limits its degradation by Regnase-1 (a.k.a. ZC3H12A).[8] The presence of an IRE-like motif in *DMT1* suggests that *DMT1* could be regulated by IRPs, similar to *TFRC*. However, the single *DMT1* IRE contains an additional 3'-bulge in its upper stem, and *DMT1* mRNA seems to lack a Regnase-1 binding site.[9] Importantly, DMT1 expression only responds to iron fluctuation in a subset of cell lines,[10,11] and the *DMT1* 3'IRE failed to exhibit iron-dependent regulation in reporter assays.[11] Furthermore, *Dmt1* transcription is controlled by HIF2α (a.k.a. EPAS1),[5,6] which itself is regulated by IRPs,[1] confounding the study of specific functions of the *Dmt1* 3'IRE.[12] Here, we address the role of this ribonucleic acid (RNA) motif using a mouse model with selective disruption of the *Dmt1* 3'IRE.

We established a mouse line lacking the 5' stem, the apical loop and part of the 3' stem of the *Dmt1* 3'IRE (Fig. 1A–D and Supplemental Materials and Methods, http://links.lww.com/HS/A91). Mutagenesis of the *Dmt1* 3'IRE impairs IRP binding. Importantly, all four DMT1 transcripts are adequately expressed in homozygous mutant mice, including those that bear the dysfunctional IRE (Supplemental Figure 1, http://links.lww.com/HS/A91). The resulting allele (designated $Dmt1^{IRE\Delta}$) is inherited in Mendelian proportions (Supplemental Table 1, http://links.lww.com/HS/A91). Both $Dmt1^{IRE\Delta/\Delta}$ males and females are viable and fertile and exhibit normal posture and activity patterns. Blood cell parameters (Supplemental Table 2, http://links.lww.com/HS/A91) are globally preserved during postnatal growth (2 weeks of age, during a period of high iron demand), early adulthood (3 months of age) and advanced age (9 months). A flow cytometry analysis did not reveal any abnormality of terminal erythroid differentiation in young adults (Supplemental Figure 2, http://links.lww.com/HS/A91). The mean weight is slightly higher in 2-week-old $Dmt1^{IRE\Delta/\Delta}$ pups but later is comparable to $Dmt1^{IRE+/+}$ littermates (Supplemental Table 3, http://links.lww.com/HS/A91). Spleen, liver, kidney, and heart weights were unchanged (Supplemental Table 3, http://links.lww.com/HS/A91). These data show that while *Dmt1* is essential during perinatal life and critical for erythroid iron acquisition,[2,3] its 3'IRE is not required under standard laboratory conditions and appears to be dispensable for normal hematopoiesis.

Interestingly, 2-week-old $Dmt1^{IRE\Delta/\Delta}$ male mice display a 40% reduction in serum iron levels, and a decrease in transferrin saturation (Fig. 1E). In spite of the hypoferremia, hepcidin concentration, which is low during postnatal growth, is not affected (Fig. 1F). Similarly, both hepatic and splenic iron stores are small and remain indistinguishable from wild-type animals

[1]German Cancer Research Center (DKFZ), Division of Virus-Associated Carcinogenesis (F170), Heidelberg, Germany
[2]Department of Nutrition, University of Massachusetts, Amherst, Massachusetts, United States
[3]Duke University School of Medicine, Department of Orthopedic Surgery, Durham, North Carolina, United States
[4]Biosciences Faculty, University of Heidelberg, Heidelberg, Germany
[5]Iron Metabolism: Regulation and Diseases Group, Department of Basic Sciences, Faculty of Medicine and Health Sciences, Universitat Internacional de Catalunya (UIC), Barcelona, Spain
[6]INSERM U1149, Paris Diderot University, Sorbonne Paris Cité, and Laboratory of Excellence GR-Ex, Paris, France
[7]Duke University School of Medicine, Department of Pharmacology and Cancer Biology and Department of Pediatrics, Durham, North Carolina, United States.
[†]Deceased
This work was supported by the Howard Hughes Medical Institute (N.C.A.) and a grant from the Deutsche Forschungsgemeinschaft to B.G. (GA2075/5-1).
The authors have no conflicts of interest to disclose.
Supplemental Digital Content is available for this article.

HemaSphere (2020) 4:5(e459). http://dx.doi.org/10.1097/HS9.0000000000000459.
Received: 22 April 2020 / Accepted: 26 June 2020

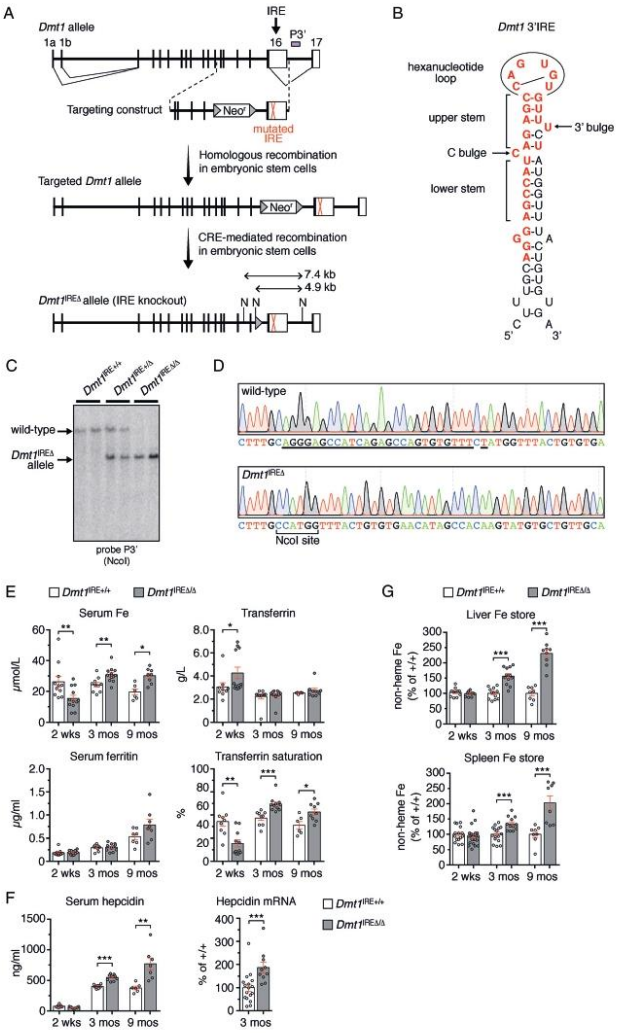

Figure 1. **Disruption of the *Dmt1* 3'IRE decreases serum iron levels during early life but leads to hyperferremia in adulthood**. (A) The *Dmt1* locus comprises 18 exons. The first exon is transcribed from 2 alternative promoters termed 1a and 1b, respectively. 3' end diversity results from alternative splicing and alternative usage of polyadenylation sites: inclusion of exon 16 gives rise to *Dmt1* mRNA isoforms bearing the 3'UTR IRE; non-IRE isoforms arise from the joining of a splice donor located upstream of the IRE within exon 16 with the splice acceptor of exon 17. The IRE stem-loop was mutagenized using a targeting construct encompassing exons 12 to 16; a CD neomycin (Neo) resistance cassette (indicated Neo^r) flanked with *LoxP* sites (depicted by grey triangles) was inserted into intron 15 and served as a selection marker. The *Dmt1* IRE was replaced by the mutated IRE through homologous recombination in embryonic stem cells. The CD-Neo cassette was subsequently removed via transient expression of CRE recombinase to obtain the $Dmt1^{IRE\Delta}$ allele. (B) Schematic representation of the murine *Dmt1* IRE stem-loop structure. The bases highlighted in red are deleted in the $Dmt1^{IRE\Delta}$ allele. (C) Southern-blot analysis of the *Dmt1* locus in $Dmt1^{IRE+/+}$, $Dmt1^{IRE+/\Delta}$, and $Dmt1^{IRE\Delta/\Delta}$ mice with a 3' external probe (P3') after digestion of genomic deoxyribonucleic acid with NcoI, indicated N in (A). (D) Total RNA from wild-type (top) and mutant (bottom) littermates was reverse transcribed and the IRE region of the *Dmt1* mRNA was PCR amplified (Supplemental Table 4, http://links.lww.com/HS/A91) and sequenced. The electropherograms confirm proper mutagenesis of the 3'IRE of the *Dmt1* mRNA. The nucleotides deleted in the wild-type IRE are underlined. The NcoI site created in the mutated IRE is shown. (E) Serum iron parameters were assessed in male mice at 2 weeks (2 wks), 3 months (3 mos) and 9 months (9 mos) of age (6–13 male mice per group). (F) Serum hepcidin concentration (left) and liver hepcidin mRNA levels (right) in 3-month-old male mice. (G) The liver and splenic iron stores were determined in male mice (8–22 mice per group) at different stages of life, as in (E). The results are expressed as percentage of wild-type littermates for each range of age. Note that the hepatic and splenic iron stores of 2 week-old mice are low compared to adults (liver: ~ 100 ± 32 mg nonheme iron/g of dry tissue in 2-week old wild-type males vs 279 ± 51 and 357 ± 62 mg/g at 3 and 9 months of age, respectively; spleen: 227 ± 14 mg/g in 2 week-old wild-type males vs 1927 ± 119 and 3887 ± 744 mg/g at 3 and 9 months of age, respectively). Histograms display averages ± SEM. p: Student *t*-test (*: $p < 0.05$; **: $p < 0.01$; ***: $p < 0.001$). CD = cytidine deaminase, IRE = iron responsive element, mRNA = messenger ribonucleic acid, RNA = ribonucleic acid.

HemaSphere (2020) 4:5 www.hemaspherejournal.com

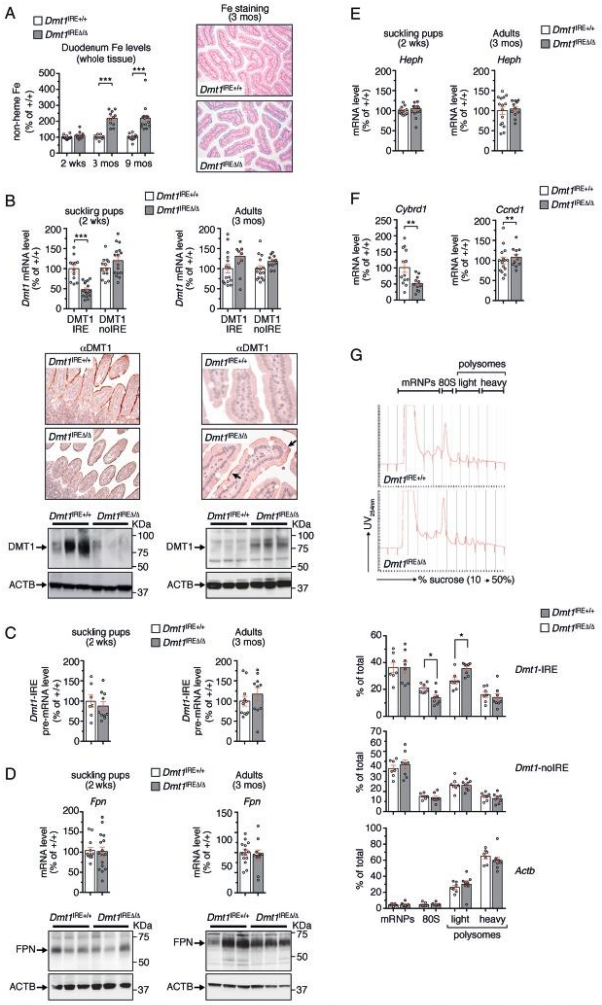

Figure 2. The *Dmt1* 3'IRE exerts divergent effects on intestinal DMT1 expression in postnatal vs adult animals. (A) Left: Duodenal nonheme iron levels were analyzed in male mice at different stages of life as in Figure 1E (9–15 mice per group). Right: Perl's staining in the duodenum of 3-month old male mice showing iron deposition in mucosal cells (counterstain: nuclear fast red). (B) Top: qPCR analysis of *Dmt1* mRNA levels in the duodenum of 2 week- (left) vs 3 month- (right) old mice using IRE vs non-IRE-specific primers (Supplemental Table 4, http://links.lww.com/HS/A91). The data display transcript levels as percentage of control (ie, $Dmt1^{IRE+/+}$) after calibration to *Actb* (n = 9–16 mice per group); similar results were obtained when using *Gapdh* and/or *Tubb5* as standard (not shown). Middle panels: immunostaining of DMT1 in the duodenum (counterstain: hematoxylin); a higher magnification is presented for adult tissues because the DMT1 signal (arrows) is fainter than in suckling pups. Bottom: representative western-blot analysis of DMT1 in whole duodenal extracts. (C) qPCR analysis of *Dmt1* pre-mRNA levels in 2-week- vs 3-month-old male mice, after calibration to the *Actb* pre-mRNA (similar results were obtained after calibration of *Gapdh* pre-mRNA, not shown). (D) qPCR (top) and western-blot (bottom) analysis of ferroportin expression in the duodenum of mice at 2 weeks (left) vs 3 months (right) of age. For western blotting (B and D), ACTB was used as loading control. In (A) and (B), pictures were acquired with a DM5000 microscope equipped with a DFC420C camera and a 10× (A), 20× (B, 2 weeks) or 40× (B, 3 months) objectives, and were processed using the Leica Application Suite (Leica Biosystems, Wetzlar, Germany). (E) qPCR analysis of *Heph* mRNA levels in the duodenum of 2 week- vs 3-month old mice. (F) qPCR analysis of HIF2-target genes in the duodenum of 3-month-old animals. The qPCR data in (D) to (F) display transcript levels as percentage of control (ie, $Dmt1^{IRE+/+}$) after calibration to *Actb* (similar results were obtained after calibration on *Gapdh* and/or *Tubb5*, not shown). (G) Duodenal scrapings from 3-month old mice were resolved through linear 10% to 50% sucrose density gradients and fractions were collected with constant UV recording (top). Fractions corresponding to untranslated mRNA (mRNP: messenger ribonucleoprotein), monosomes (80S), as well as light and heavy polysomes were collected. The amount of *Dmt1* (IRE and non-IRE isoforms) and *Actb* mRNAs in those fractions was determined by qPCR. The histograms (bottom) represent mRNA levels across the fractions as a percentage (mean ± SEM, n = 7–8) of the sum of all fractions. Histograms display averages ± SEM. p: Student *t*-test (*: $p < 0.05$; **: $p < 0.01$; ***: $p < 0.001$). IRE = iron responsive element, mRNA = messenger ribonucleic acid, RNA = ribonucleic acid.

Letter

(Fig. 1G). In contrast to suckling pups, 3 month-old *Dmt1*$^{IRE\Delta/\Delta}$ males exhibit high serum iron and transferrin saturation values (Fig. 1E) and an increase in tissue iron stores (Fig. 1G), accompanied by an augmentation of serum hepcidin (Fig. 1F, left) attributable to stimulation of the hepcidin transcript in liver (Fig. 1F, right). Nine-month-old *Dmt1*$^{IRE\Delta/\Delta}$ males display a comparable hyperferremia and a trend towards high serum ferritin (Fig. 1E), associated with hepatic and splenic iron loading (Fig. 1G). *Dmt1*$^{IRE\Delta/\Delta}$ female mice show a similar, albeit less pronounced iron phenotype (Supplemental Figure 3, http://links.lww.com/HS/A91) at 2 weeks and 3 months. Enlargement of tissue iron stores in *Dmt1*$^{IRE\Delta/\Delta}$ adults is not associated with aberrantly high expression of mRNAs encoding known iron import or sequestration genes, nor with marked suppression of transcripts coding for iron export molecules (Supplemental Figure 4, http://links.lww.com/HS/A91), suggesting that tissue iron loading is secondary to the elevation of serum iron rather than a consequence of aberrant iron management in liver and spleen cells.

Iron dyshomeostasis in *Dmt1*$^{IRE\Delta/\Delta}$ mice could result from altered intestinal iron absorption.[1,4] At 2 weeks of age, duodenal nonheme iron levels are indistinguishable from wild type (Fig. 2A). However, *Dmt1*$^{IRE\Delta/\Delta}$ pups exhibit a selective downregulation of the *Dmt1*-IRE mRNA isoform, associated with a decrease in total DMT1 protein levels and reduced DMT1 immunostaining at the apical membrane of enterocytes (Fig. 2B). The downregulation of the *Dmt1*-IRE mRNA is largely posttranscriptional, since *Dmt1*-IRE pre-mRNA levels are not significantly altered (Fig. 2C). This is in agreement with the predicted role of 3'UTR IREs, based on analogy to *TFRC*, where IRP binding decreases mRNA decay.[1,8] Considering that FPN protein and *Heph* mRNA levels are not reduced (Fig. 2D and E), the hypoferremia in *Dmt1*$^{IRE\Delta/\Delta}$ pups could be explained by downregulation of intestinal DMT1 expression. During adulthood, *Dmt1*$^{IRE\Delta/\Delta}$ mice exhibit an approximately 2-fold increase in enterocyte iron accumulation (Fig. 2A), associated with normal expression of FPN and *Heph* (Fig. 2D and E). In contrast to its partial suppression in *Dmt1*$^{IRE\Delta/\Delta}$ pups, IRE-containing *Dmt1* mRNA is expressed at nearly wild-type levels in adult intestine (Fig. 2B). It is unlikely that this is due to compensatory stimulation of *Dmt1* transcription by HIF2.[5,6] Indeed, mRNA levels of *Fpn* and *Ccnd1*, both HIF2-target genes, are not increased (Fig. 2D and F). *Cybrd1*, another HIF2-target, appears to be repressed (Fig. 2F). Moreover, *Dmt1* pre-mRNA levels are unchanged (Fig. 2C). Hence, the 3'IRE of *Dmt1* exerts a positive effect on intestinal DMT1 expression during the postnatal period of growth but not during adult life. This age-dependent effect of the *Dmt1* 3'IRE appears to be tissue-specific. While it is also observed in heart, it is not detected in spleen or kidney (Supplemental Figures 4 and 5, http://links.lww.com/HS/A91). Surprisingly, while *Dmt1*$^{IRE\Delta/\Delta}$ adults express nearly wild-type levels of *Dmt1*-IRE mRNA, duodenal DMT1 protein expression is increased (Fig. 2B). Although we cannot exclude changes in protein turnover,[13] we speculated that disruption of the *Dmt1* 3'IRE could alter mRNA translation. Supporting this notion, we observed a significant shift of the *Dmt1*-IRE mRNA isoform from monosomes to polysomes (Fig. 2G), suggesting that the *Dmt1* 3'IRE partially represses *Dmt1* mRNA translation in the adult duodenum. As we did not detect obvious signs of altered urinary iron excretion (not shown), the relatively mild iron accumulation in *Dmt1*$^{IRE\Delta/\Delta}$ animals could reflect a modest increase in dietary iron absorption secondary to intestinal DMT1 protein upregulation, leading to progressive accretion of iron in the body over time.

The functionality of the *DMT1* 3'IRE has been questioned. Although it exhibits weaker affinity for IRPs than other IREs, the *DMT1* 3'IRE does bind IRP1 in the native cellular environment.[14] Our work confirms that the 3'IRE of *Dmt1* plays a role in controlling DMT1 expression and systemic iron homeostasis and reveals an age-dependent switch in its activity. During postnatal growth, the *Dmt1* 3'IRE promotes intestinal DMT1 expression and secures iron sufficiency; in adulthood, it suppresses DMT1 and prevents systemic iron loading.

Surprisingly, the IRE of *Dmt1* seems to influence different aspects of RNA fate in the intestine at different times – abundance and stability during early life and mRNA translation in adulthood. The molecular details of this age-related switch in the function of the *Dmt1* 3'IRE remain unknown. 3'UTR based-gene regulation is often mediated through the binding of proteins and/or microRNAs to specific RNA sequences and/or structures. We speculate that factors with tissue- and/or age-specific activity or expression might influence the way the *Dmt1* 3'IRE modulates DMT1 levels. Of note, single 3'IREs have been identified in other transcripts, including the *Cdc14a* and *Pfn2* mRNAs.[1] Like *DMT1*, the regulation of those mRNAs appears to be cell type-specific and different from the regulation of *TFRC*. Whether those other single 3'IREs regulate gene expression through a mechanism similar to the *DMT1* 3'IRE remains to be determined.

It is well established that *Dmt1* regulation in the duodenal mucosa is strongly dependent on HIF2.[15] In that context, the precise role of the age-dependent switch in the activity of the *Dmt1* 3'IRE remains to be defined. The *Dmt1* 3'IRE may contribute to maintaining baseline homeostasis of immature intestinal absorption early in life, whereas, in adulthood, the 3'IRE may help to fine-tune DMT1 expression to avoid excessive iron assimilation.

Acknowledgements

We thank Sandro Altamura (University of Heidelberg, Germany) for fruitful discussions. We are grateful to the staff of the DKFZ animal facility for their dedicated care of the animals. We thank the "Plateforme de Biochimie" at the "Centre de Recherche sur l'Inflammation" (Paris, France) for their measurement of serum parameters. This work was supported by the Howard Hughes Medical Institute (NCA) and a grant from the Deutsche Forschungsgemeinschaft to B.G. (GA2075/5-1).

References

1. Muckenthaler MU, Rivella S, Hentze MW, et al. A red carpet for iron metabolism. *Cell*. 2017;168:344–361.
2. Gunshin H, Mackenzie B, Berger UV, et al. Cloning and characterization of a mammalian proton-coupled metal-ion transporter. *Nature*. 1997; 388:482–488.
3. Fleming MD, Trenor CC, Su MA, et al. Microcytic anaemia mice have a mutation in Nramp2, a candidate iron transporter gene. *Nat Genet*. 1997;16:383–386.
4. Shawki A, Anthony SR, Nose Y, et al. Intestinal DMT1 is critical for iron absorption in the mouse but is not required for the absorption of copper or manganese. *Am J Physiol Gastrointest Liver Physiol*. 2015;309: G635–G647.
5. Shah YM, Matsubara T, Ito S, et al. Intestinal hypoxia-inducible transcription factors are essential for iron absorption following iron deficiency. *Cell Metab*. 2009;9:152–164.
6. Mastrogiannaki M, Matak P, Keith B, et al. HIF-2alpha, but not HIF-1alpha, promotes iron absorption in mice. *J Clin Invest*. 2009;119: 1159–1166.

7. Hubert N, Hentze MW. Previously uncharacterized isoforms of divalent metal transporter (DMT)-1: implications for regulation and cellular function. *Proc Natl Acad Sci USA*. 2002;99:12345–12350.
8. Yoshinaga M, Nakatsuka Y, Vandenbon A, et al. Regnase-1 maintains iron homeostasis via the degradation of transferrin receptor 1 and prolyl-hydroxylase-domain-containing protein 3 mRNAs. *Cell Rep*. 2017;19:1614–1630.
9. Mino T, Murakawa Y, Fukao A, et al. Regnase-1 and roquin regulate a common element in inflammatory mRNAs by spatiotemporally distinct mechanisms. *Cell*. 2015;161:1058–1073.
10. Wardrop SL, Richardson DR. The effect of intracellular iron concentration and nitrogen monoxide on Nramp2 expression and non-transferrin-bound iron uptake. *Eur J Biochem*. 1999;263:41–49.
11. Gunshin H, Allerson CR, Polycarpou-Schwarz M, et al. Iron-dependent regulation of the divalent metal ion transporter. *FEBS Lett*. 2001; 509:309–316.
12. Galy B, Ferring-Appel D, Becker C, et al. Iron regulatory proteins control a mucosal block to intestinal iron absorption. *Cell Rep*. 2013;3: 844–857.
13. Foot NJ, Leong YA, Dorstyn LE, et al. Ndfip1-deficient mice have impaired DMT1 regulation and iron homeostasis. *Blood*. 2011;117:638–646.
14. Connell GJ, Danial JS, Haastruthers CX. Evaluation of the iron regulatory protein-1 interactome. *Biometals*. 2018;31:139–146.
15. Schwartz AJ, Das NK, Ramakrishnan SK, et al. Hepatic hepcidin/intestinal HIF-2α axis maintains iron absorption during iron deficiency and overload. *J Clin Invest*. 2019;129:336–348.

9. Acknowledgements

En primer lloc m'agradaria donar les gracies a Mayka per haver-me donat l'oportunitat de fer un doctorat al seu laboratori. Va ser un començament un poc difícil, però amb treball crec que hem portat la tesi a bon port. M'has ajudat amb la teua proactivitat, la teua energia i tota la teua experiència com a investigadora guiant-me i ajudant a que pugui assolir un dels meus somnis. Gracies també per la paciència i per la velocitat amb la que em passaves les correccions.

Vull també fer una menció especial a Gonzalo, el meu co-director i el que ha anat supervisant el meu treball des de que va arribar. M'has ajudat moltíssim amb els experiments que no sortien, amb els maleïts EMSAs, els westerns que de repent van deixar de funcionar i els primers que en la vida han funcionat. M'has ensenyat a pensar com un científic a proposar solucions i a mirar tot des d'un altre punt de vista.

Gracies a tota la resta del grup d'Iron Metabolism: Lídia, Vero, Xènia, Dani i Melina. Per l'ajuda, les preguntes interessants durant els seminaris i per crear un ambient "fantàstic" on treballar es fa un poc menys avorrit. Com no, vull agrair també el bon rotllo a tota la resta del laboratori: Marta, Andrea, Nuria, Jesús, Anna M, Cris, Anna F, Xavi, Sara, Ainoa, Tadeo, Blanca, Eva i la gent que ja no està Pau, Marta Pera i Reyes. Espero no deixar-me a ningú i si es així i ho veus et convido a una cervesa!. M'agradaria fer una menció especial per a Ana, Rocío, Joan i Alessandro. Amb vosaltres he passat els millors i els pitjors moments de la tesi: des de els sopars a casa Alessandro, els vermuts i les festes, fins les tardes i/o cerveses de "dramitas". Segur que en poc de temps estem celebrant les vostres tesis!

No voldria oblidar-me en aquest apartat dels col·laboradors que han fet alguns d'aquests experiments possibles. Com el Dr. Bruno Galy, del DKFZ, per la seva paciència amb els EMSAs, Lucía Gutierrez i Mª Puerto Morales de la Universitat de Zaragoza i del ICMM-CSIC per la seva disponibilitat 24/7 i amabilitat. Com no, a la Dra. Mar García del IRB; sense la teva ajuda i amabilitat no haguera pogut dur a terme la meva tesis, no tenies per què ajudar-me ni deixar-me entrar al teu laboratori i vas acollir-me amb els braços oberts. Gracies, també, per contestar els correus en qüestió de segons.

Ara ja fora de la feina, voldria donar les gracies als compis de pis: Isaac, Vicente, Joan (encara que ja no estas) i sobretot Edu. Hem sigut quasi com una família i heu creat un bon ambient a casa on poder estar a gust, evadir-se del treball i poder relaxar-se i descansar. Cosa que ha sigut fonamental moltes vegades durant la tesi.

No em vull oblidar de donar les gracies a la xicoteta part del poble que tinc per Barcelona: Uri, Patri, Juan i Alba. No sabeu tot el que m'heu ajudat només amb les vostres bromes, nits de festa, riures i mes anècdotes que no poden anar apuntades en un text massa formal com aquest. Mentre escric això encara no se que faré després del doctorat (ni en la vida en general, per a què enganyar-nos), però encara que no em quedi a Barcelona espero que la confiança que ens tenim no es perdi mai.

Gracies mama i gracies papa per haver fet això possible. No heu deixat de creure en mi a pesar de que en moltes ocasions no enteníeu en què estic treballant. Vau ser els primers en ensenyar-me i vau donar-me les ferramentes per desenvolupar la meua curiositat. Moltes gracies per tot l'esforç econòmic que suposa haver costejat els meus estudis i mes sacrificis personals que ni imagino que heu fet.

Per últim, moltes gracies a mi mateix. Pot sonar egoista, però considero necessari valorar els meus esforços i sacrificis. Vull agrair-me el treball realitzat, el no renunciar mai i el creure en mi quan pocs o ningú ho han fet. M'he demostrat a mi mateix que puc amb qualsevol cosa.